Supporting Information

Light controlled shape-changing azomacrocycles exhibiting reversible modulation of pyrene fluorescence emission

Anjali Srivastava,[a] Surbhi Grewal,[a] Naimat K Bari,[b] Mayank Saraswat,[a] Sharmistha Sinha,*[b] and Sugumar Venkataramani*[a]

[a]Indian Institute of Science Education and Research Mohali (IISERM), Sector 81, SAS Nagar, Knowledge City, Manauli – 140 306, Punjab, India.
[b]Institute of Nano Science and Technology (INST), Sector 64, Mohali-160 062, Punjab, India.
E-mail: sugumarv@iisermohali.ac.in, sinhas@inst.ac.in

List of Contents

S1. General methods:

All the solvents and chemicals were purchased from commercially available sources such as Sigma Aldrich, TCI, Avra chemicals, Rankem, Promochem, CIL, etc., and all of them have been used for synthesis as purchased. For purification, distilled solvents have been used, wherever necessary. For UV-Vis experiments, HPLC or spectroscopy grade solvents have been used. For dry and inert condition reactions, oven-dried glasswares, and the dry solvents obtained from MBRAUN solvent purification system (SPS) have been used. Reactions were monitored by thin-layer chromatography (TLC) using Merck Silica gel 60 F_{254} TLC plates under UV light (λ = 254 nm) in a UV chamber. Compounds were purified using column chromatography on a silica gel (mesh size 100-200 Å) and neutral alumina using n-hexane/ethyl acetate mixture as an eluent. MPs (Melting Point) were recorded on a Stuart SMP20 melting point apparatus and are uncorrected. The NMR spectra have been recorded in Bruker Avance-III 400 MHz spectrometer. ^{1}H and ^{13}C NMR were recorded at operational frequencies 400 MHz and 100 MHz, respectively. For recording NMR spectra, $CDCl_3$ and DMSO-d_6 have been used as solvents, and the residual solvent signals have been used for calibration. The chemical shift values are reported in parts per million (ppm) and the coupling constants (*J*) are reported in Hz. High-resolution mass spectra (HRMS) have been recorded using Waters Synapt G2-Si Q-TOF mass spectrometer. HRMS data were obtained from a TOF mass analyzer in both positive and negative modes using either electrospray ionization (ESI) or Matrix-assisted laser desorption ionization (MALDI) methods. The electronic absorption spectra were recorded using a Cary 5000 UV-Vis-NIR spectrophotometer or Cary 60 UV-Vis spectrophotometer equipped with Peltier controller for variable temperature measurements. Commercially available UV (Nichia 365 nm) LED, Applied Photophysics with different wavelengths of LEDs, and 405 nm LED light sources have been used for the forward and reverse photoisomerization processeses and screening of irradiation wavelengths. FT-IR spectra were recorded using Bruker Alpha spectrometer in transmittance mode using a ZnSe Attenuated Total Reflectance (ATR) assembly and are reported in cm^{-1}. Atomic force microscopy (AFM) studies were performed on Innova atomic force microscope using NanoDrive (v8.03) software. The AFM images were processed and analyzed using WSxM software. The height profiles were plotted using Origin 8. Field emission-scanning microscopy (FE-SEM) was performed by using the JEOL JSM-7600F instrument. Dynamic light Scattering (DLS) has been performed by using the instrument DLS (Malvern). Fluorescence studies have been done by using a Fluoromax-4 spectrophotometer (Horiba Scientific) and Hitachi F700 fluorescence spectrophotometer. Fluorescence Lifetime studies have been done by using Horiba Jobin Yvon using DAS6 analysis software. Isothermal titration calorimetry (ITC) experiments were performed using Malvern MicroCal PEAQ-ITC200.

S2. Synthesis and characterization :[1-6]

S2.1 Synthesis of core unit (*E*)-4,4'-(diazene-1,2-diyl) diphenol (2):[1]

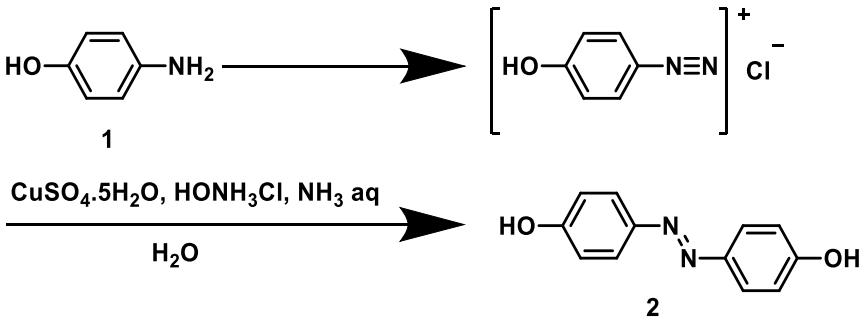

In a 500 ml RB, a solution of *p*-aminophenol **1** (2.0 g, 18.3 mmol) in 40 ml of water was taken. To this, 37 % HCl (7.3 ml) in 30 ml water was added dropwise over 30 min at rt, then an aqueous solution (108 mL) of $NaNO_2$ (1.3 g, 18.8 mmol) was slowly added over 2 hours at 0 °C to get a purple coloured diazotised solution. Into another 500 RB, an aqueous solution was prepared consisting of water (18.3 mL), $CuSO_4 \cdot 5H_2O$

(8.2 g, 32.8 mmol), 28% NH_3 (5.5 mL), and hydroxylammonium chloride (1.3 g, 8.3 mmol). To this yellow-coloured solution, the above prepared diazotised solution was added dropwise followed by the addition of diethyl ether (18ml), and the coupling reaction was carried out. The solution was stirred for 6 hrs. The brown precipitate was filtered, washed with 1 M HCl, and dried. Pure compound **2** was obtained by purification by chromatography on silica gel using ethyl acetate/hexane (2:5) as eluent column chromatography with 72 % yield.

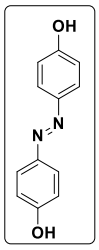

(*E*)-4,4'-(diazene-1,2-diyl) diphenol (**2**): brown solid, mp = 204 °C, 72% yield. ^{1}H NMR (400 MHz, DMSO-d_6): δ (ppm) 10.15 (s, 2H), 7.73 (d, J = 8.3 Hz, 4H), 6.92 (d, J = 8.3 Hz, 4H); ^{13}C NMR (100 MHz, DMSO-d_6): δ (ppm) 160.1, 145.3, 124.3, 115.9; FT-IR (ATR): 3309,1579, 1505, 1471, 1409, 1383, 1365, 1255, 1209, 1117, 833, 813, 769, 646 cm^{-1}; HRMS (ESI): *m/z* calcd. for $C_{12}H_{10}N_2O_2[M+H]^+$: 215.0800; found: 215.0808.

S2.2 Synthesis of *(E)*-1,2-bis(4-(prop-2-yn-1-yloxy) phenyl) diazene (3):

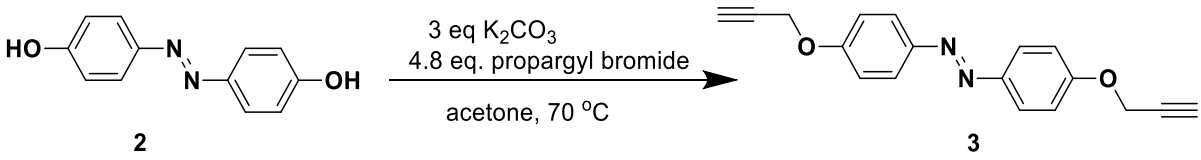

Compound **2** (500 mg, 2.33 mmol) and K_2CO_3 (774 mg, 5.6 mmol) were dissolved in dry acetone (25mL) in 100 ml RB at rt. To the above RB, propargyl bromide (1.2 mL, 11.2 mmol) was added and the mixture was stirred for 16 h under gentle reflux. Solids were filtered off and the solvent was removed under reduced pressure. A saturated solution of NH_4Cl and water were added and the mixture was extracted with DCM. The organic layers were dried over Na_2SO_4. The solvent was removed under reduced pressure to yield the desired compound **3** (667 mg, 2.30 mmol, isolated yield: 88 %).

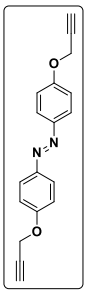

(E)-1,2-bis(4-(prop-2-yn-1-yloxy) phenyl) diazene (**3**): crystalline golden colour, mp = 192-194 °C, 88% yield. ^{1}H NMR (400 MHz, $CDCl_3$): δ (ppm) 7.89 (d, J = 8.8 Hz, 4H), 7.08 (d, J = 8.8 Hz, 4H), 4.77 (d, J = 2.0 Hz, 4H), 2.56 (t, J = 2.0 Hz, 2H); ^{13}C NMR (100 MHz, $CDCl_3$): δ (ppm) 159.6, 147.7, 124.5, 115.2, 78.2, 76.1, 56.1; FT-IR (ATR): 3272, 2925, 2128, 1592, 1495, 1451, 1375, 1243, 1230, 1107, 1014, 972, 842, 808, 781, 700, 666 cm^{-1}; HRMS (ESI): *m/z* calcd. for $C_{18}H_{14}N_2O_2$ $[M+H]^+$: 291.1133; found : 291.1144.

S2.3. Synthesis of *(E)*-1,2-bis(4-(2-bromoethoxy) phenyl) diazene (4a):[2]

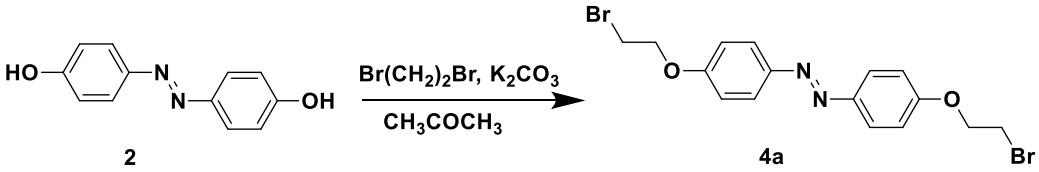

4,4'-Dihydroxyazobenzene **2** (1.34 g, 6.3 mmol), potassium carbonate (6.06 g, 43.8 mmol), 1,2- Dibromoethane (11.8 g, 62.6 mmol) was dissolved in dry acetone and were heated to reflux for 50 hours at 70 ^{o}C. After 50 hours, the reaction mixture was cooled to room temperature, the solvent was removed under reduced pressure to get the crude product. The residue was purified by column chromatography on silica gel using hexane as an eluent to get compound **4a** as a yellow powder with 30 % yield (1.59 g, 3.71 mmol).

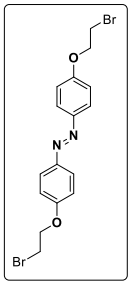

(E)-1,2-bis(4-(2-bromoethoxy) phenyl) diazene **(4a):** yellow powder, mp = 156 °C, 30% yield. ^{1}H NMR (400 MHz, $CDCl_3$): δ (ppm) 7.88 (d, J = 8.7 Hz, 4H), 7.01 (d, J = 8.7 Hz, 4H), 4.37 (t, J = 6.2 Hz, 4H), 3.68 (t, J = 6.2 Hz, 4H); ^{13}C NMR (100 MHz, $CDCl_3$): δ (ppm) 160.2, 147.6, 124.6, 115.0, 68.1, 29.0; FT-IR (ATR): 2969, 2924, 2863, 1710, 1598, 1492, 1454, 1417, 1379, 1314, 1234, 1143, 1072, 1013, 963, 883, 851, 814, 747, 667 cm^{-1}; HRMS (ESI): *m/z* calcd. for$C_{16}H_{16}Br_2N_2O_2$[M+H] $^{+}$: 426.9657; found: 426.9644.

S2.4. Synthesis of *(E)*-1,2-bis(4-(3-bromopropoxy) phenyl) diazene (4b):[3]

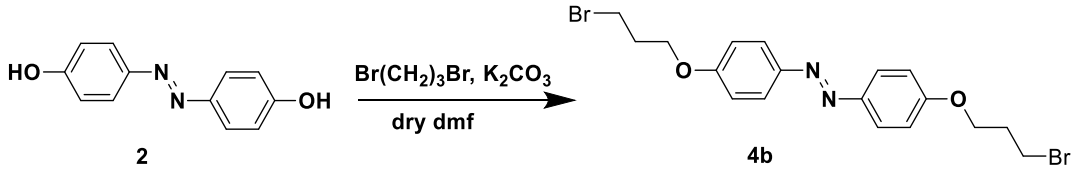

4,4'-dihydroxyazobenzene **2** (0.50 g, 2.33 mmol), anhydrous potassium carbonate (3.06 g, 22.4 mmol) was dissolved in dry DMF and stirred for 30 min. After 30 min, 1,3dibromopropane (4.52 g, 22.4 mmol) was added to the above solution. The reaction mixture was allowed to be stirred for 24 hours. The solution was extracted with CH_2Cl_2 3 times. The organic layer was washed several times with water, dried over anhydrous Na_2SO_4, and the solvent was removed under reduced pressure. The residue was purified by column chromatography on silica gel using hexane as an eluent to get compound **4b** as a yellow powder with 45 % yield.

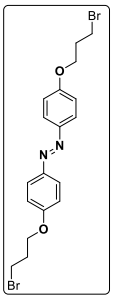

(E)-1,2-bis(4-(3-bromopropoxy) phenyl) diazene**(4b):** yellow powder, mp = 138-139 °C, 45% yield. ^{1}H NMR (400 MHz, $CDCl_3$): δ (ppm) 7.87 (d, J = 8.2 Hz, 4H), 7.00 (d, J = 8.2 Hz, 4H), 4.19 (t, J = 5.8 Hz, 4H), 3.63 (t, J = 5.8 Hz, 4H), 2.39-2.33 (m, 4H) ; ^{13}C NMR (100 MHz, $CDCl_3$): δ (ppm) 160.8, 147.3, 124.5, 114.8, 65.7, 32.4, 30.0; FT-IR (ATR): 3071, 2952, 2862, 1599, 1578, 1494, 1464, 1380, 1314, 1234, 1206, 1141, 1055,1027, 921, 843, 807, 732, 655, 639 cm^{-1}; HRMS (ESI): *m/z* calcd$C_{18}H_{20}Br_2N_2O_2$ $[M+H]^+$: 454.9970; found : 454.9951.

S2.5 Synthesis of (*E*)-1,2-bis(4-(4-bromobutoxy)phenyl)diazene (4c):[4]

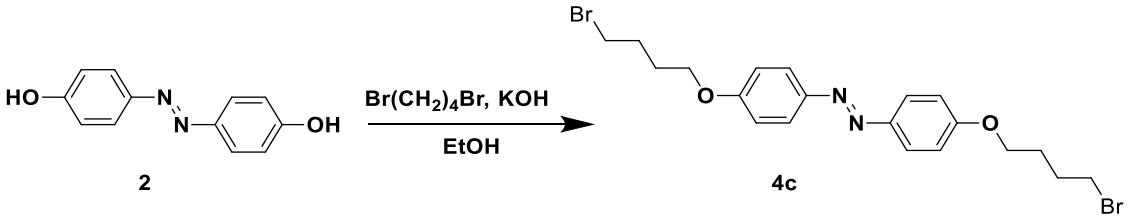

4,4'-dihydroxyazobenzene **2** (0.50 g, 2.33mmol) was dissolved in ethanol and was heated to reflux. To the reaction mixture, potassium hydroxide (0.39 g, 7 mmol) was added, followed by the addition of 1,4-dibromobutane (0.50 g, 23.3 mmol). The reaction mixture was then refluxed at 80 °C for 4 hours. After cooling, a precipitate was formed, which was filtered and washed with ethanol. The crude product was dissolved in toluene, filtered while hot, and then recrystallized to get yellow coloured compound **4c** with 56 % yield.

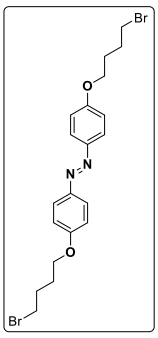

(E)-1,2-bis(4-(4-bromobutoxy)phenyl)diazene (**4c**): yellow solid, mp = 157-162 °C, 56% yield. ^{1}H NMR (400 MHz, $CDCl_3$): δ (ppm) 7.87 (d, J = 8.0 Hz, 4H), 6.98 (d, J = 8.1 Hz, 4H), 4.07 (t, J = 5.9 Hz, 4H), 3.51 (t, J = 6.3 Hz, 4H), 2.04 (dq, J = 45.2, 6.6 Hz, 8H); ^{13}C NMR (100 MHz, $CDCl_3$): δ (ppm) 161.0, 147.1, 124.5, 114.7, 67.2, 33.6, 29.5, 28.0; FT-IR (ATR): 2945, 2874, 1601, 1580, 1495, 1474, 1462, 1435, 1348, 1317, 1279, 1210, 1149, 1107, 1043, 1027, 1011, 843, 775, 732, 652, 641 cm^{-1}; HRMS (ESI): *m/z* calcd. for $C_{20}H_{24}Br_2N_2O_2$ $[M+H]^+$: 483.0283; found : 483.0341.

S2.6. General procedure for azide synthesis (5a-5c):

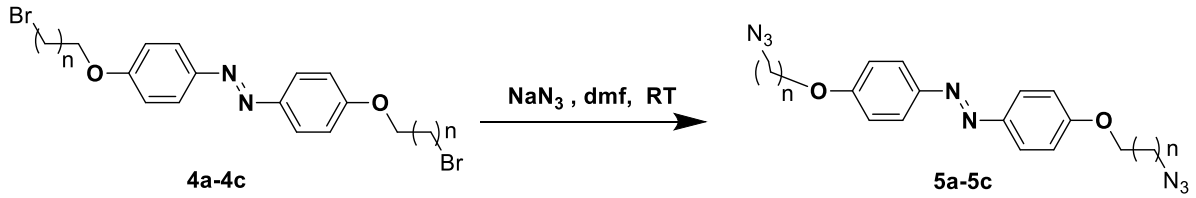

General Procedure: In a 50 ml round-bottom flask, dibromide (**4a-4c**) (0.5 mmol) was dissolved in 10 ml dry DMF. After this, sodium azide (1.5 mmol) was added and stirred for 24 hours at room temperature. Then, the mixture was extracted with ethyl acetate and the combined organic extracts were washed with H_2O, dried over anhydrous Na_2SO_4, filtered,

concentrated in vacuo, and then subjected to purification by column chromatography using neutral alumina.

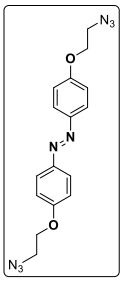

(E)-1,2-bis(4-(2-azidoethoxy)phenyl)diazene (**5a**): crystalline yellow, mp = 119-123 °C, 72% yield. ^{1}H NMR (400 MHz, $CDCl_3$): δ (ppm) 7.89 (d, J = 8.4 Hz, 4H), 7.03 (d, J = 8.4 Hz, 4H), 4.23 (t, J = 4.8 Hz, 4H), 3.65 (t, J = 4.7 Hz, 4H); ^{13}C NMR (100 MHz, $CDCl_3$): δ (ppm) 160.3, 147.5, 124.6, 115.0, 67.3, 50.2; FT-IR (ATR): 2929,2108, 1594, 1579, 1495, 1457, 1348, , 1300, 1250, 1145, 1105, 1050, 920, 842, 817, 731, 637 cm^{-1}; HRMS (ESI): *m/z* calcd. for $C_{16}H_{16}N_8O_2$ $[M+H]^+$: 353.1474; found : 353.1469.

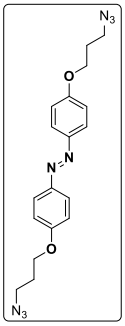

(E)-1,2-bis(4-(3-azidopropoxy) phenyl) diazene (**5b**): crystalline yellow, mp = 110-112 °C, 68% yield. ^{1}H NMR (400 MHz, DMSO-d_6): δ (ppm) 7.83 (d, J = 8.2 Hz, 4H), 7.12 (d, J = 8.2 Hz, 4H), 4.14 (t, J = 5.8 Hz, 4H), 3.53 (t, J = 6.5 Hz, 4H), 2.05-1.99 (m, 4H); ^{13}C NMR (100 MHz, DMSO-d_6): δ (ppm) 160.6, 146.2, 124.2, 115.0, 65.1, 40.1, 28.1; FT-IR (ATR): 2966, 2872, 2091, 1592, 1497, 1469, 1458, 1391, 1301, 1247, 1142, 1102, 1048, 955, 845, 732, 639 cm^{-1}; HRMS (ESI): *m/z* calcd. for $C_{18}H_{20}N_8O_2$ $[M+H]^+$: 381.1787; found : 381.1771.

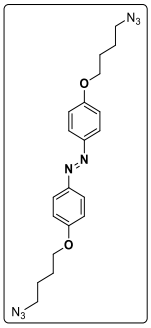

(E)-1,2-bis(4-(4-azidobutoxy) phenyl) diazene(**5c**): crystalline orange, mp = 97-100 °C, 65% yield. ^{1}H NMR (400 MHz, $CDCl_3$): δ (ppm) 7.87 (d, J = 8.0 Hz, 4H), 6.98 (d, J = 8.1 Hz, 4H), 4.06 (t, J = 5.4 Hz, 4H), 3.38 (t, J = 6.6 Hz, 4H), 1.86 (dq, J = 37.2, 5.7 Hz, 8H); ^{13}C NMR (100 MHz, $CDCl_3$): δ (ppm) 160.9, 147.1, 124.4, 114.7, 67.5, 51.3, 26.6, 25.8; FT-IR (ATR): 2957, 2929, 2918, 2852, 2210, 2181, 2091, 1599, 1576, 1497, 1471, 1455, 1395, 1347, 1312, 1238, 1143, 1105, 999, 945, 827, 802, 772, 756, 730, 621 cm^{-1}; HRMS (ESI): *m/z* calcd. for $C_{20}H_{24}N_8O_2$ $[M+H]^+$: 409.2100; found : 409.2112.

S2.7 Synthesis of *(E)*-(diazene-1,2-diylbis(4,1-phenylene))dimethanol(7):[6]

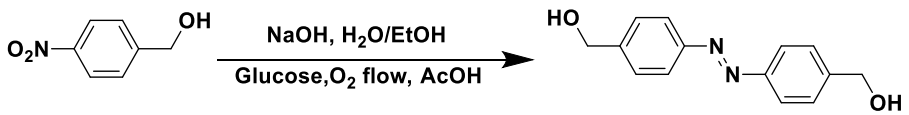

6 **7**

Sodium hydroxide was dissolved in a 3-necked round bottom flask equipped with a reflux condenser and heated at 50 °C. To this, Nitrobenzyl alcohol **6** (6.0 g, 0.04 mol) dissolved in 60 mL EtOH was added to this above prepared solution. This reaction mixture was stirred for 30 min under a continuous inert gas flow. Subsequently, a glucose solution (75 g, 0.42 mol) in 50 ml water was added drop-wise (within 90 min) at 50 °C with continuous stirring under an inert gas flow. The reaction mixture was then aerated for 3 h at 50 °C and then cooled to room temperature, and aerated additionally overnight with vigorous stirring. The final mixture was

acidified with a dilute acetic acid (50 %) until pH>5. The generated solid was filtered off, washed with water excessively. The crude product was purified by column chromatography on silica gel using ethyl acetate as an eluent to get compound **7** as a yellow-orange powder with 55 % yield.

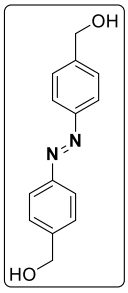

(E)-(diazene-1,2-diylbis(4,1-phenylene))dimethanol (**7**)**:** Dark orange solid, mp = 230 °C, 55% yield. ^{1}H NMR (400 MHz, DMSO-d_6): δ (ppm) 7.86 (d, J = 7.8 Hz, 4H), 7.53(d, J = 8.0 Hz, 4H), 5.40 (t, J = 5.6 Hz, 2H), 4.60 (d, J = 5.2 Hz, 4H); ^{13}C NMR (100 MHz, DMSO-d_6): δ (ppm) 150.9, 146.3, 127.2, 122.4, 62.5; FT-IR (ATR): 3291, 3206, 2911, 2855, 1930, 1601, 1500, 1449, 1345, 1302, 1289, 1206, 1151, 1024, 1005, 851, 832, 639 cm^{-1}; HRMS (ESI): *m/z* calcd. for $C_{14}H_{14}N_2O_2$[M+H]$^+$: 243.1133; found : 243.1120.

S2.8 Synthesis of *(E)*-1,2-bis(4-((prop-2-yn-1-yloxy) methyl) phenyl) diazene (8*)*:

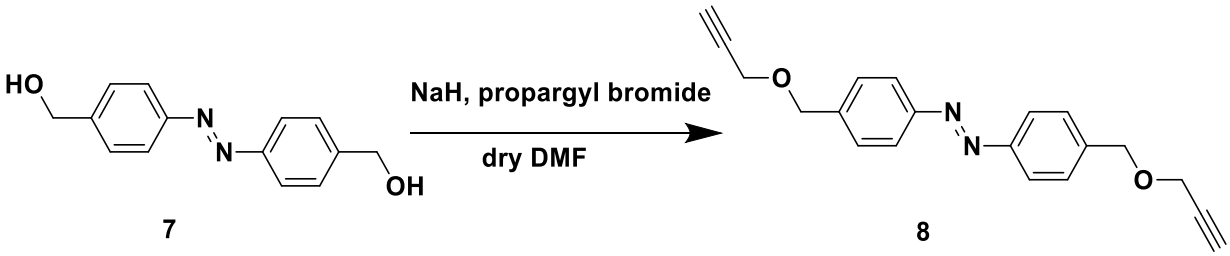

Compound **7** (500 mg, 2 mmol) was dissolved in dry DMF (20 mL) in a 100 ml round bottom flask and cooled to 0 °C. To this solution, sodium hydride was added (192 mg, 8 mmol). The resulting mixture was stirred at room temperature until the evolution of hydrogen gas subsided, and then was added propargyl bromide (0.6 mL, 8 mmol) at 0 °C. The reaction was stirred at rt and the reaction progress was monitored using TLC analysis. After the reaction was complete, the reaction was quenched with saturated aq. NH_4Cl. The quenched mixture was poured into H_2O and extracted three times with EtOAc. The combined organic layers were washed with an equal volume of saturated aq. NaCl and dried over anhydrous $MgSO_4$. After filtration and concentration, the crude product was purified using silica gel flash column chromatography [eluent: 2% EtOAc/Hexane] to get the desired compound **8** isolated.

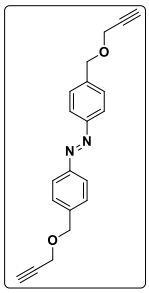

(E)-1,2-bis(4-((prop-2-yn-1-yloxy) methyl) phenyl) diazene **(8*):** crystalline orange, mp = 97-101 °C, 74% yield. ^{1}H NMR (400 MHz, $CDCl_3$): δ (ppm) 7.91 (d, J = 8.3 Hz, 4H), 7.51 (d, J = 8.3 Hz, 4H), 4.69 (s, 4H), 4.23 (d, J = 2.4 Hz, 4H), 2.50 (t, J = 2.3 Hz, 2H); ^{13}C NMR (100 MHz, $CDCl_3$): δ (ppm) 152.3, 140.5, 128.7, 123.1, 79.5, 75.0, 71.1, 57.5; FT-IR (ATR): 3247, 2874, 2853, 2111, 1603, 1578, 1310, 1259, 1095, 1068, 833, 707, 650, 606 cm^{-1}; HRMS (ESI): *m/z* calcd. for $C_{20}H_{18}N_2O_2$ [M+H]$^+$: 319.1446; found : 319.1434.

S2.9 Synthesis of *(E)*-1,2-bis(4-methoxyphenyl)diazene (9):

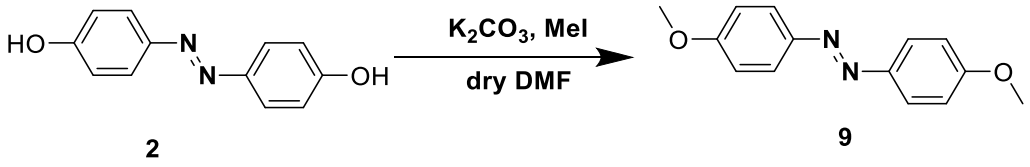

2 9

Compound **2** (200 mg, 0.93 mmol) was dissolved in 7 mL DMF and then, K_2CO_3 (386 mg, 2.8 mmol) was added to the solution. After that, methyl iodide (528 mg, 3.72 mmol) was added to the mixture. The mixture was then heated at 100 °C in a sealed tube for 12 hours and was monitored by TLC. After completion, the reaction mixture was cooled down to room temperature and poured into distilled water to afford yellow precipitate, which was filtered and washed with water to give pure **9** as yellow solid.

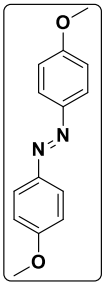

(E)-1,2-bis(4-methoxyphenyl)diazene (**9**)**:** yellow solid, mp = 160-162 °C, 90% yield. ^{1}H NMR (400 MHz, $CDCl_3$): δ (ppm) 7.84 (d, J = 8.9 Hz, 4H), 7.10 (d, J = 9.0 Hz, 4H), 3.84 (s, 6H); ^{13}C NMR (100 MHz, $CDCl_3$): δ (ppm) 161.9, 146.6, 124.6, 115.0, 56.0; FT-IR (ATR): 1581, 1478, 1234, 1123, 1014, 830, 736 cm^{-1}; HRMS (ESI): m/z calcd. for $C_{14}H_{14}N_2O_2$ $[M+Na]^+$: 265.0953; found : 265.0952.

S2.10 Synthesis of macrocycles (AM1a- AM1c):

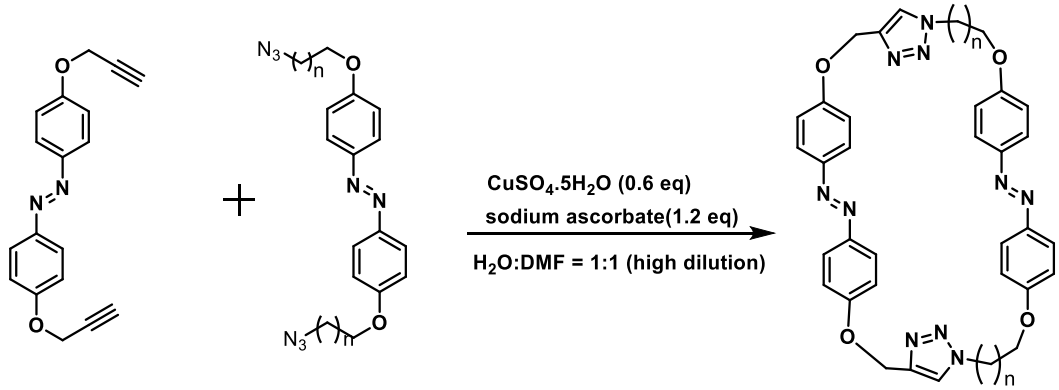

3 5a-c AM1a-c n=1, 2, 3

General Procedure: Macrocycles **AM1a- AM1c** have been synthesized by click chemistry. For click chemistry, core **3**(0.2 mmol, 1.0 eq for **AM1a**-**AM1c**) was dissolved in 20 ml DMF and subsequently irradiated with 365 nm for 20 min in one neck 100 ml RB under dark conditions. Similarly, the corresponding azides **5a**-**5c**, (1eq, 0.2 mmol) for macrocycles **AM1a**-**AM1c** respectively) dissolved in 20 ml DMF and subsequently irradiated separately with 365 nm for 20 min in another one neck 100 ml RB under dark condition. The above two separate solutions were poured into 500 ml RB followed by the addition of 110 ml more DMF. Subsequently, $CuSO_4 \cdot 5H_2O$ (0.6 eq) in 50 ml water and sodium ascorbate (1.2 eq) in 50 ml water was added to the above reaction mixture. The reaction was stirred for4 days at room

temperature. The resulting yellow coloured precipitate was filtered off and was washed three times with H_2O and acetone.

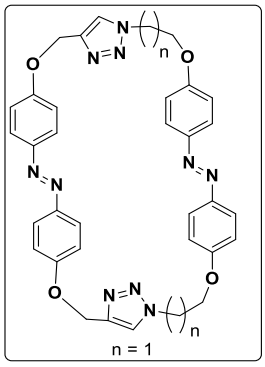

AM1a: yellow solid, 75% yield. ^{1}H NMR of *ZZ*-form (400 MHz, DMSO-d_6): δ (ppm) 8.27 (s, 2H), 6.96 (d, J = 8.0 Hz, 4H), 6.84-6.75 (m,12H), 5.09 (s,4H), 4.73 (t, J = 4.6 Hz, 4H), 4.34 (t, J = 4.0 Hz, 4H); ^{13}C NMR of *ZZ*-form (100 MHz, DMSO-d_6): δ (ppm) 157.0, 156.7, 147.1, 147.0, 125.4, 122.16, 122.14, 114.8, 114.7, 114.5 66.2, 61.2, 49.0; FT-IR (ATR): 2949, 2932, 2875, 2361, 2097, 1597, 1581, 1497, 1469, 1391, 1316, 1242, 1148, 1049, 1004, 841, 730, 641 cm^{-1}; HRMS (ESI): *m/z* calcd. for $C_{34}H_{30}N_{10}O_4$ $[M+H]^+$: 643.2529; found : 643.2533.

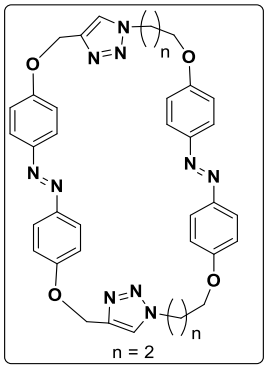

AM1b: yellow solid, 77% yield: ^{1}H NMR of *ZZ*-form (400 MHz,DMSO-d_6): δ (ppm) 8.23 (s, 2H), 6.96-6.77 (m, 16H), 5.08 (s, 4H), 4.50 (br,4H), 3.92 (br, 4H), 2.22 (br, 4H); ^{13}C NMR of *ZZ*-form (100 MHz, DMSO-d_6): δ (ppm) 157.7, 157.4, 147.3, 147.2, 125.3, 124.6, 122.6, 115.7, 115.2, 115.0, 65.2, 61.7, 47.1, 29.8; FT-IR (ATR): 2945, 2937, 2877, 2359, 2110, 1597, 1583, 1498, 1461, 1297, 1239, 1106, 1046, 1047, 1004, 840, 667, 641 cm^{-1}; HRMS (ESI): *m/z* calcd. for $C_{36}H_{34}N_{10}O_4$ $[M+H]^+$: 671.2842; found : 671.2859.

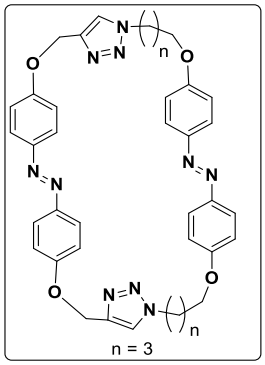

AM1c: yellow solid, 74% yield: ^{1}H NMR of *ZZ*-form (400 MHz, DMSO-d_6): δ (ppm) 8.23 (s, 2H), 6.96 (br, 4H), 6.82 (br, 12H), 5.09 (br, 4H), 4.04 (br, 4H), 3.92 (br, 4H), 7.92 (br, 4H), 1.62 (br, 4H); ^{13}C NMR of *ZZ*-form (100 MHz, DMSO-d_6): δ (ppm) 157.9, 157.4, 147.09, 147.07, 125.1, 124.6, 122.6, 115.4, 115.2, 115.0, 67.4, 61.7, 49.5, 27.0, 26.0; FT-IR (ATR): 3048, 2945, 2873, 2359, 2337, 1596, 1581, 1497, 1470, 1392, 1316, 1296, 1240, 1147, 1106, 1104, 839, 730, 641 cm^{-1}; HRMS (ESI): *m/z* calcd. for $C_{38}H_{38}N_{10}O_4$ $[M+Na]^+$: 721.2975; found : 721.2963.

S2.11. Synthesis of macrocycles (AM2a-AM2c):

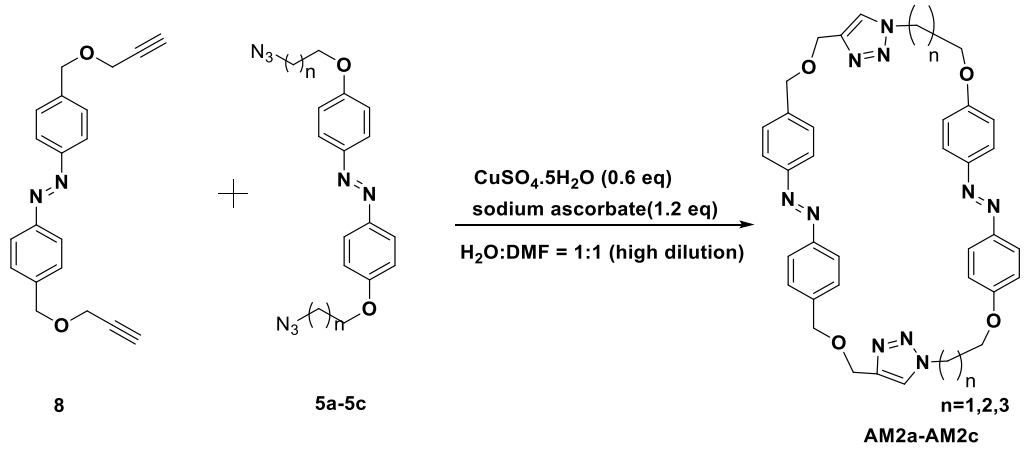

General Procedure: Macrocycles **AM2a-AM2c** have been synthesized by click chemistry. For click chemistry, core **8** (0.2 mmol, 1.0 eq for **AM2a-AM2c**) was dissolved in 20 ml DMF and subsequently irradiated with 365 nm for 20 min in one neck 100 ml RB under dark conditions. Similarly, the corresponding azides **5a-5c**, (1eq, 0.2 mmol) for macrocycles **AM2a -AM2c** respectively)dissolved in 20 ml DMF and subsequently irradiated separately with 365 nm for 20 min in another one neck 100 ml RB under dark condition. The above two separate solutions were poured into 500 ml RB followed by the addition of 110 ml more DMF. Subsequently, $CuSO_4 \cdot 5H_2O$ (0.6 eq) in 50 ml water and sodium ascorbate (1.2 eq) in 50 ml water was subsequently added to the above reaction mixture. The reaction was stirred for 4 days at room temperature. The resulting yellow coloured precipitate was filtered off and was washed three times with H_2O and acetone.

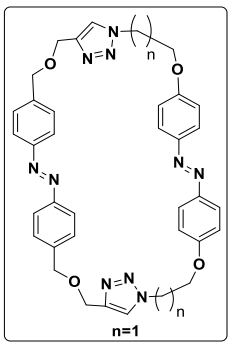

AM2a: yellow solid, 71% yield. ^{1}H NMR of *ZZ*-form (400 MHz, DMSO-d_6): δ (ppm) 8.16 (s, 2H), 7.21(d, J = 6.9 Hz, 4H), 6.92-6.79 (m, 12H), 4.70 (br,4H), 4.51 (br, 4H), 4.41-4.35 (m, 8H); ^{13}C NMR of *ZZ*-form (100 MHz, DMSO-d_6): δ (ppm) 156.7, 152.7, 146.9, 145.2, 137.2, 128.0,122.13, 122.12, 120.0, 114.7, 70.5, 66.3, 63.0, 48.9; FT-IR (ATR): 3057, 2946, 2865, 2360, 2341, 1598, 1583, 1498, 1458, 1298, 1226, 1147, 1080, 1046, 907, 838, 715, 640 cm^{-1}; HRMS (ESI): *m/z* calcd. for $C_{36}H_{34}N_{10}O_4$ $[M+H]^+$: 671.2842; found: 671.2852.

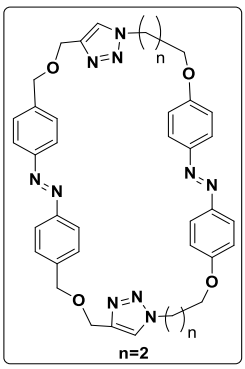

AM2b: yellow solid, 69% yield. ^{1}H NMR of *EE*-form (400 MHz, DMSO-d_6): δ (ppm) 8.20 (s, 2H), 7.79 (d, J = 24.0 Hz, 8H), 7.49 (br,4H), 7.01 (br, 4H), 4.80-4.30 (m, 12H), 4.03 (br, 4H), 2.31 (br, 4H); of *ZZ*-form 8.13 (s, 2H), 7.22 (d, J = 6.6 Hz, 4H), 6.81 (br,12H), 4.03 (br, 4H), 2.31 (br, 4H); ^{13}C NMR of *ZZ*-form (100 MHz, DMSO-d_6): δ (ppm) 157.3, 152.7, 146.74, 146.72, 137.2, 128.0, 124.1, 122.1, 120.0, 114.5, 70.5, 64.7, 63.0, 46.4, 29.4; FT-IR (ATR): 2935, 2865, 2359, 2348, 2096, 1598, 1582, 1499, 1471, 1298, 1240, 1147, 1047, 1012, 837, 729, 639 cm^{-1}; HRMS (ESI): *m/z*calcd. for $C_{38}H_{38}N_{10}O_4$ $[M+Na]^+$: 721.2975; found: 721.3004.

0

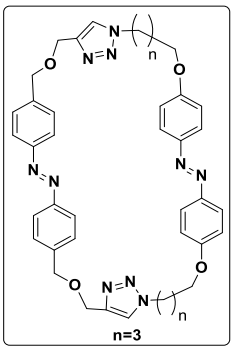

AM2c: yellow solid, 71% yield. ^{1}H NMR of *ZZ*-form (400 MHz,DMSO-d_6): δ (ppm) 8.11 (s, 2H), 7.23(br, 4H), 6.80- 6.78 (m, 12H), 4.50-4.35 (m, 12H), 3.90 (br, 4H), 1.90 (br, 4H), 1.61 (br, 4H); ^{13}C NMR of *ZZ*-form (100 MHz, DMSO-d_6): δ (ppm) 157.5, 153.0, 146.67, 146.65, 137.3, 128.1, 124.0, 122.2, 120.0, 114.5, 70.6, 67.0, 63.1, 49.0, 26.5, 25.6; FT-IR (ATR): 3057, 2940, 2866, 2359, 2340, 1598, 1581, 1498, 1471, 1418, 1297, 1248, 1147, 1049, 1084, 839, 729, 640 cm^{-1}; HRMS (ESI): *m/z* calcd. for $C_{40}H_{42}N_{10}O_4$ $[M+H]^+$:727.3468; found: 727.3459.

S3. Photoswitching of macrocycles AM1a-c and AM2a-c

S3.1. Photoswitching of macrocycles AM1a-c and AM2a-c: UV-Vis spectroscopic studies

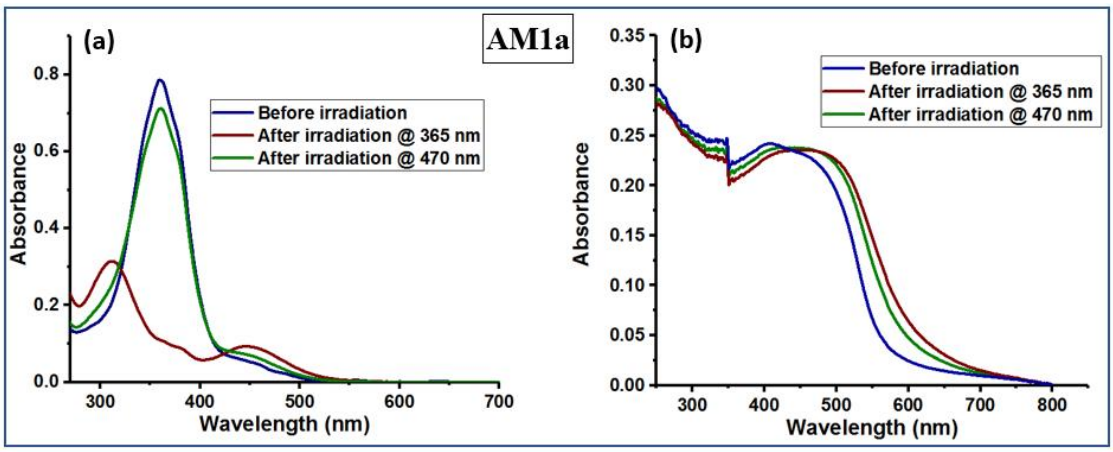

Figure S3.1. UV-Vis spectroscopic data of **AM1a**: (a) Photoswitching studies performed in DMSO; (b) Photoswitching studies performed in KBr medium.

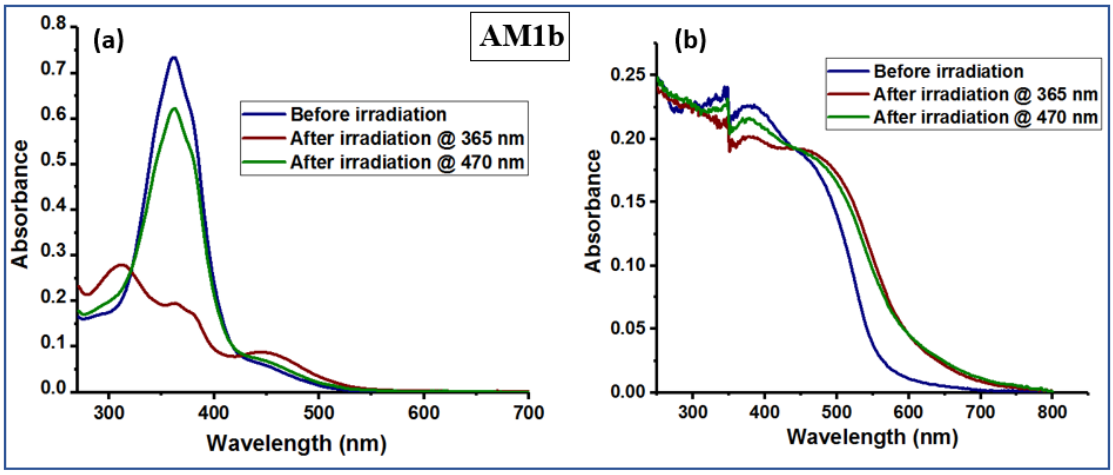

Figure S3.2. UV-Vis spectroscopic data of **AM1b**: (a) Photoswitching studies performed in DMSO; (b) Photoswitching studies performed in KBr medium.

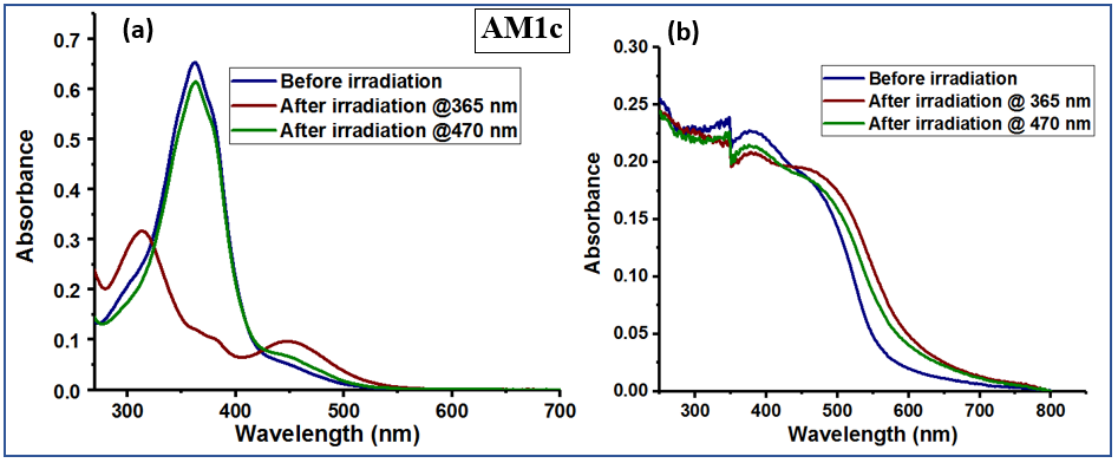

Figure S3.3. UV-Vis spectroscopic data of **AM1c**: (a) Photoswitching studies performed in DMSO; (b) Photoswitching studies performed in KBr medium.

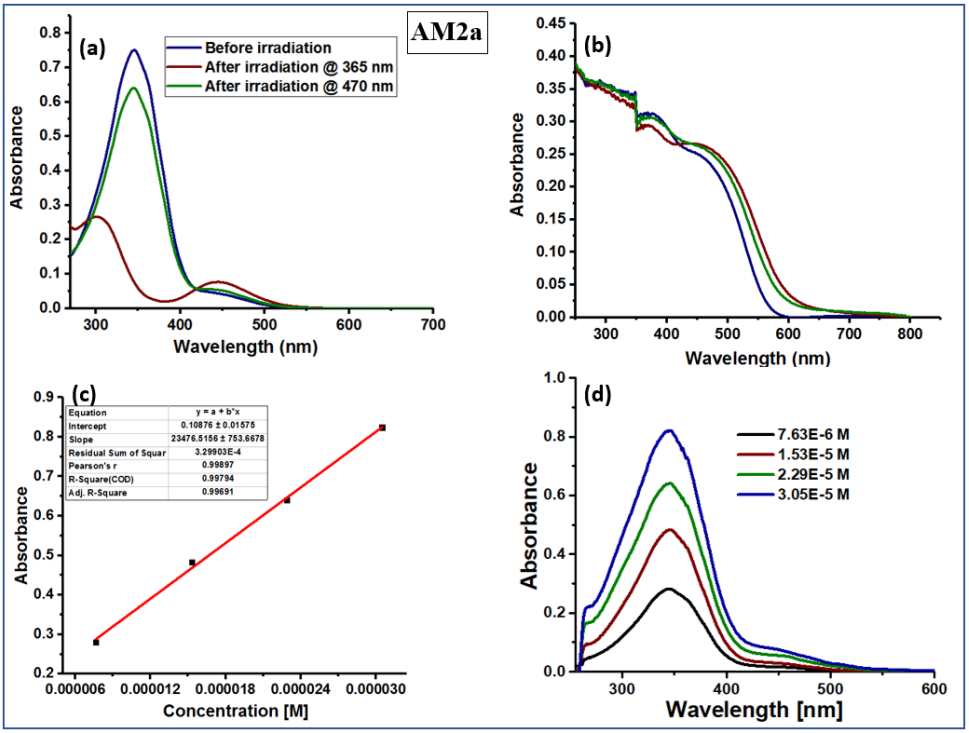

Figure S3.4. UV-Vis spectroscopic data of **AM2a**: (a) Photoswitching studies performed in DMSO (32 μM); (b) Photoswitching studies performed in KBr medium; Estimation of the molar absorption coefficient for (c) π−π* absorption maxima (d) Absorption spectra at different concentration.

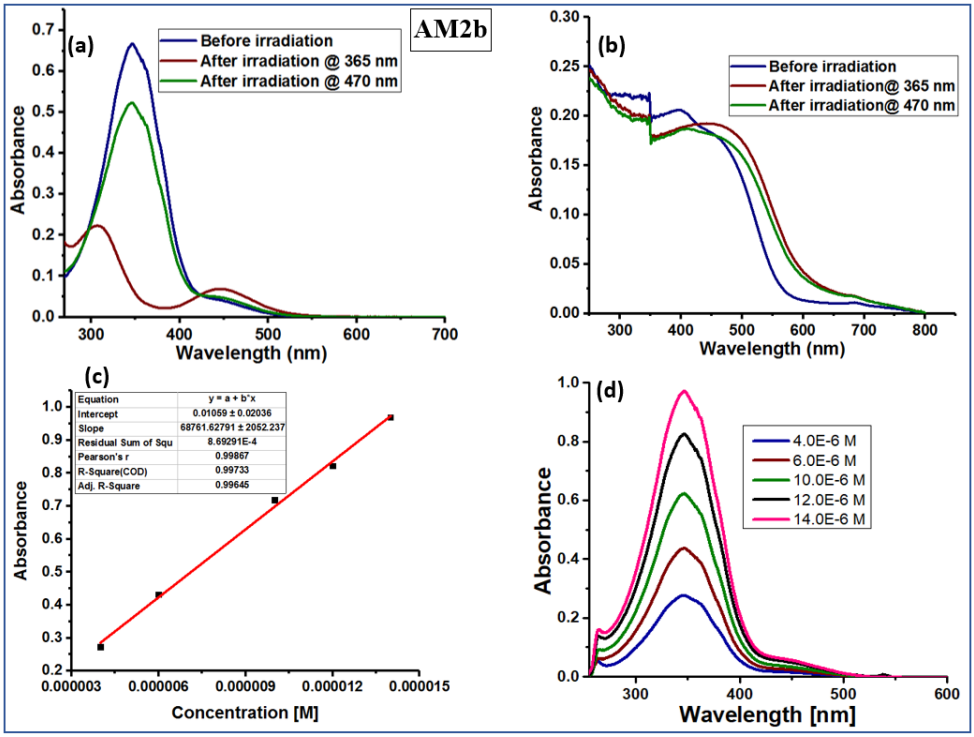

Figure S3.5. UV-Vis spectroscopic data of **AM2b**: (a) Photoswitching studies performed in DMSO (9.7 μM); (b) Photoswitching studies performed in KBr medium; Estimation of the

molar absorption coefficient for (c) π−π* absorption maxima (d) Absorption spectra at different concentration.

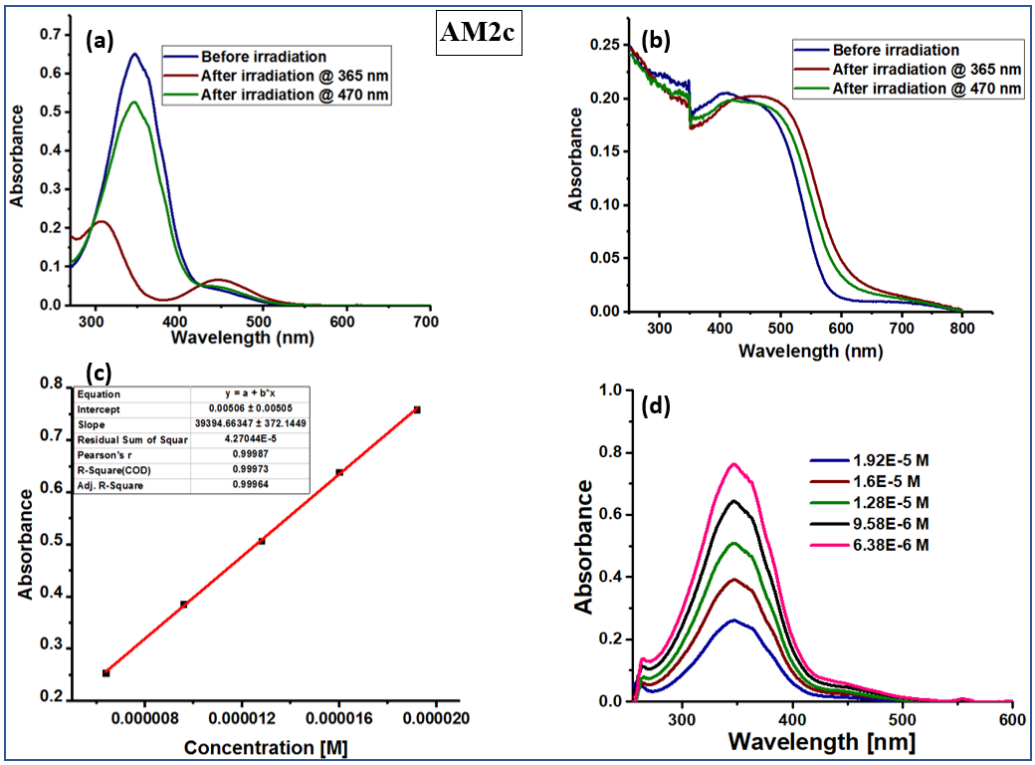

Figure S3.6. UV-Vis spectroscopic data of **AM2c**: (a) Photoswitching studies performed in DMSO (16 μM); (b) Photoswitching studies performed in KBr medium; Estimation of the molar absorption coefficient for (c) π−π* absorption maxima (d) Absorption spectra at different concentration.

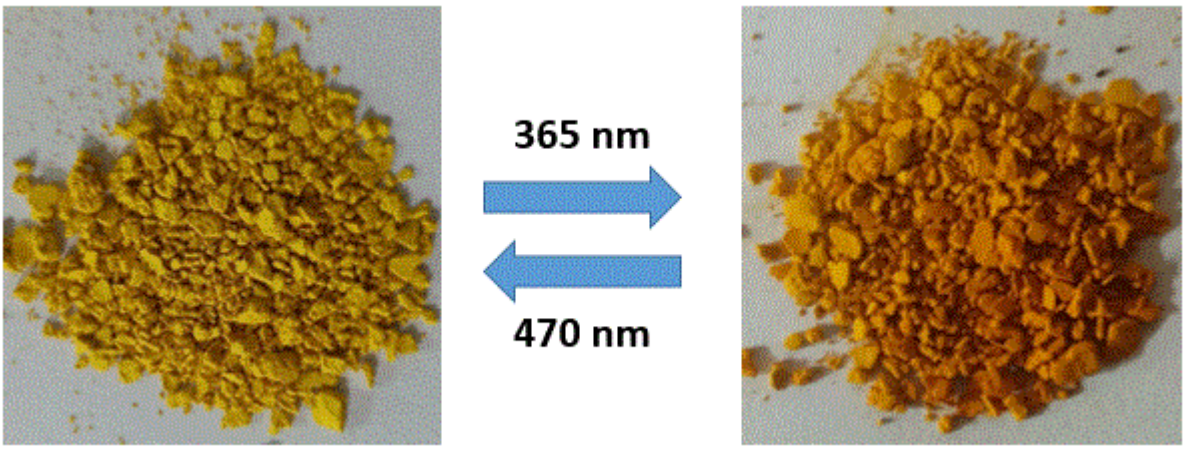

Figure S3.7. Photochromic behaviour of **AM2b**. The solid-state colour changes from yellow to light brown and *vice versa* on irradiation with 365 nm and 470 nm light, respectively.

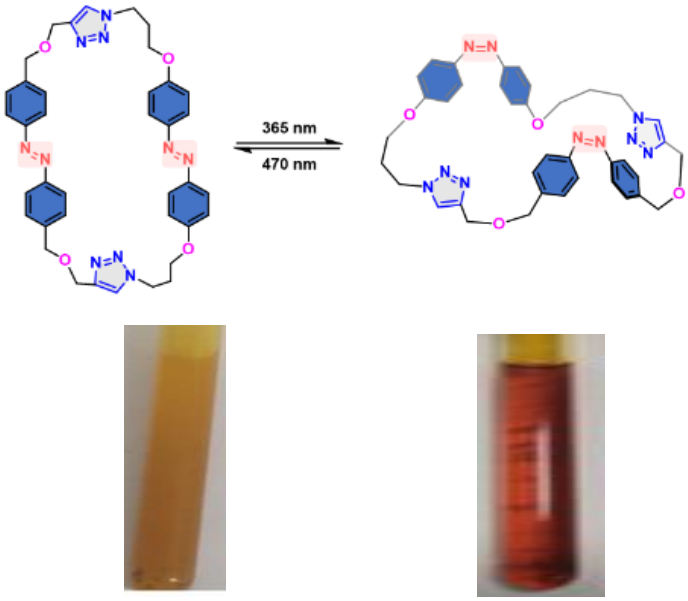

Figure S3.8. Photoisomerization of **AM2b** and enhancement in solubility accompanied by the irradiation at 365 nm (colour changes from yellow to red also observed).

Table S3.1. Absorption spectral data of the target macrocycles and estimation of at PSS composition for the forward and reverse isomerization steps.

S. No	Compound	*E*-isomer[a]		*Z*-isomer[a]				Concentration (μM)
		π–π* λ_{max},	*E-Z* PSS[b] (%*Z*)	π–π* λ_{max}	n–π* λ_{max}	$\Delta\lambda_{cis}$	*Z-E* PSS (%*E*)	
1	**AM1a**	359	86	312	446	134	91	-
2	**AM1b**	362	73	312	445	133	85	-
3	**AM1c**	363	82	313	448	135	94	-
4	**AM2a**	345	90	301	445	144	85	32
5	**AM2b**	347	90	307	445	138	78	9.7
6	**AM2c**	347	90	307	448	141	81	16

[a,b]The exact method for estimation has been followed as in the literature.[7,8] [c]470 nm wavelength; Estimation of %*E*/%*Z* conversion at PSS in solid-state and solution phases was done by UV-vis spectroscopy using the following expressions, respectively:

$$\%\ \text{conversion of } E\text{-isomer} = 1 - \frac{A(n-\pi*)\ absorption\ before\ irradiation}{A(n-\pi*)\ absorption\ after\ irradiation\ at\ 365\ nm}$$

$$\%\ \text{conversion of } E\text{-isomer} = 1 - \frac{A(\pi-\pi*)\ absorption\ after\ irradiation\ at\ 365\ nm}{A(\pi-\pi*)\ absorption\ before\ irradiation}$$

S3.2. Photoswitching stability: UV-Vis spectroscopic studies

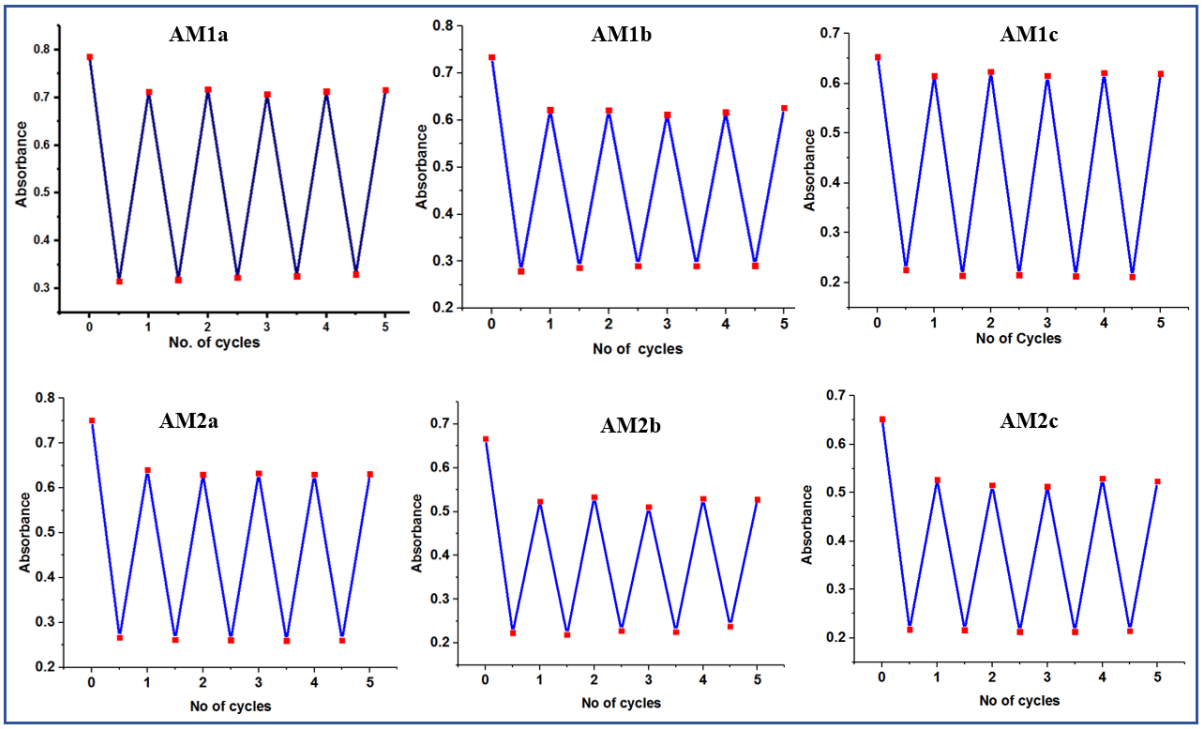

Figure S3.9. Photoswitching stability of macrocycles **(AM1a-c and AM2a-c).** For the forward isomerization step, 365 nm light was used, whereas for the reverse isomerization step, 470 nm light was used; Both the irradiation steps were repeated over five cycles. (Solvent: DMSO).

S3.3. Photoisomerization studies in AM2b using ^{1}H-NMR spectroscopy

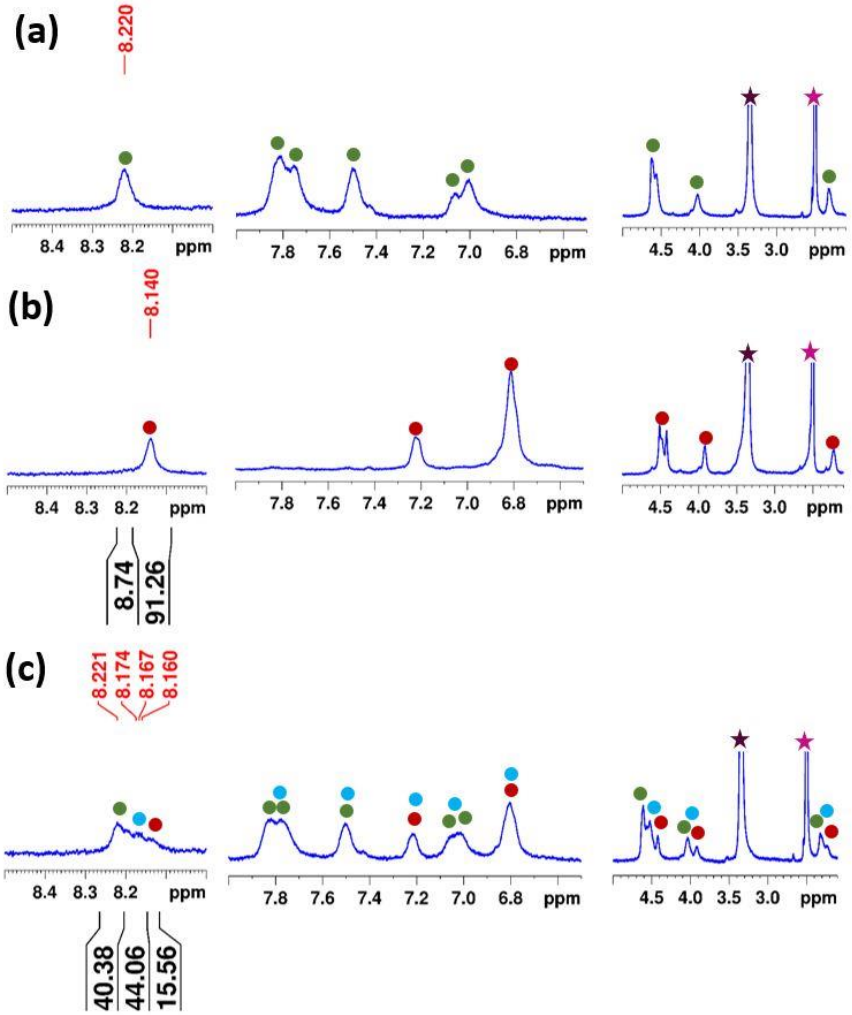

Figure S3.10. ^{1}H-NMR spectral data (DMSO-d_6, 5 mM) corresponding to (a) before irradiation; (b) after irradiation at 365 nm for 90 minutes; (d) after irradiation at 470 nm for 30 minutes. (The indicated normalized integration values of the triazole protons have been used to quantify the individual photoisomers; green, red, and cyan circles correspond to *EE*, *ZZ*, and *EZ/ZE*-isomers, respectively; The stars in purple and pink represents the signals due to water and the residual solvent in DMSO-d_6, respectively).

S4. Thermal reverse isomerization kinetics (AM1a-c and AM2a-c)

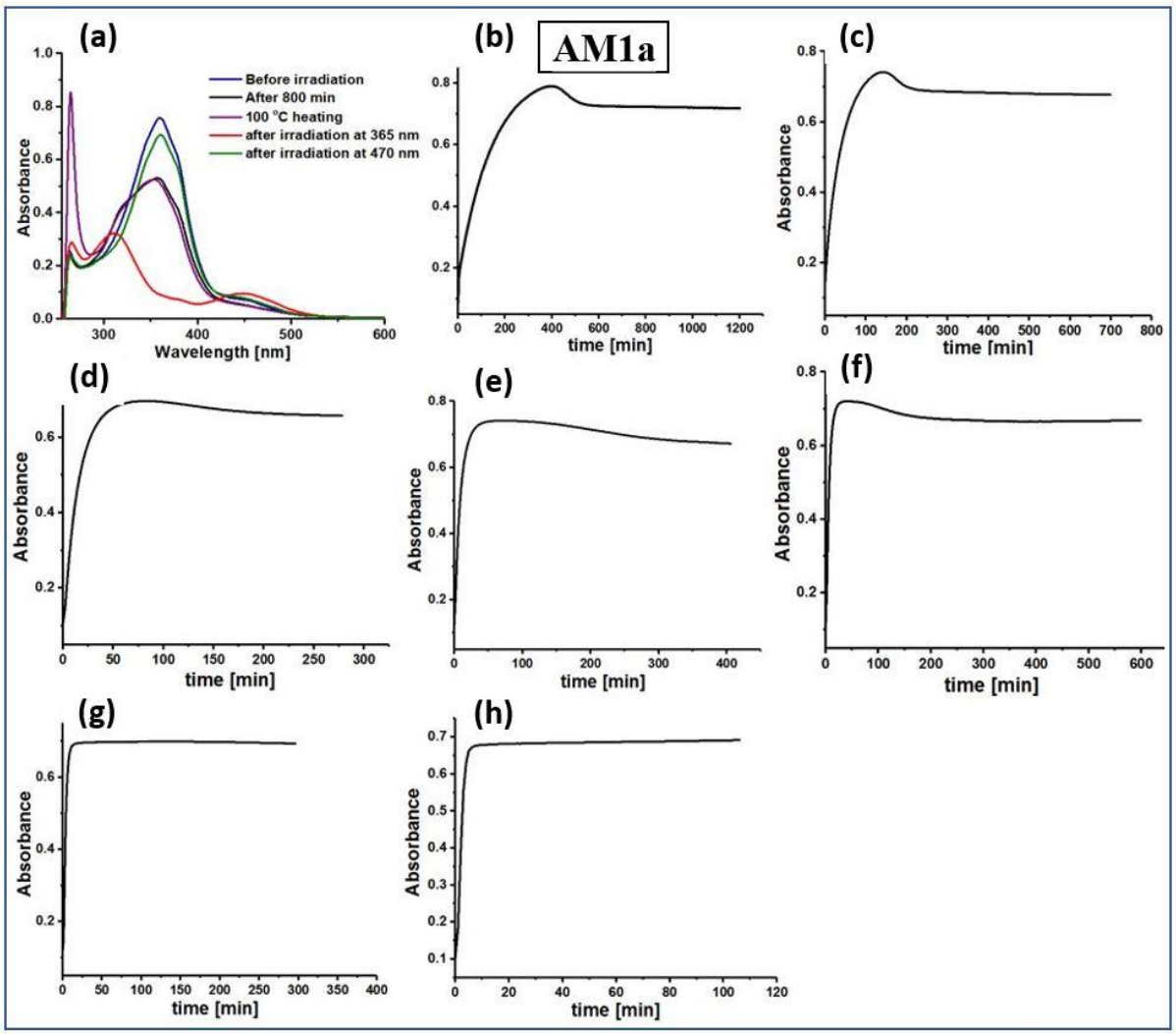

Figure S4.1. Aggregation phenomena in **AM1a**. (a) UV-Vis spectroscopic data at the indicated conditions depicting the influence of temperature and light in the making and breaking of aggregates. Variable temperature kinetics profile of **AM1a** (DMSO): at (b) 40 °C, (c) 50 °C, (d) 60 °C, (e) 65 °C, (f) 70 °C, (g) 80 °C, and (h) 90 °C; the λ_{max} corresponding to the π–π* band of the *EE*-isomer.

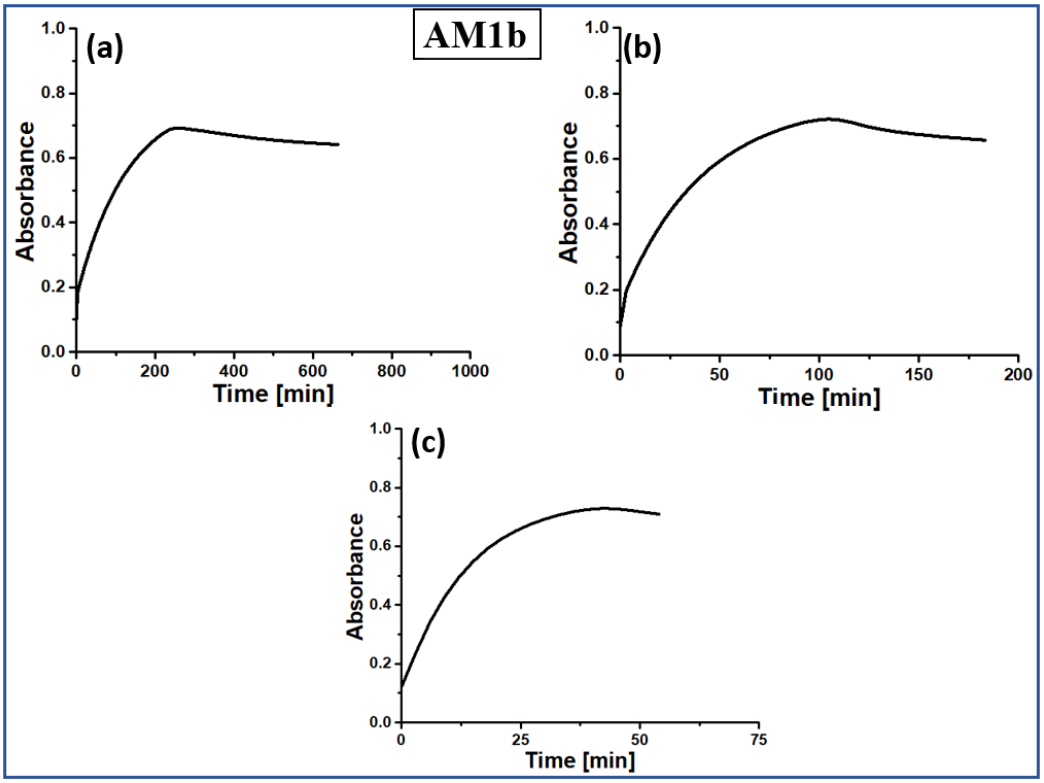

Figure S4.2. Thermal reverse isomerization kinetics plots of macrocycle **AM1b** in DMSO at (a) at 40 ± 2 °C; (b) 50 ± 2 °C and (c) 60 ± 2 °C measured using UV-Vis spectroscopy.

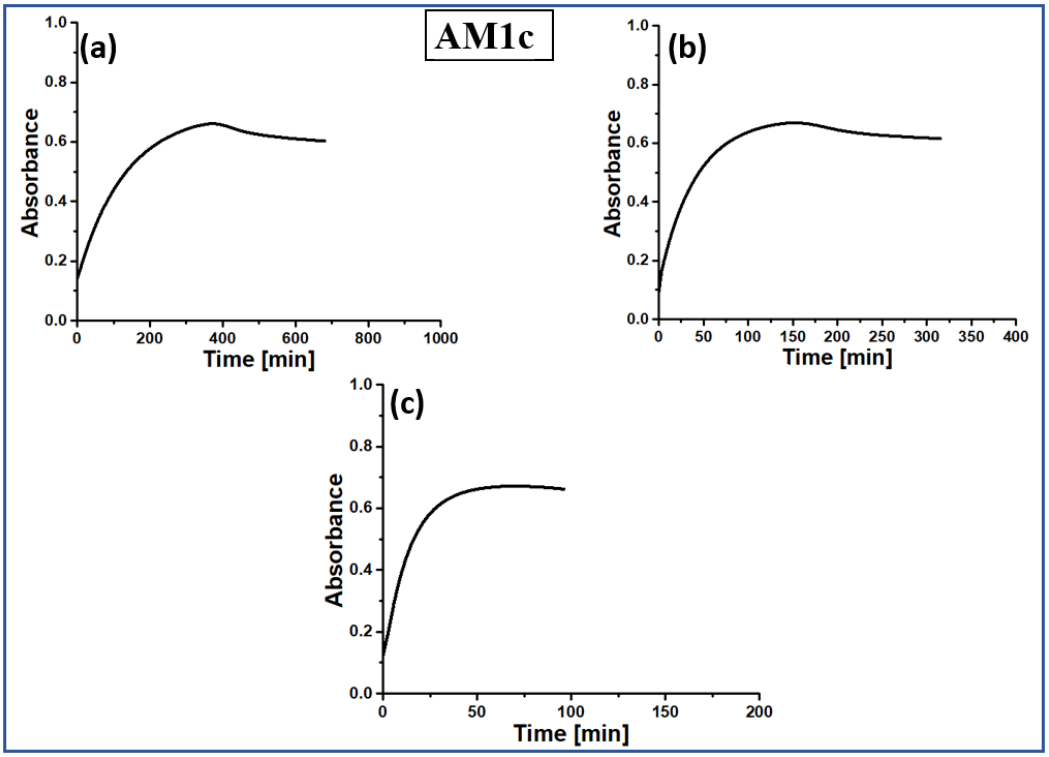

Figure S4.3. Thermal reverse isomerization kinetics plots of macrocycle **AM1c** in DMSO at (a) at 40 ± 2 °C; (b) 50 ± 2 °C and (c) 60 ± 2 °C measured using UV-Vis spectroscopy.

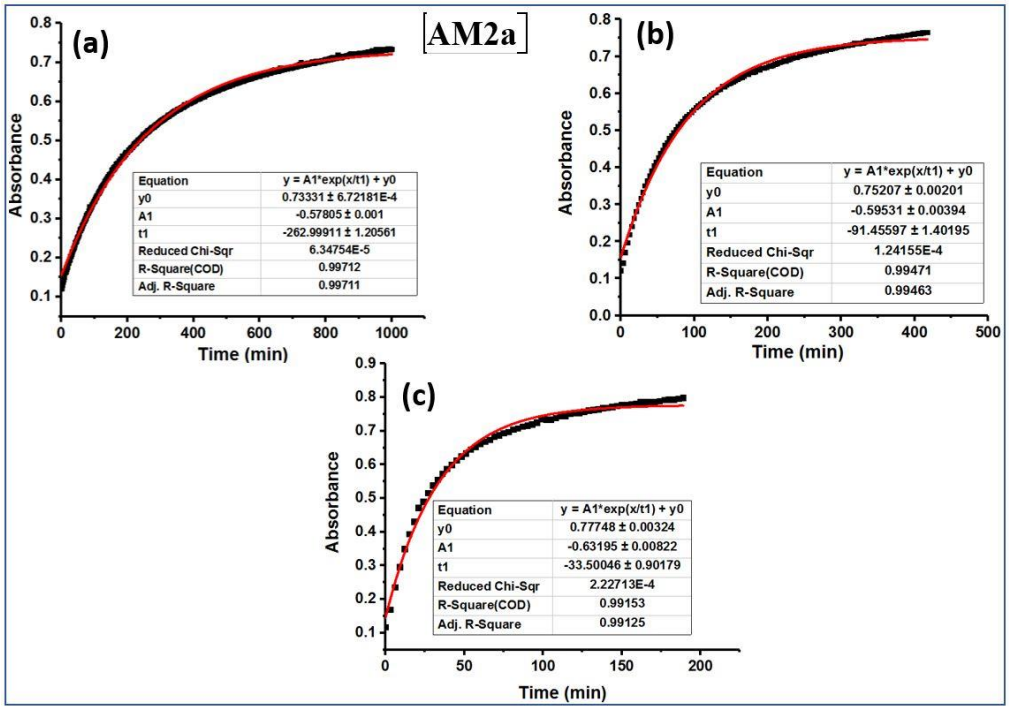

Figure S4.4. Thermal reverse isomerization kinetics plots of macrocycle **AM2a** in DMSO at (a) at 40 ± 2 ºC; (b) 50 ± 2 ºC and (c) 60 ± 2 ºC measured using UV-Vis spectroscopy.

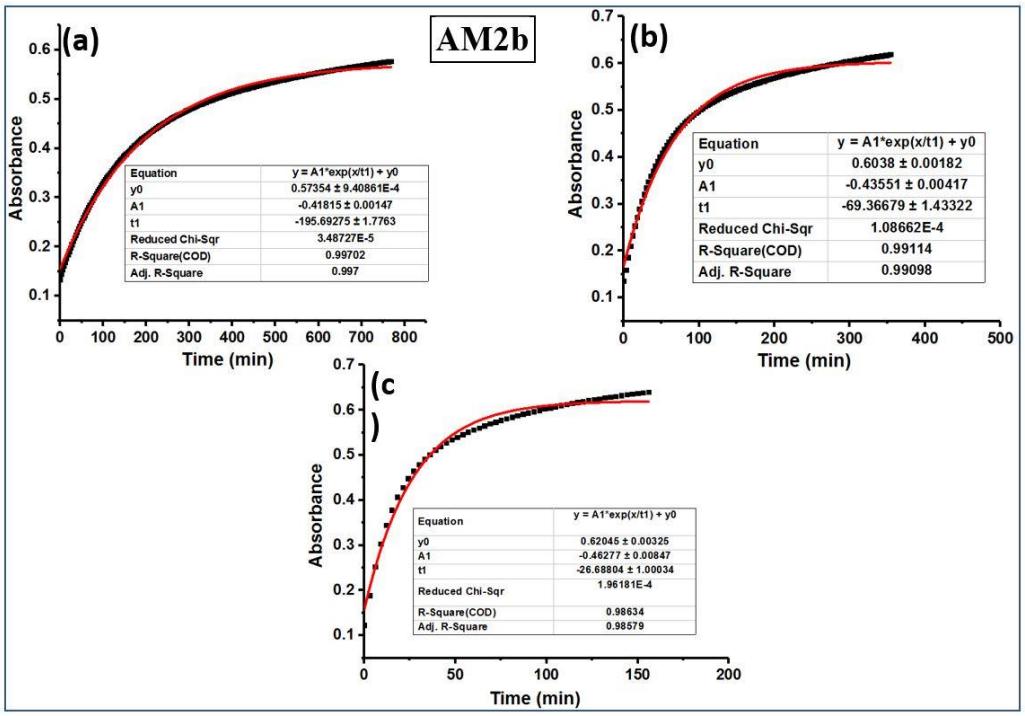

Figure S4.5. Thermal reverse isomerization kinetics plots of macrocycle **AM2b** in DMSO at (a) at 40 ± 2 ºC; (b) 50 ± 2 ºC and (c) 60 ± 2 ºC measured using UV-Vis spectroscopy.

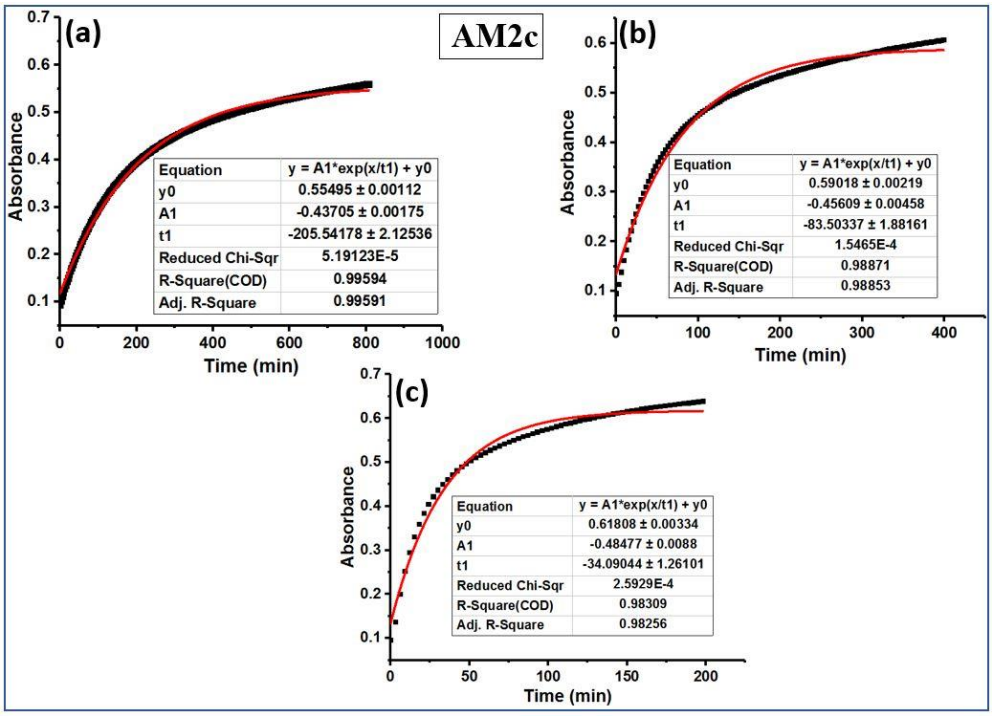

Figure S4.6. Thermal reverse isomerization kinetics plots of macrocycle **AM2c** in DMSO at (a) at 40 ± 2 ^{o}C; (b) 50 ± 2 ^{o}C and (c) 60 ± 2 ^{o}C measured using UV-Vis spectroscopy.

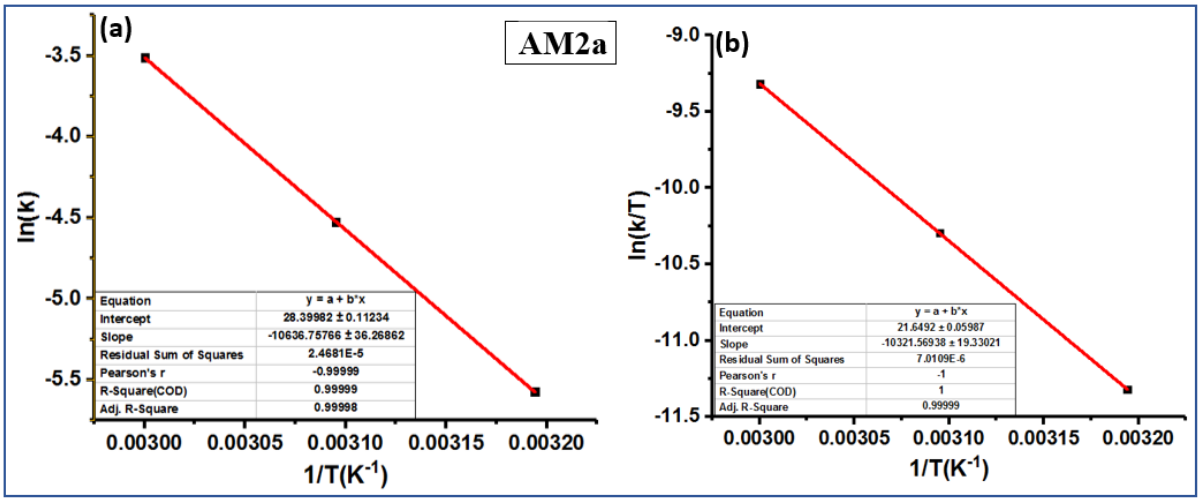

Figure S4.7. (a) Arrhenius plot and (b) Eyring plot depicting the thermal reverse isomerization of macrocycle **AM2a** in DMSO.

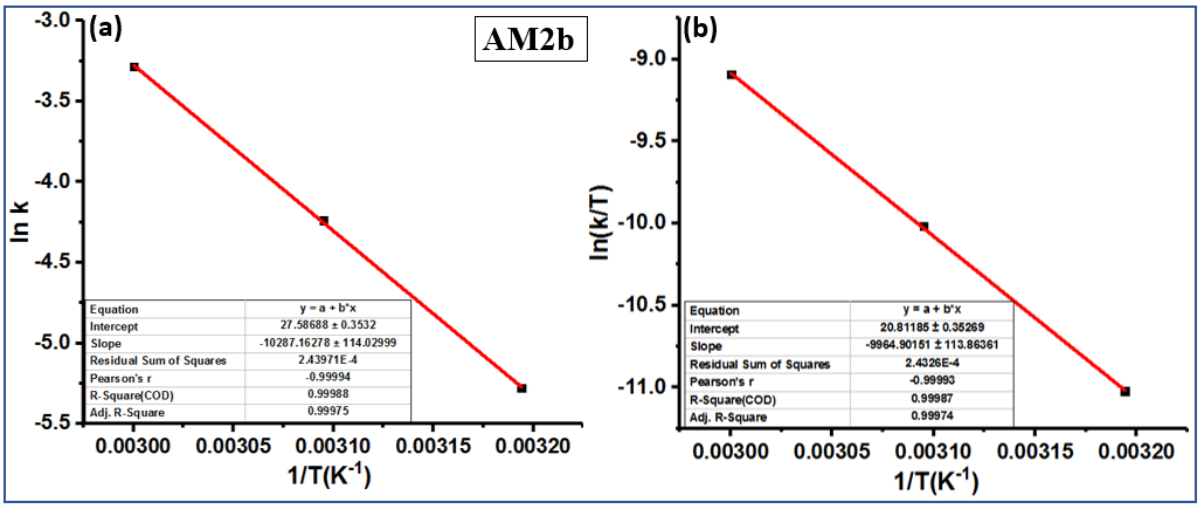

Figure S4.8. (a) Arrhenius plot and (b) Eyring plot depicting the thermal reverse isomerization of macrocycle **AM2b** in DMSO.

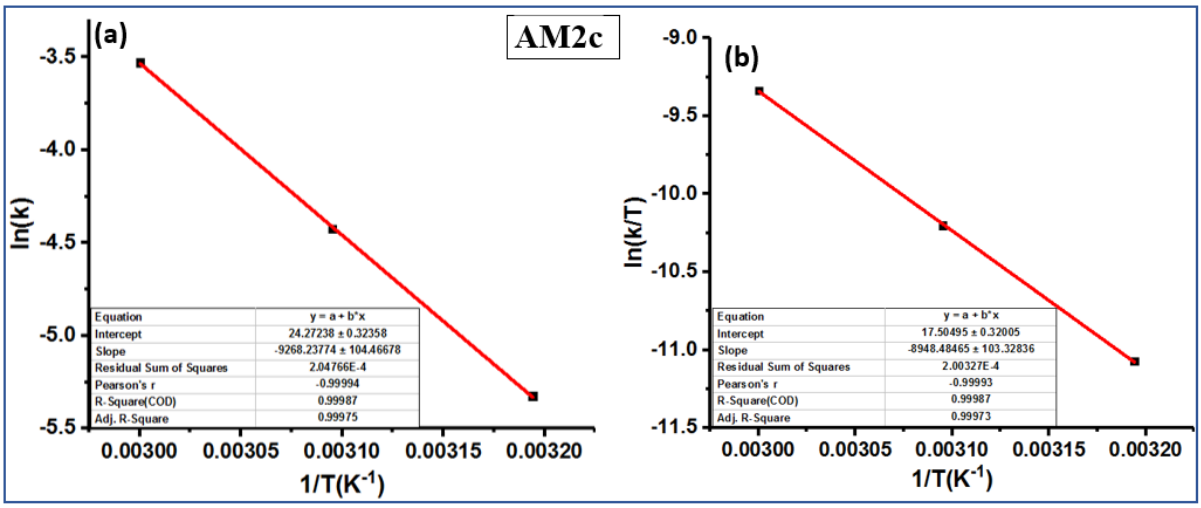

Figure S4.9. (a) Arrhenius plot and (b) Eyring plot depicting the thermal reverse isomerization of macrocycle **AM2c** in DMSO.

Table S4.1. Estimation of Kinetic and activation parameters **(AM2a-c)**

S. No	Compound	Temperature (°C)	Kinetics data		Activation Parameters				Concentration (µM)
			k (min^{-1})	$t_{½}$ (min)	E_a[a]	$\Delta H^{‡}$[a]	$\Delta S^{‡}$[b]	$\Delta G^{‡}$[a]	
1	**AM2a**	40 50 60	$3.8 \times 10^{-3} \pm 1.7 \times 10^{-5}$ $1.1 \times 10^{-2} \pm 1.7 \times 10^{-4}$ $3.0 \times 10^{-2} \pm 8.0 \times 10^{-4}$	182 63 23	88.4 ± 0.3	85.8 ± 0.1	-17.5 ± 0.5	91.0 ± 0.2	31.3
2	**AM2b**	40 50 60	$5.1 \times 10^{-3} \pm 4.6 \times 10^{-5}$ $1.4 \times 10^{-2} \pm 3.0 \times 10^{-4}$ $3.7 \times 10^{-2} \pm 1.4 \times 10^{-3}$	136 48 18	85.5 ± 0.9	82.8 ± 0.9	-24.0 ± 2.9	90.0 ± 1.3	9.7
3	**AM2c**	40 50 60	$4.9 \times 10^{-3} \pm 5.0 \times 10^{-5}$ $1.2 \times 10^{-2} \pm 2.7 \times 10^{-4}$ $2.9 \times 10^{-2} \pm 1.1 \times 10^{-3}$	142 58 24	77.0 ± 0.8	74.4 ± 0.8	-52.0 ± 2.7	90.0 ± 1.2	16.0

[a] $kJ.mol^{-1}$, [b] $J.K^{-1}mol^{-1}$

S5. Aggregation studies in macrocycles AM1a-c and AM2a-c.

S5.1 Spectroscopic studies on aggregation in macrocycle AM1a-c and AM2a-c

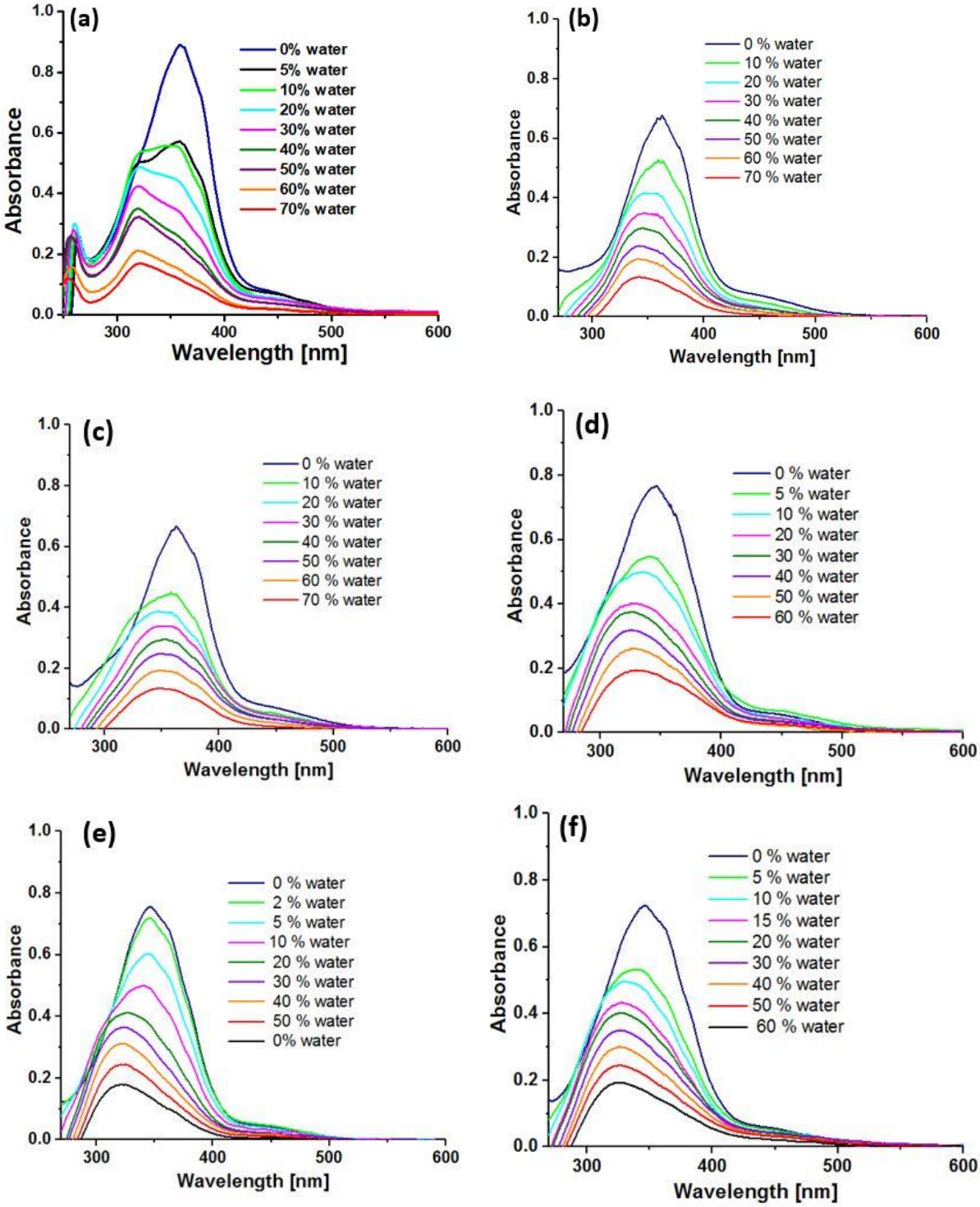

Figure S5.1. Effect of varying water content on the UV-Vis spectra of **(a-c) AM1a-c**, and **(d-f) AM2a-c** in water/DMSO solvent mixtures. The volume percentage of water in the solvent mixture is indicated in the figure.

S5.2. Aggregation studies:

We presume aggregation as one of the factors for the poor solubility. Particularly, the presence of azobenzene and triazole units in the macrocycles can influence them to aggregate through π–π stacking.[8c-f] To shed further light on the aggregation phenomena, and the light-induced disaggregation, we have performed the self-aggregation studies of all the macrocycles **AM1a-c** and **AM2a-c**. The UV-Vis spectroscopic studies have been carried out for the macrocycle solutions in DMSO (μM concentrations) before and after photoisomerization. Upon adding water into the DMSO solution of macrocycles, we observed changes and shifts in the absorption spectral features, particularly in the π–π* band of the azo group. For instance, **AM1a** in pure DMSO solvent exhibited a reasonably sharp π–π* absorption that showed a decrease in the intensity with a significant blue shift and broadening on the addition of an increasing amount of water.

A closer inspection of the spectral features indicates the appearance of two features, which we attribute to the bands due to monomer and the aggregate.[10] As the amount of water increases, the features corresponding to the aggregate form increase in intensity.

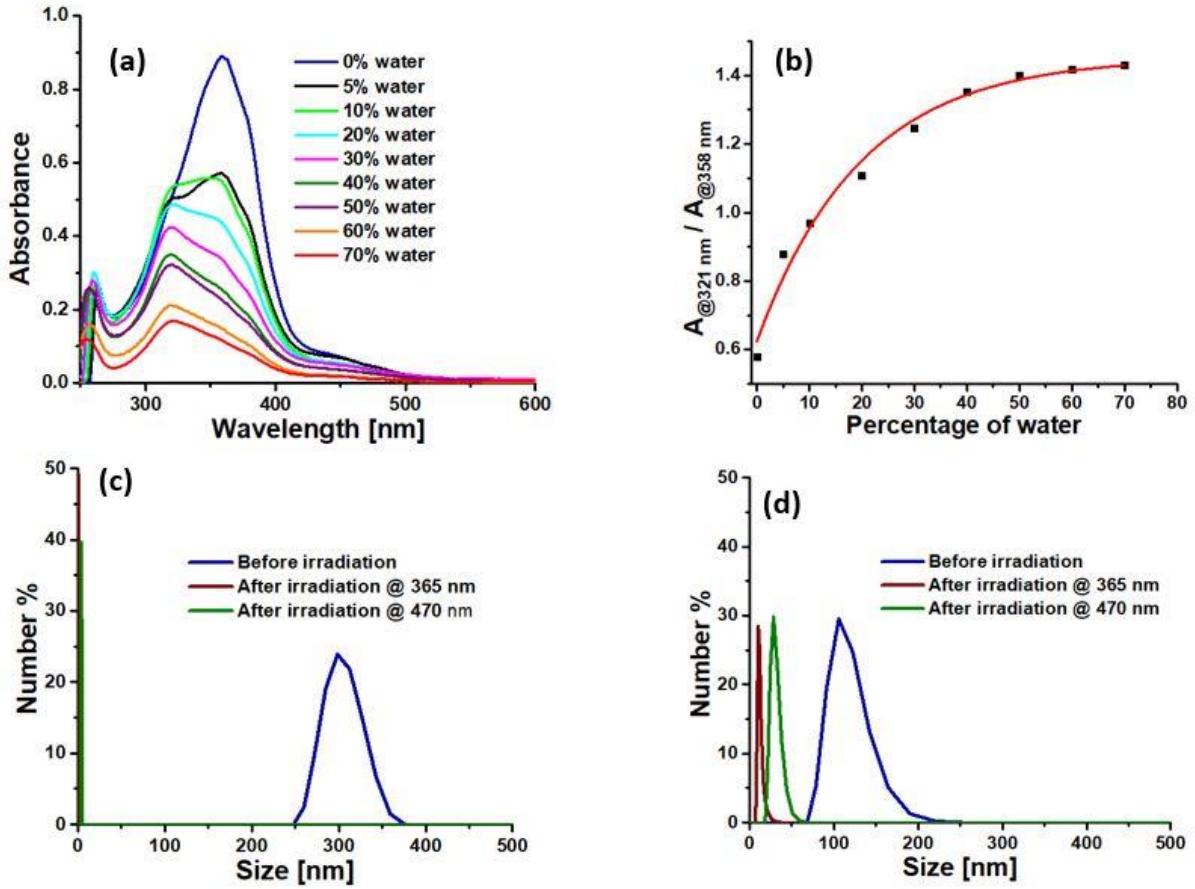

Figure S5.2. Aggregation studies on macrocycles. (a) Concentration dependence on the absorption spectra of **AM1a** in DMSO as a result of varying % of water; (b) A plot depicting exponential growth of aggregate/monomer absorption ratio of **AM1a** in DMSO with the increasing % of water; Dynamic light scattering (DLS) experiments in (c) **AM1a** (DMSO, undetermined mM concentration), and (d) **AM2b** (DMSO, 1 mM)

Again, the proximity of these two bands caused the broadness in the absorption feature. Based on these observations, and the blue shift of the absorption maxima, we assume the formation of H-aggregates.[8g] To understand the trend, we also plotted the ratio between the aggregated and the monomeric forms of **AM1a** against the percentage of water content, which revealed an exponential growth curve (Figure S5.2b). All these studies envisage the formation of aggregates of macrocycles responsible for poor solubility.

S5.3. Effect of photoisomerization and influence of temperature on aggregation:

After obtaining the preliminary evidences for aggregation, we paid our attention to obtain the effect of photoisomerization on it. In this regard, a solution of the macrocycle **AM1a** in DMSO has been subjected to dynamic light scattering (DLS) experiments, which indicate the native state (*EE*-isomer) of it exhibiting aggregation based on the average size (328.0 nm) of the molecules (Figure S5.2c). On the other hand, the irradiation at 365 nm led to the isomerization accompanied by the aggregation's breaking, which can be inferred from the smaller average size of the molecular particles (0.5 nm). Indeed, the reverse isomerization at 470 nm does not lead to an increase in the particle size (3.9 nm), indicating that thermodynamic and kinetic factors control the aggregation step. Surprisingly, when such experiments are carried out using the macrocycle **AM2b** (1.0 mM), we have observed a relatively smaller particle size in the range of 100 to 200 nm (114.7 nm), which might be responsible for better solubility (Figure S5.2d). However, the irradiation at 365 and 470 nm in alternate steps shows the breaking (11.7 nm) and a small re-aggregation (30.1 nm). Thus, the DLS experiments clearly demonstrate the light-induced *E*-*Z* and *Z*-*E* isomerization steps of the macrocycles in reversibly breaking and (slow) formation of aggregates.

Next, we attempted to understand the unusual trends in the thermal reverse isomerization kinetic profiles of **AM1a-c**. As indicated earlier, the kinetics profile of the photoswitched macrocycle **AM1a** (in DMSO) exhibits exponential growth. However, after attaining a limiting value, it displays a small exponential decay pattern (Figure S4.1.b-f in the supporting information). The primary component of the kinetics profile corresponds to the typical *Z*-*E* thermal isomerization channel of azobenzene units (growth of the *EE*-isomer), whereas the latter part of it can be correlated to the aggregation phenomenon. Notably, the variable temperature experiments confirm it. As the temperature increases, the growth component becomes faster, and consequently, the decay component or aggregation step slows down. Indeed at 80 ^{o}C and beyond (Figure S4.1.g-h in the supporting information), the second step is absent. This can also be accountable for the solubility of the macrocycles at higher temperatures, where the tendency of aggregation is reasonably hindered. To provide additional support on the aggregation behavior, we have performed further studies using scanning electron microscopic (SEM) and atomic force microscopic (AFM) techniques. The studies on **AM1a** reveal the aggregation of particles with an irregular shape and average height profiles of 500 nm (see section S5.4 supporting information).

S5.4. Morphology of AM1a: SEM and AFM studies

S5.4.1. Morphology of AM1a before irradiation

Investigation on a microscopic level (SEM and AFM studies) were carried out in DMF solvent to envision the surface morphology of **AM1a** aggregates**.** The solution of **AM1a** in DMF was drop costed on a silicon wafer and allowed to dry for 3 days in the desiccator. The presence of an extensive network of irregularly shaped particles aggregated together has been observed. The height profile of the aggregate was found to be around 500 nm in size.

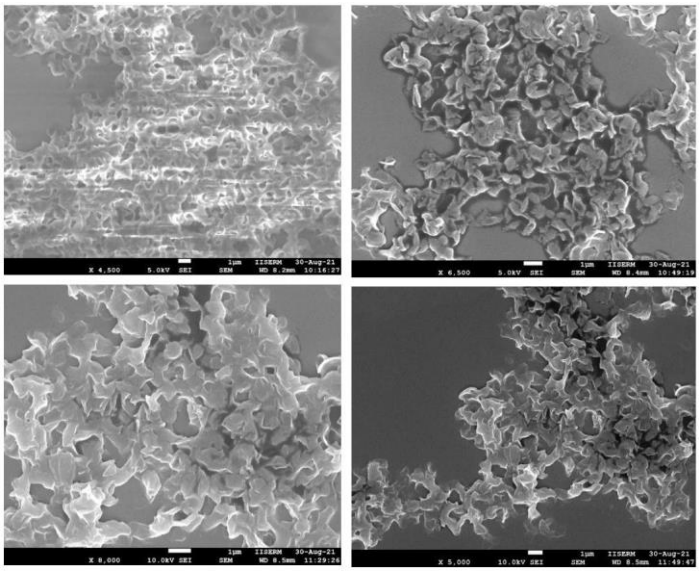

Figure S5.3 SEM images showing the morphological structure of **AM1a** aggregate in DMF solvent

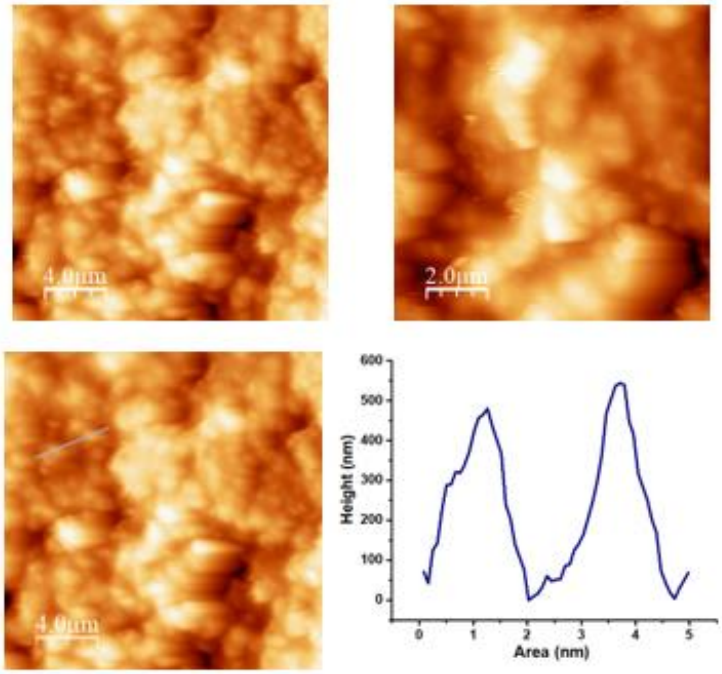

Figure S5.4. AFM images showing the morphological structure of **AM1a** aggregate in DMF solvent.

S5.4.2. Morphology of AM1a after irradiation

The solution of **AM1a** in DMF was irradiated for 20 minutes and then drop casted on a silicon wafer and allowed to dry for 3 days in the desiccator under dark. The morphological changes have been observed in the irradiated sample. The separated spherical aggregates were observed in the irradiated state showing the breaking of aggregation.

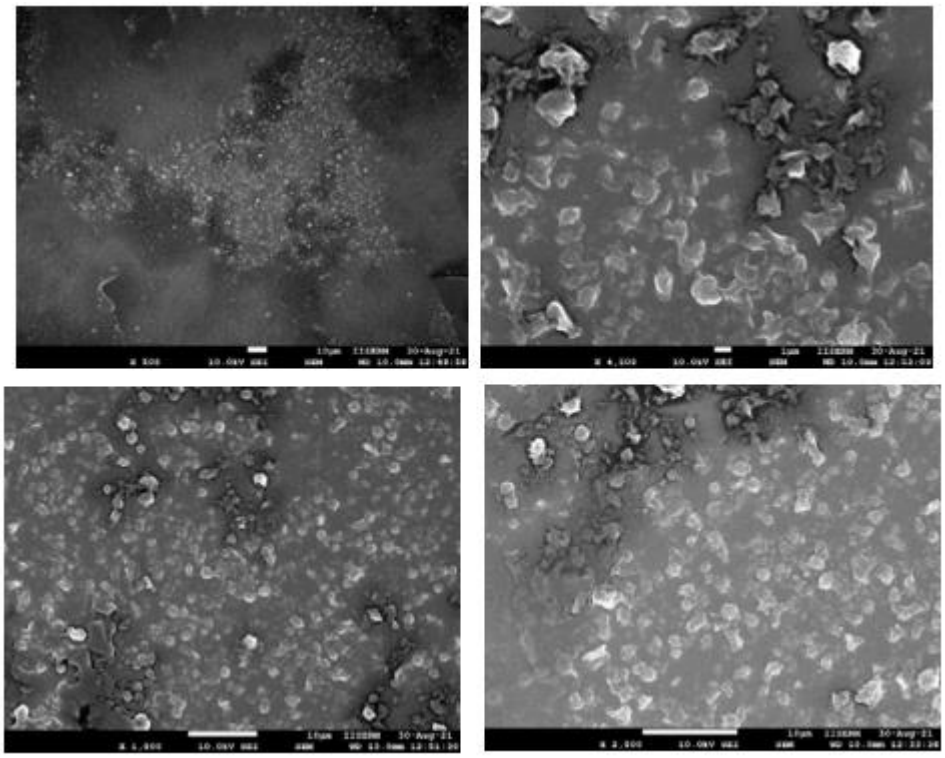

Figure S5.5. SEM images showing the morphological structure of 365 nm irradiated **AM1a** aggregate in DMF solvent.

S6. Reversible modulation of fluorescence response and control experiments

S6.1. Fluorescence titration experiments

S6.1.1 Titration experiment of pyrene Vs Macrocycle AM2b

A 20 micromolar solution of pyrene and macrocycle **AM2b** was prepared as stock solutions. In a fluorescence cuvette, 100 µL of 20 µm solution of macrocycle **AM2b** was added to a cuvette containing 1800 µL of DMSO. In the cuvette, 100 µL of 20µm solution of pyrene was added. The sample was excited at the pyrene's excitation wavelength (339 nm) and the fluorescence emission spectra were recorded. Both the excitation slit width and the emission slit width were 0.5 and 1 nm, respectively. The same sample was irradiated with 365 nm light for 3 minutes and again the spectra were recorded. The same experiment was repeated with 300 µL, 500 µL, 600 µL,700 µL, 800 µL, 1000 µL, 1200 µL, 1500 µL, 1800 µL solution of pyrene, keeping the total volume of solution 2000 µL by subsequent addition of DMSO. Other samples were also irradiated with 365 nm light for 3 minutes and again the fluorescence emission spectra were recorded. Their fluorescence spectral intensity at constant pyrene has been plotted against the increasing concentrations of macrocycle **AM2b**.

S6.1.2 Titration experiment of Macrocycle AM2b Vs pyrene

A 20 micromolar solution of pyrene and macrocycle **AM2b** were prepared as stock solutions. In a fluorescence cuvette, 100 µL of 20 µm solution of pyrene was added to a cuvette containing 1800 µL of DMSO. In the cuvette, 100 µL of 20 µm solution of macrocycle **AM2b** was added. The sample was excited at the pyrene's excitation wavelength (339 nm) and the fluorescence emission spectra were recorded. Both the excitation slit width and the emission slit width were 0.5 and 1 nm, respectively. The same sample was irradiated with 365 nm light for 3 minutes and again the spectra were recorded. The same experiment was repeated with 300 µL, 500 µL, 600 µL,700 µL, 800 µL, 1000 µL, 1200 µL, 1500 µL, 1800 µL solution of macrocycle **AM2b**, keeping the total volume of solution 2000 µL by subsequent addition of DMSO. Other samples were also irradiated with 365 nm light for 3 minutes and again the fluorescence emission spectra were recorded. Their fluorescence spectral intensity at constant concentatration of macrocycle **AM2b** has been plotted against the increasing concentrations of pyrene.

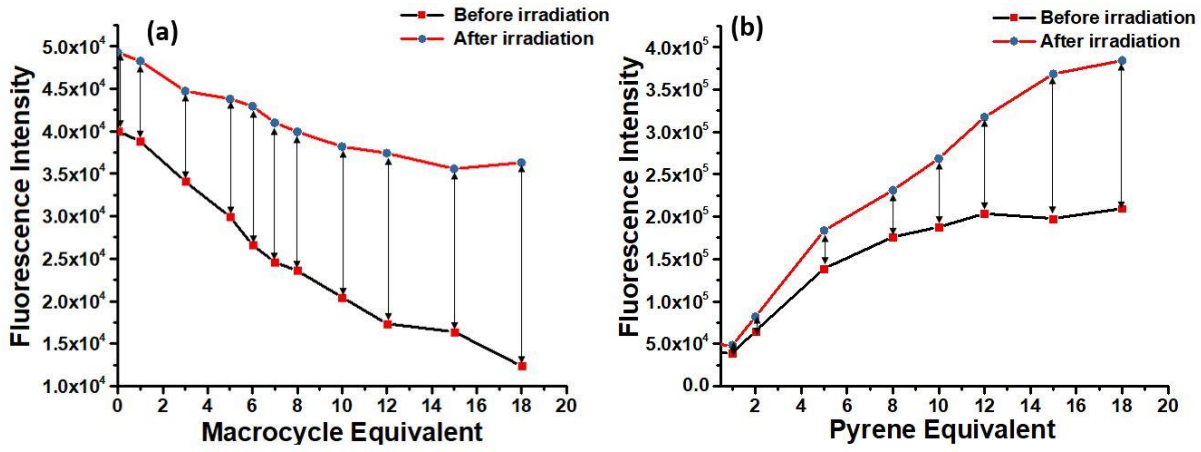

Figure S6.1. (a) Titration experiment of pyrene with increasing concentration of the macrocycle **AM2b** before irradiation (black) and after irradiation (red). (b) Titration experiment of the macrocycle **AM2b** with increasing concentration of pyrene before irradiation (black) and after irradiation (red).

S6.1.3 Titration experiment of compound 9 Vs pyrene

Similar studies as indicated in the section **S6.1.1** and **S6.1.2** have been performed with the compound **9** under similar experimental conditions. Their fluorescence spectral intensity at constant pyrene has been plotted against the increasing concentrations of the compound **9**. In a separate experiment, a reversal of the plot, i.e. at constant concentration of the compound 9 was plotted against the increasing concentaions of pyrene. In both the cases, the excitation wavelength λ_{ex} = 339 nm and emission wavelength λ_{em} = 372 nm were the same.

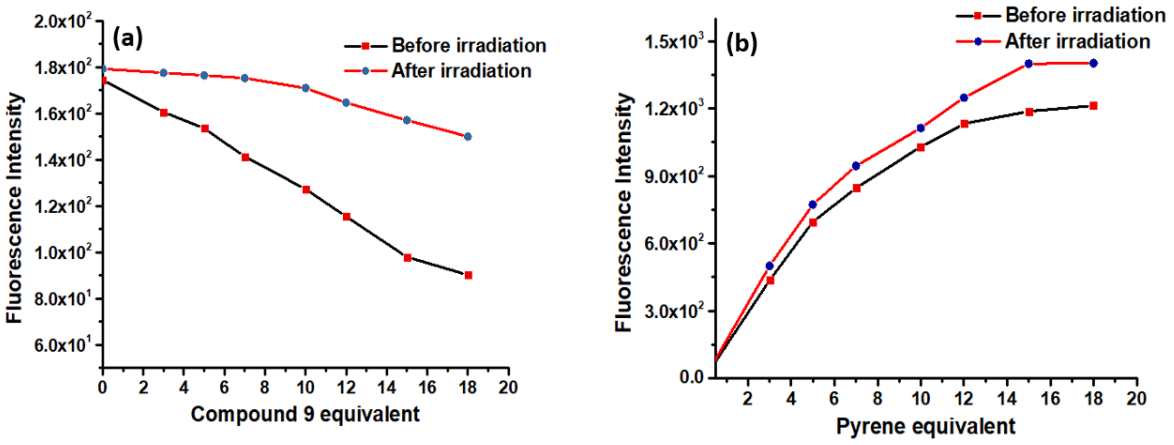

Figure S6.2. (a) Titration experiments of pyrene with increasing concentration of the compound **9** {before irradiation (black) and after irradiation (red)}. (b) Titration experiments of the compound **9** with increasing concentration of pyrene {before irradiation (black) and after irradiation (red)}.

S6.2 Benesi-Hildebrand (B-H) plot.[11b]

The binding constant or association constant, Ka indicates the binding affinity between host and guest species and can be calculated from the slope of Benesi-Hildebrand (B-H) plot.

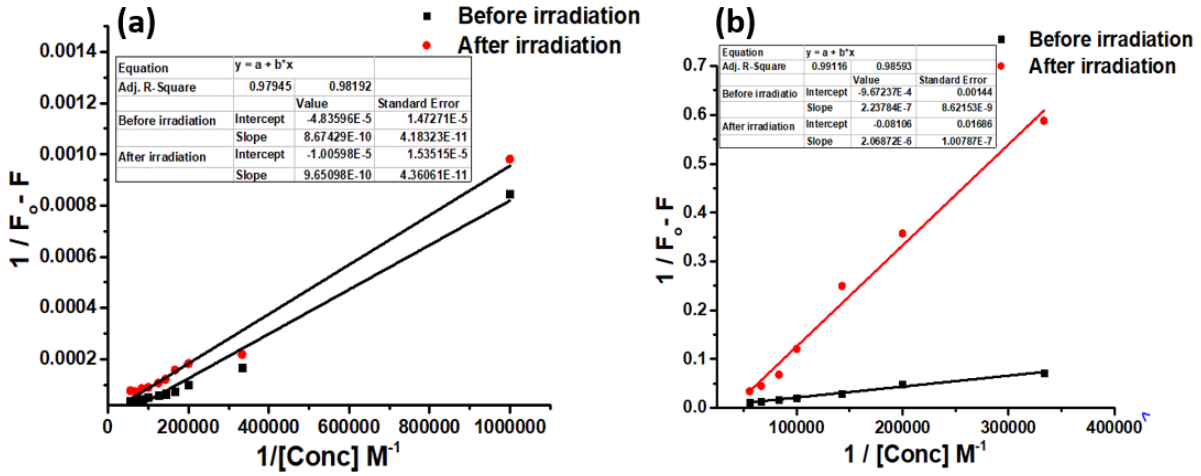

Figure S6.3. Benesi-Hilderbrand plot with increasing concentration of (a) the macrocycle **AM2b** at the constant concentration of pyrene (1 μM): before irradiation (black dot) and after irradiation (red dot). (The association constant K_a was estimated to be 4.2 x 10^4 ± 2.1 x 10^3 M^{-1} and 7.6 x 10^4 ± 3.4 x 10^3 M^{-1}, before and after irradiation, respectively indicating a strong quenching in the native state of the macrocycle.); (b) the compound **9** at the constant concentration of pyrene (1 μM): before irradiation (black dot) and after irradiation (red dot). (The association constant K_a was estimated to be 5.3 x 10^4 ± 2.0 x 10^3 M^{-1} and 1.6 x 10^4 ± 8.1 x 10^2 M^{-1}, before and after irradiation)

The B-H equation (3) used in this work is given below:

$$\frac{1}{F_x - F_O} = \frac{1}{K_a\,[M](F_{max} - F_O)} + \frac{1}{(F_{maz} - F_O)}$$

where, F_{max}, F_x and F_0 represent the fluorescence intensity of host in the presence of guest at saturation, guest at intermediate concentration and of free host respectively.

K_a is the binding constant or association constant, [M] is the concentration of guest.

S6.3 Stern-Volmer plot [11a]

Using the experimental data corresponding to figure S10.1(a), Stern-Volmer plot has been made by fitting the F_o/F against the concentration of pyrene. (F_o = fluorescence intensity in the absence of quencher; F = fluorescence intensity in the presence of quencher)

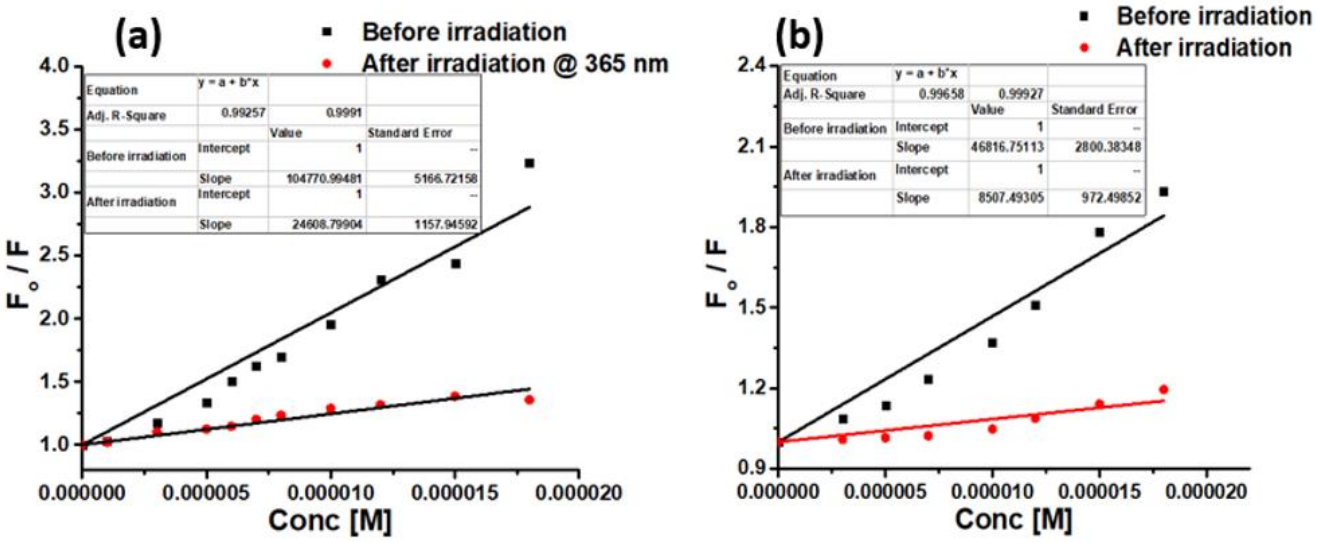

Figure S6.4. Stern-Volmer plot with increasing concentration of (a) the macrocycle **AM2b** at the constant concentration of pyrene (1 μM): before irradiation (black dot) and after irradiation (red dot). (The Stern-Volmer constant K_{sv} was estimated to be 1.0 X 10^5 M^{-1} ± 5.2 x 10^3 and 2.5 X 10^4 ± 1.2 x 10^3 M^{-1}, before and after irradiation, respectively indicating a strong quenching in the native state of the macrocycle.); (b) the compound **9** at the constant concentration of pyrene (1 μM): before irradiation (black dot) and after irradiation (red dot). (The Stern-Volmer constant K_{sv} was estimated to be 4.7 x 10^4 ± 2.8 x 10^3 M^{-1} and 8.5 x 10^3 ± 9.7 x 10^2 M^{-1}, before and after irradiation, respectively indicating a strong quenching in the native state of the compound **9**.)

The relative fluorescence intensity in the absence of quenchers (F_o) can be written as

$$F_o = \frac{k_f F^*}{(k_f + k_o)} = \frac{k_f}{k_f + k_o} = k_f \tau_o$$

When quenchers are present in a concentration of [Q] the equation modifies to

$$F = \frac{k_f}{k_f + k_o + k_+ [Q]} = k_f \tau$$

$$\frac{F_o}{F} = \frac{\tau_o}{\tau} = 1 + k_+ \tau_o [Q] = 1 + K_{SV} [Q]$$

Where K_{SV} is the Stern–Volmer constant

S6.4. Job's Plot

A 20 micromolar solution of pyrene and macrocycle **AM2b** was prepared as stock solutions in DMSO solvent. From this two stock solutions, eleven new solutions were made comprising of the ratio 0:10, 1:9, 2:8, 3:7, 4:6, 5:5, 6:4, 7:3, 8:2, 9:1, 10:1 (pyrene:**AM2b)**. The prepared solutions were allowed to stand for 2 days for maximum interaction. The absorption spectra were recorded for each sample before irradiation and after irradiation for 3 min with 365 nm light.. The absorbance vs. molefraction of pyrene on the x-axis were plotted.

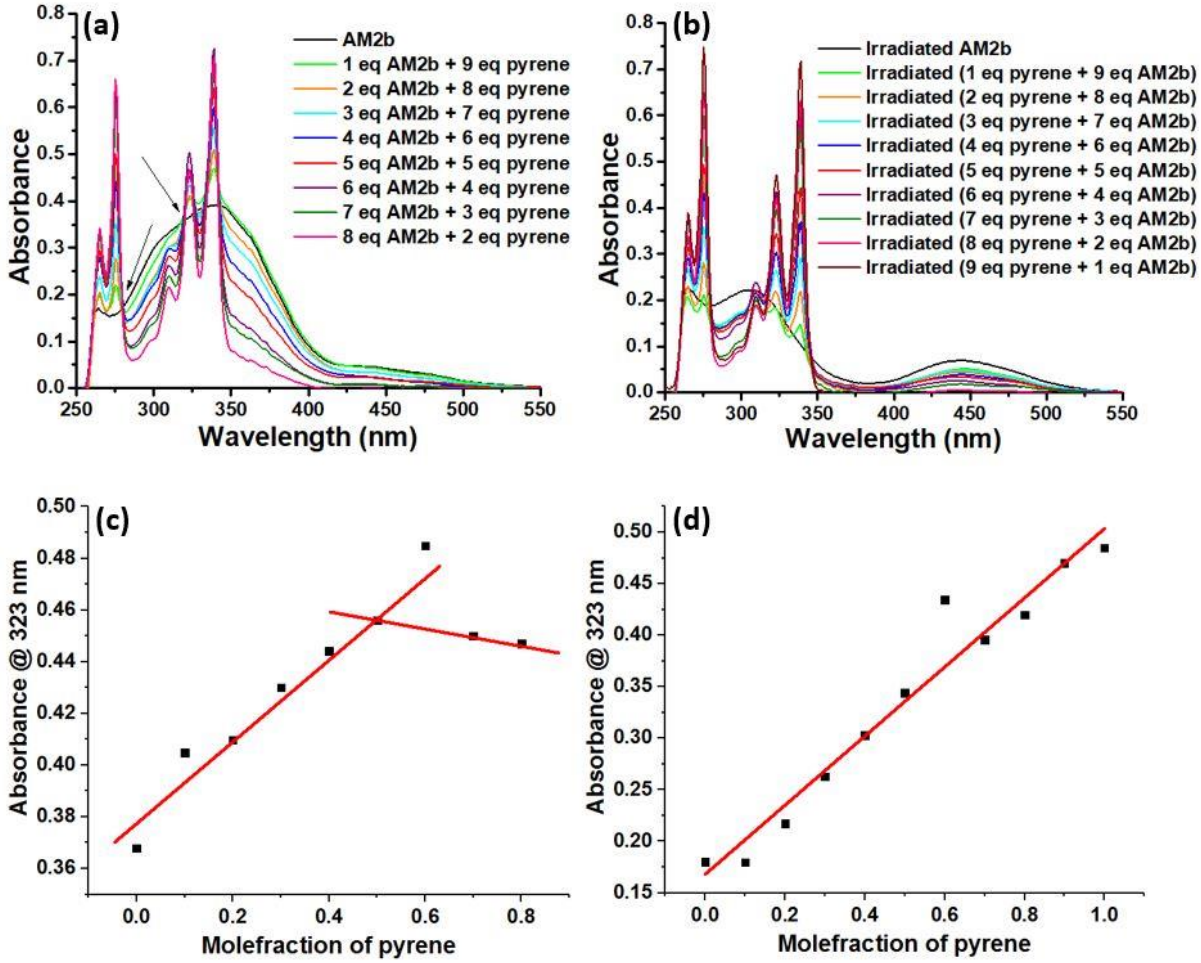

Figure S6.5. Absorption spectral data corresponding to the mixture of **AM2b** and pyrene at different mole fractions to determine their stoichiometry of binding: (a) before irradiation and (b) after irradiation; The corresponding Job's plot based on the absorbance changes at 323 nm: (c) before irradiation (depicting 1:1 stoichiometry), and (d) after irradiation at 365 nm.

S6.5 Titration experiment of *ZZ*-AM2b vs pyrene using ^{1}H-NMR spectroscopy

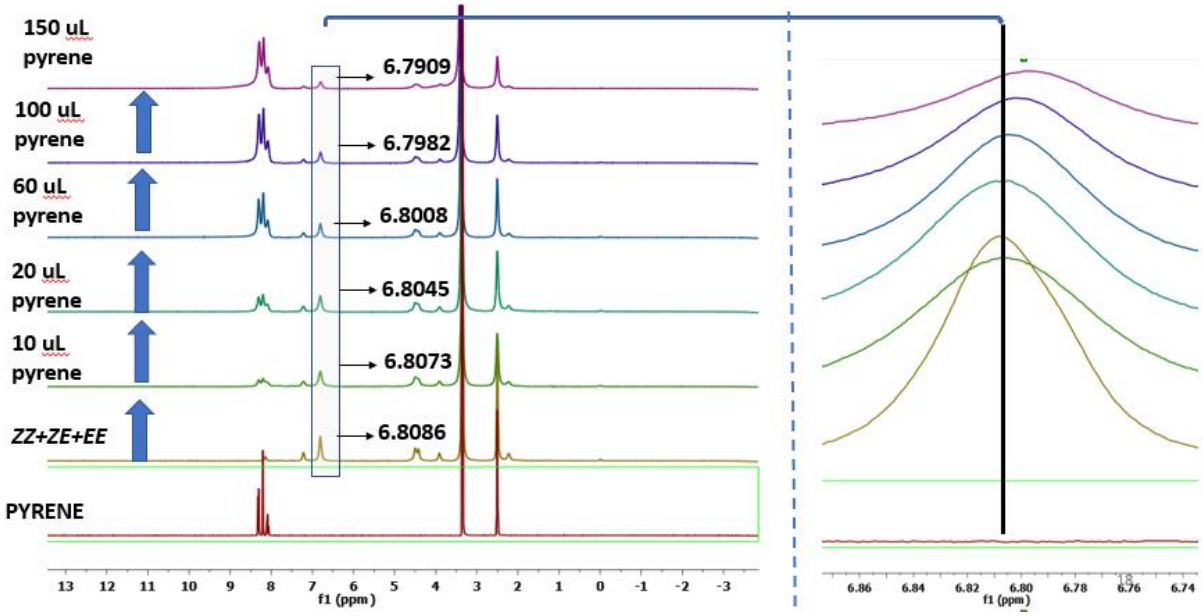

Figure S6.6 ^{1}H-NMR experiment depicting the shifts in *ZZ*-**AM2b** upon titration with the increasing concentration of pyrene {Concentrations: 6 mM **AM2b** in DMSO-[d6]}.

S6.6 Wide-angle X-ray scattering (WAXS) data

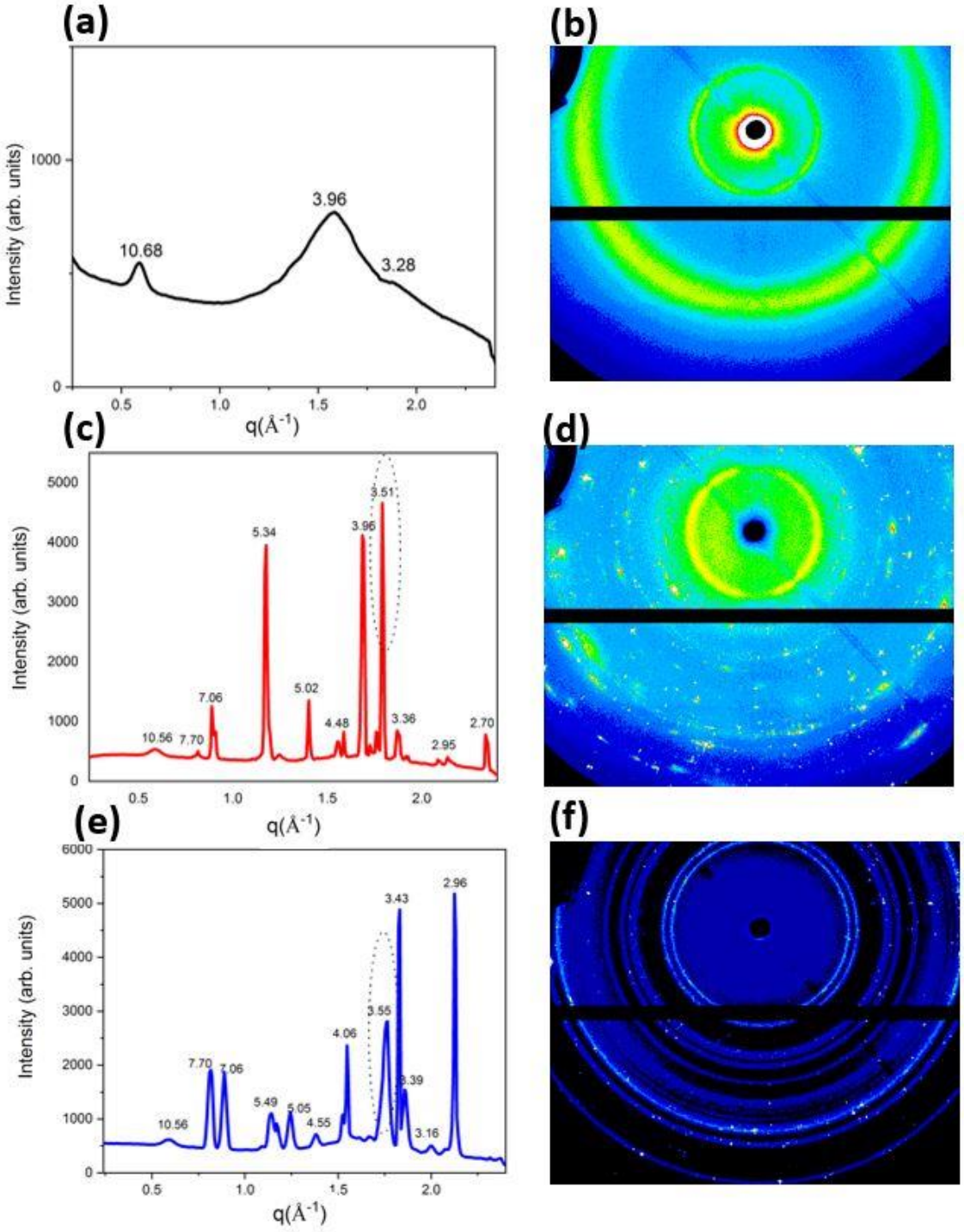

Figure S6.7. X-ray diffraction data depicting the involvement of π–π stacking between the pyrene and the azomacrocycle **AM2b**. The 1D XRD pattern through wide-angle X-ray scattering (WAXS) of (a) **AM2b**, (c) pyrene, and (e) their homogeneously ground 1:1 mixture as; The corresponding 2D XRD pattern of (b) **AM2b**, (d) pyrene, and (f) their homogeneously ground 1:1 mixture. The peaks corresponding to π–π stacking in pyrene and the mixture are indicated in the plots "c" and "e".

S6.7 Fluorescence response of pyrene in the presence of macrocycle (*EE*-AM2b and *ZZ*-AM2b)

Stock solutions of 20 micromolar concentrations of pyrene and **AM2b** were prepared in DMSO solvent. In a fluorescence cuvette, 1 ml each of 20 micromolar solutions of pyrene and macrocycle **AM2b** in DMSO were taken and mixed well. The fluorescence response of this 1:1 mixture in DMSO has been recorded at an excitation wavelength of 339 nm.Then the kinetics of the fluoresence response has been carried out at room temperature. Similarly, in yet another experiment, 1 ml of 20 micromolar solutions of **AM2b** was irradiated for 15 min at 365 nm in a fluorescence cuvette, and 1 ml of 20 micromolar solutions of pyrene was added to it. The mixture was mixed well, and fluorescence response was followed as a function of time. In both the experiments, the excitation slit width, and the emission slit width were kept at 2.5 nm. The results were plotted as fluorescence intensity on the y-axis against time on the x-axis. (**Figure S6.8**).

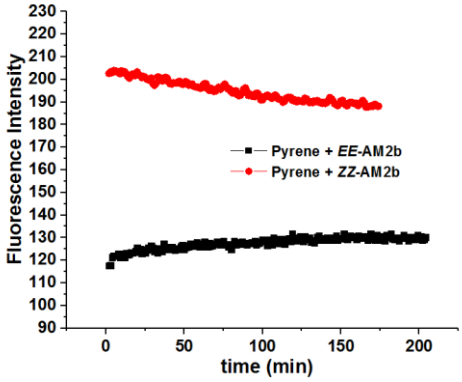

Figure S6.8. Fluorescence response as a function of time in pyrene in the presence of macrocycle **AM2b** in native state (black) and photoswitched state (red)

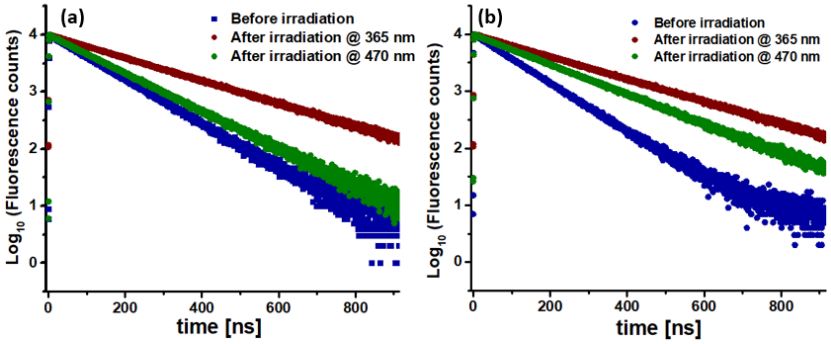

Figure S6.9 Plots depicting fluorescence lifetime decay traces of pyrene in DMSO (10 μM): (a) without macrocycle (b) with macrocycle **AM2b** (10 μM, 1:1 ratio) (blue trace – before irradiation; brown trace – after irradiation at 365 nm for 15 min; green trace – after irradiation at 470 nm for 15 min.) {Lifetimes: before irradiation: (i) Pyrene = 109 ns, (ii) Pyrene + **AM2b** = 100 ns; after irradiation at 365 nm: (i) Pyrene = 195 ns, (ii) Pyrene + **AM2b** = 196 ns; after irradiation at 470 nm: (i) Pyrene = 127 ns, (ii) Pyrene + **AM2b** = 156 ns}

S6.8 Titration experiment of pyrene with and without macrocycle Vs TBAC

A 4 millimolar solution of TBAC was prepared as stock solution in DMSO solvent. In a fluorescence cuvette, 2 ml 10 micromolar solution of 1:1 pyrene and macrocycle **AM2b** in DMSO was taken. The 1:1 solution was excited at the pyrene's excitation wavelength (339 nm) and the fluorescence emission spectra were recorded. TBAC from a stock solution has been added to it in small portions (5 μL, 10 μL, 15 μL, 20 μL, 25 μL, 30 μL, 40 μL, 50 μL, 70 μL, 80 μL). After each addition, fluorescence spectrum was immediately recorded. Similarly, in another fluorescence cuvette, 2 ml 10 micromolar solution of 1:1 pyrene and macrocycle **AM2b** in DMSO was taken and the sample was irradiated with 365 nm light for 15 minutes and the spectra were recorded at the pyrene's excitation wavelength (339 nm). Similarly, TBAC from stock solution has been added to it in small portion (5 μL, 10 μL, 15 μL, 20 μL, 25 μL, 30 μL, 40 μL, 50 μL, 70 μL, 80 μL). After each addition, fluorescence emission spectrum was immediately recorded. Both the excitation slit width and the emission slit width were 0.5 and 1 nm, respectively for both the sets of experiment. The fluorescence intensity on y axis vs. TBAC equivalence on the x-axis.

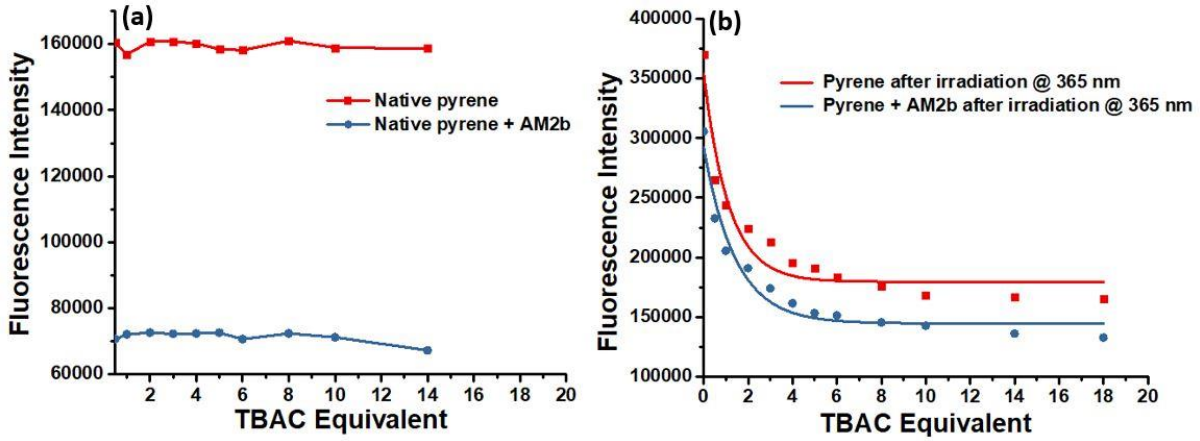

Figure S6.10. Titration experiment of pyrene (a) without (red) and with the macrocycle **AM2b** (blue) in the native state (no irradiation), and (b) without (red) and with the macrocycle **AM2b** (blue) in the photoirradiated state (after irradiation at 365 nm for 15 min).

S6.9 Titration experiment of *ZZ*-AM2b vs TBAC using ^{1}H-NMR spectroscopy

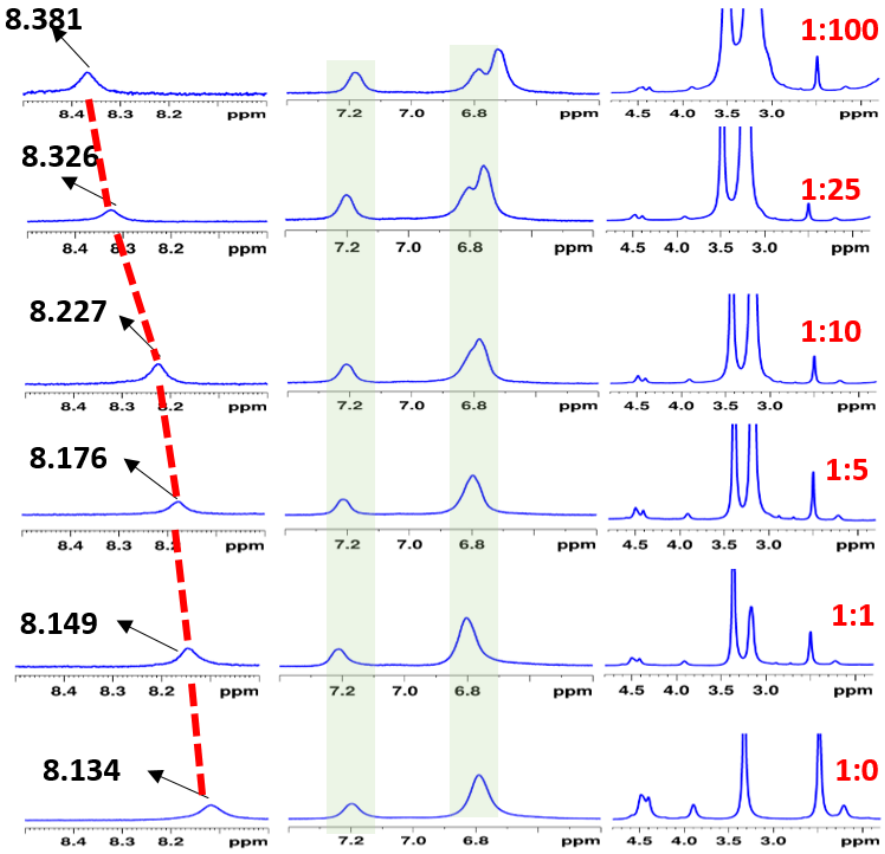

Figure S6.11. ^{1}H-NMR experiment depicting the shifts in *ZZ*-**AM2b** upon titration with TBAC with the stoichiometric ratios (**AM2b**:**TBAC**) as follows (bottom to top): 1:0; 1:1; 1:5; 1:10; 1:25 1:100. [Concentrations: **AM2a** -7 mM in DMSO-d_6].

S7. Isothermal Titration Calorimetry (ITC)

Preferential binding of the Tripodal Triazole linked Azoarenes (Azo-M5/Macrocycle) with TBAC over pyrene is measured using Isothermal Titration Calorimetry (ITC). This approach can help us to determine the dissociation constant (K_d), the number of binding sites (N), and Thermodynamic parameters i.e., ΔH, ΔS, ΔG and). The experiment was carried out by MicroCal PEAQ-ITC200 (Malvern) at 293.15K, by titrating the ligand (TBAC) and the substrate (Tripodal Triazole linked Azoarenes, Catalyst) (0.73 mM) (AM2b), wherein the ligand (TBAC) (7.33 mM) was kept in the syringe (Volume = 40 µl) and the substrate (native as well as in photo-switched state) was filled in the cell (Volume = 280 µl) (AM2b, 0.73 mM). The ligand (TBAC) was injected through an automated injector in the volume of 2 ul each for a duration of 4 seconds. Total 20 (1+19) injections were carried out, with an interval of 150 seconds between two injections (First injection after 60 sec and then subsequent injections at the interval of 150 sec). To assure proper mixing of the ligand and the substrate the mixing speed was kept at 750 rpm. Blank experiment was also carried out where ligand (TBAC) was made to interact with the solvent only (DMSO) and the obtained curve was subtracted from the sample curve. To check for the preferential binding of macrocycle with TBAC as compared to pyrene, the mixture of pyrene and macrocycle is kept in the cell and titrated with TBAC. To observe the change in conformation from EE to ZZ form and thus preferential binding of TBAC by replacing pyrene, the mixture of the macrocycle (**AM2b**) and pyrene is irradiated (photoswitching) and then titrated with TBAC. For this, a control experiment is carried out where pyrene is titrated with TBAC. Post subtraction the fitting of the curve was carried out to determine the various parameters and were carried out for the native and the photo-switched state. In order to check the binding affinity of the chloride ion with the photo-switched state, the native catalyst is exposed to UV light (365 nm) for a duration of 30 min, prior to start of the experiment.

S8. Computational Data

To gain more insights into the encapsulation of pyrene with macrocycle, quantum chemical calculations have been performed for **AM2b**. Both *EE* and *ZZ* geometries have been optimized in their lowest energy structures on the potential energy using density functional M062X[12]/6-311G(d,p)[13] level of theory. Frequency calculations have confirmed the energy minima with no imaginary frequencies. Similarly, both pyrene encapsulation complexes in native and photoswitched form (*EE*-pyrene and *ZZ*-pyrene) have been optimized at the above-mentioned levels of theory. In addition to that, binding energies[14] have been estimated for pyrene in encapsulation with *EE* and *ZZ* form. Furthermore, binding of pyrene has also been estimated with native form of macrocycle (*EE*) without encapsulation. Based on these calculations, the native state of the macrocycle (**AM2b**) is found to be more stable compared to its photoswitched state. However, the encapsulation of pyrene is found to be stronger in the photoswitched state (*ZZ*) compared to the native state (*EE*).

In order to obtain UV-Vis spectral data, TD-DFT calculations have been performed for native and photoswitched state of macrocycle (**AM2b**) with or without encapsulation of pyrene at M062X/6-311G(d,p) optimized geometries with n=20 states. All these calculations were performed using Gaussian09 suite of program. [15]

Table S8.1: Thermodynamic parameters for the encapsulation of pyrene with macrocycle **AM2b** at M062X/6-311G(d,p) level of theory.

Change in thermodynamic parameters	Complex		
	***EE*-AM2b**-pyrene	***ZZ*-AM2b**-pyrene	***EE*-AM2b**-pyrene(out)
Δ*E* (in kcal/mol)	−21.3	−24.5	−11.1
Δ*H* (in kcal/mol)	−21.9	−25.2	−11.6
Δ*G* (in kcal/mol)	−7.2	−8.6	−0.9
ΔS (Cal/mol-kelvin)	−43.6	−55.4	−42.0

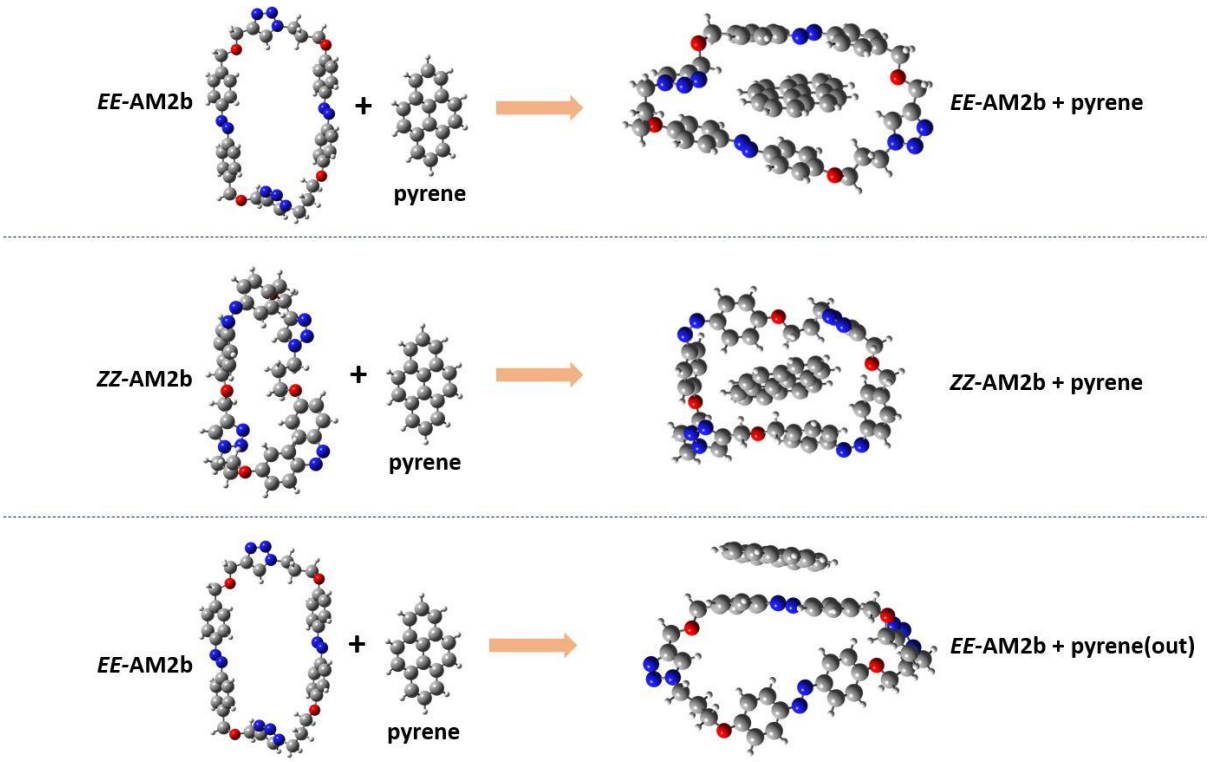

Figure S8.1: Optimized geometries of *EE*, *ZZ*, pyrene and their encapsulation complexes corresponding to **AM2b** macrocycle at M062X/6-311G(d,p) level of theory.

Table S8.2: Electronic and thermodynamic parameters at M062X/6-311G(d,p) level of theory.

Species	Thermal corrected Electronic energy (E)	ZPVE (Hartree)	Lowest frequency (cm^{-1})	Free Energy (G) (Hartree)	Enthalpy (H) (Hartree)	Entropy (S) (Cal/mol-kelvin)
***EE*-AM2b**	−2318.019731	0.731655	8.6	−2318.147445	−2318.018787	270.784
***ZZ*-AM2b**	−2317.975270	0.730905	7.6	−2318.103727	−2317.974326	272.348
Pyrene	−615.435060	0.208434	98.3	−615.479109	−615.434116	94.695
***EE*-AM2b-pyrene**	−2933.488846	0.941271	5.8	−2933.640815	−2933.487901	321.835
***EE*-AM2b-pyrene (out)**	−2933.472401	0.940466	8.9	−2933.625132	−2933.471457	323.436
***ZZ*-AM2b - pyrene**	−2933.449449	0.941307	14.8	−2933.596561	−2933.448504	311.610

Table S8.3: Vibrational frequencies (C−H stretching) of selected phenyl hydrogens (labeled in the figure) at M062X/6-311G(d,p) level of theory.

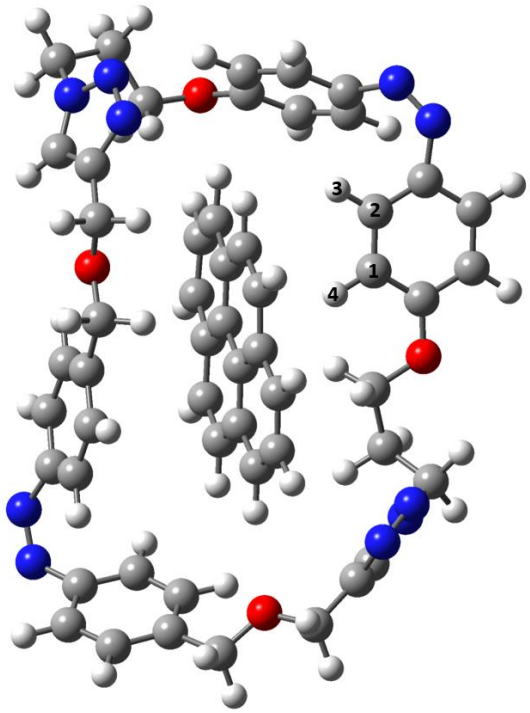

Stretching frequencies corresponding to	Vibrational frequencies (cm^{-1})	
	ZZ-AM2b	**ZZ-AM2b-pyrene**
C1−H4	3248.4	3268.0
C2−H3	3218.6	3224.6

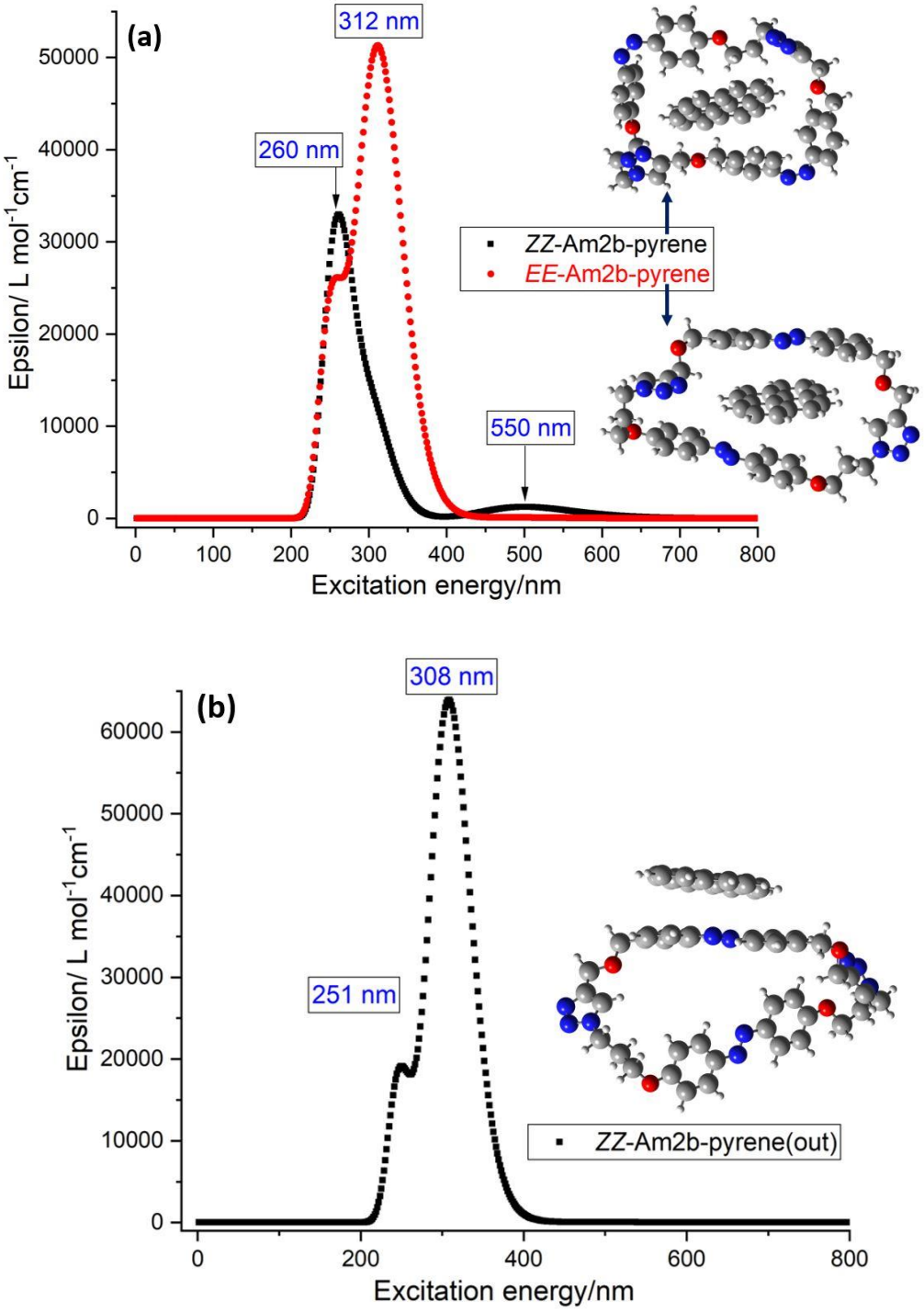

Figure S8.2: Computed UV-vis spectra of macrocycle (**AM2b**) with pyrene (a) encapsulation in native (*EE*) and photoswitched (*ZZ*) form; (b) without encapsulation in native (*EE*) form using TD-DFT (at M062X/6-311G(d,p)) calculations.

S9. Characterization Data

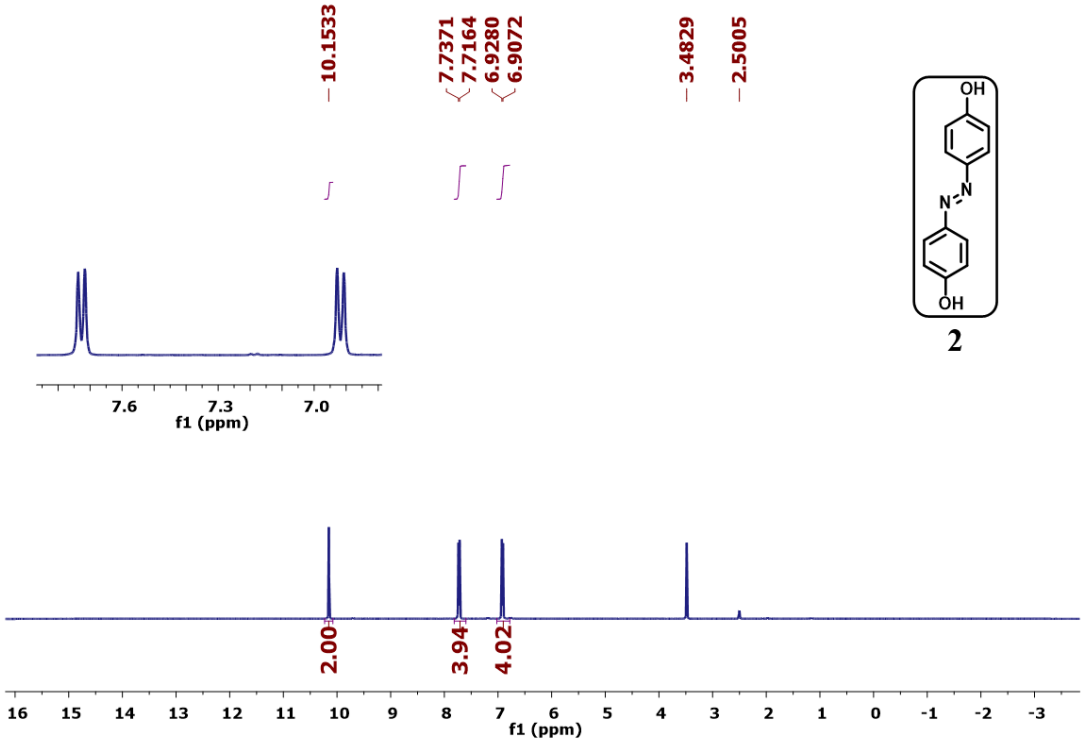

^{1}H NMR spectrum of **(*E*)-4,4'-(diazene-1,2-diyl)diphenol** (**2**) in DMSO-d_6

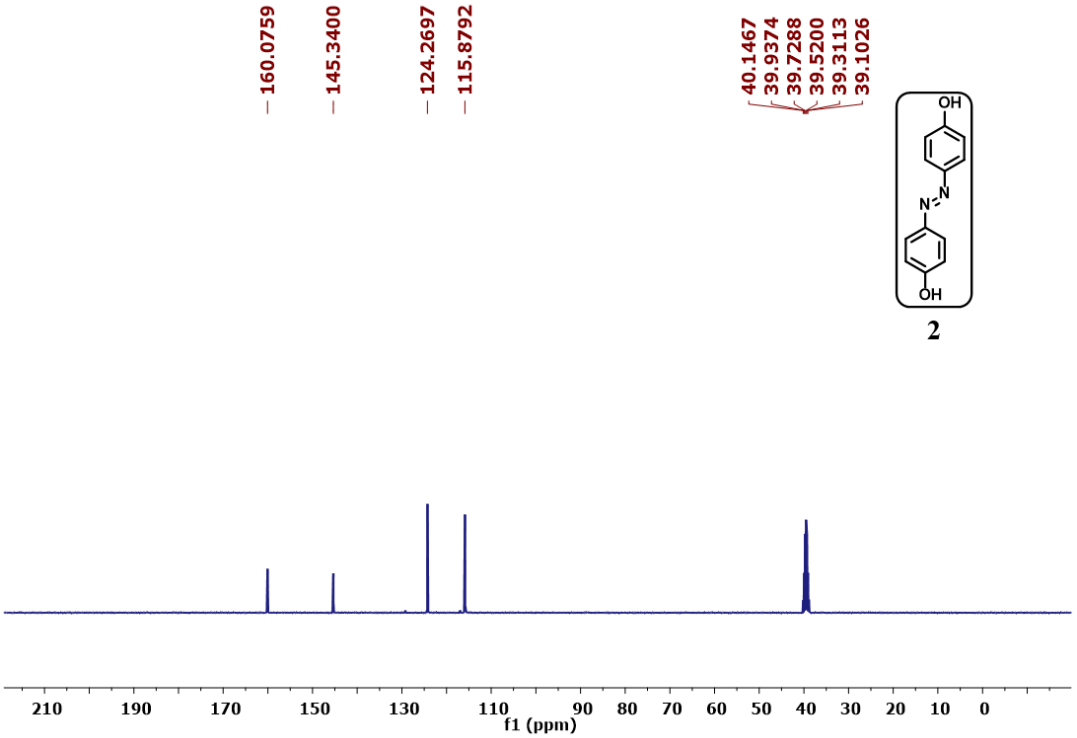

^{13}C NMR spectrum of **(*E*)-4,4'-(diazene-1,2-diyl)diphenol** (**2**) in DMSO-d_6

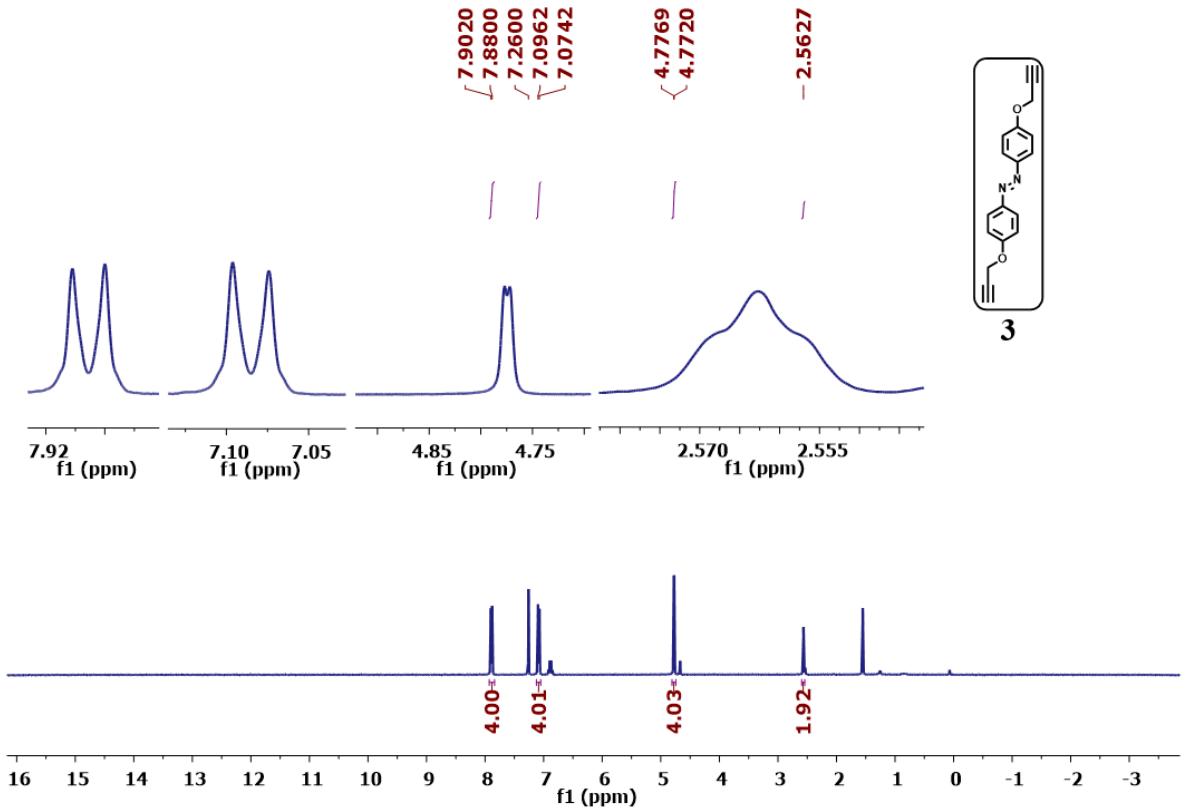

^{1}H NMR spectrum of ***(E)*-1,2-bis(4-(prop-2-yn-1-yloxy)phenyl)diazene (3)** in $CDCl_3$

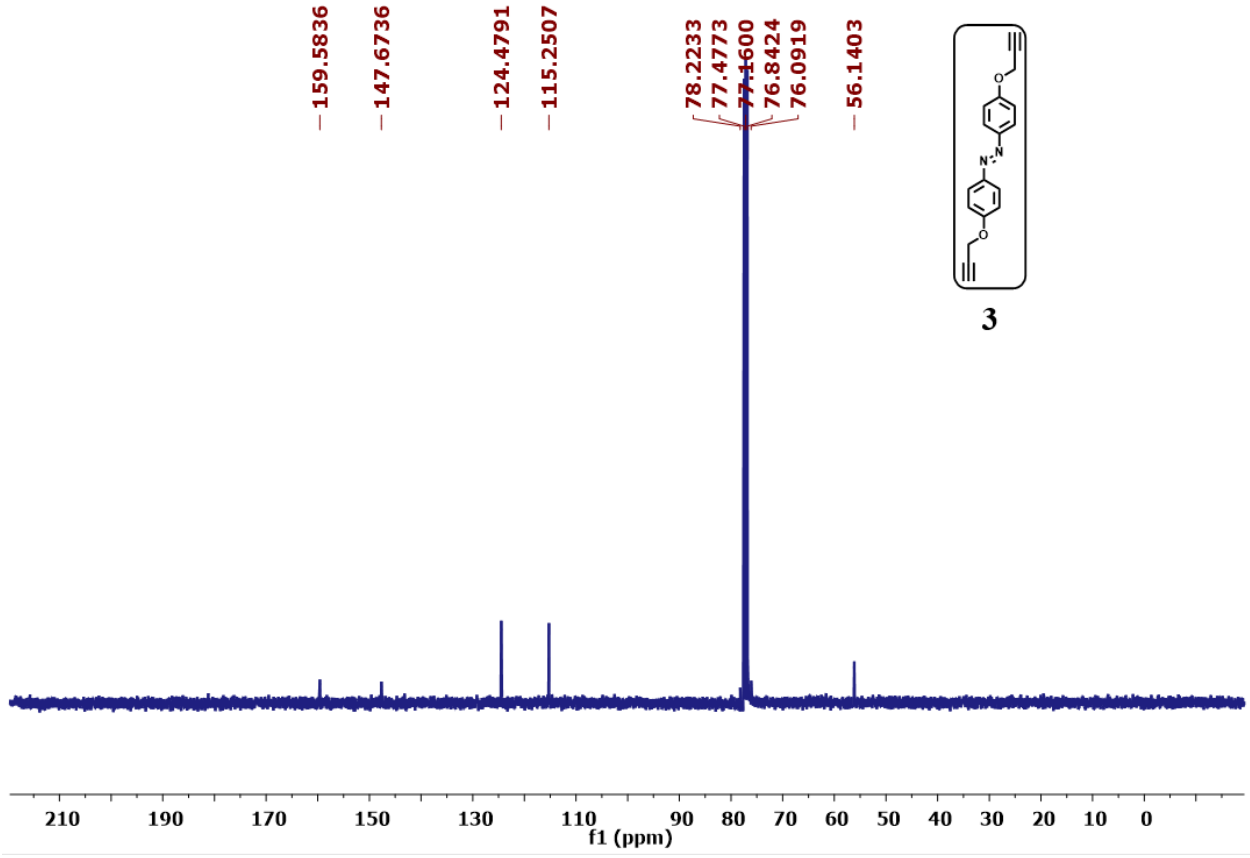

^{13}C NMR spectrum of ***(E)*-1,2-bis(4-(prop-2-yn-1-yloxy)phenyl)diazene (3)** in $CDCl_3$

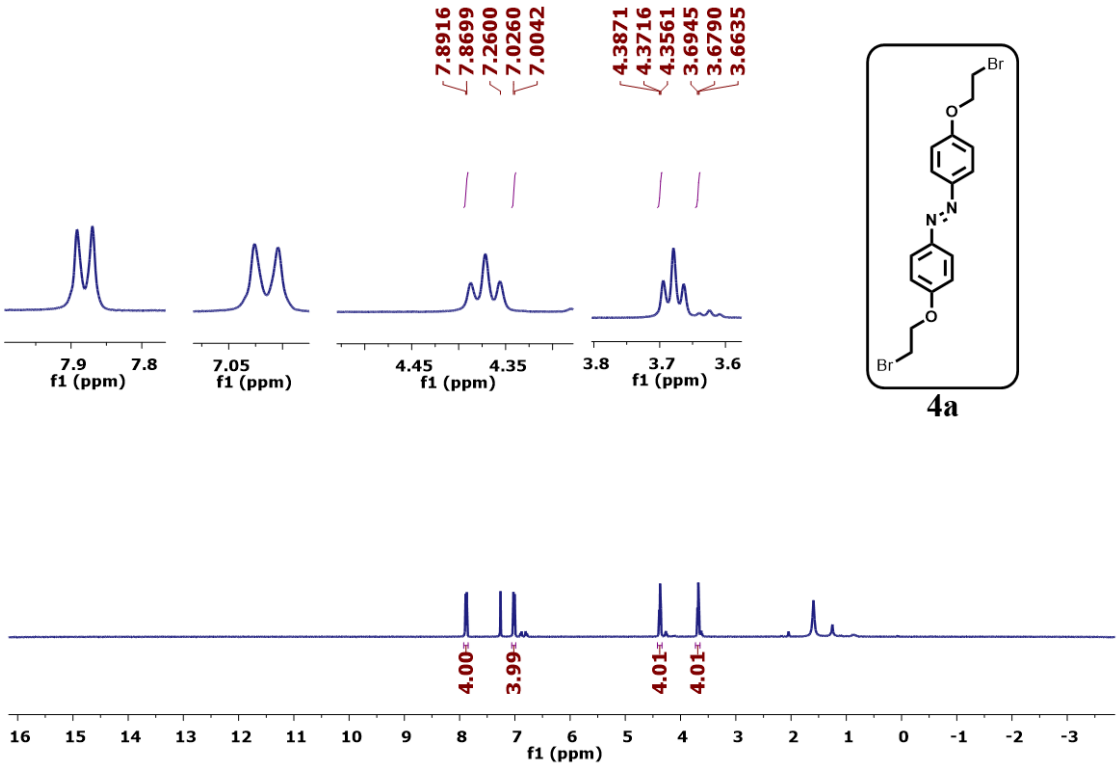

^{1}H NMR spectrum of ***(E)*-1,2-bis(4-(2-bromoethoxy)phenyl)diazene (4a)** in $CDCl_3$

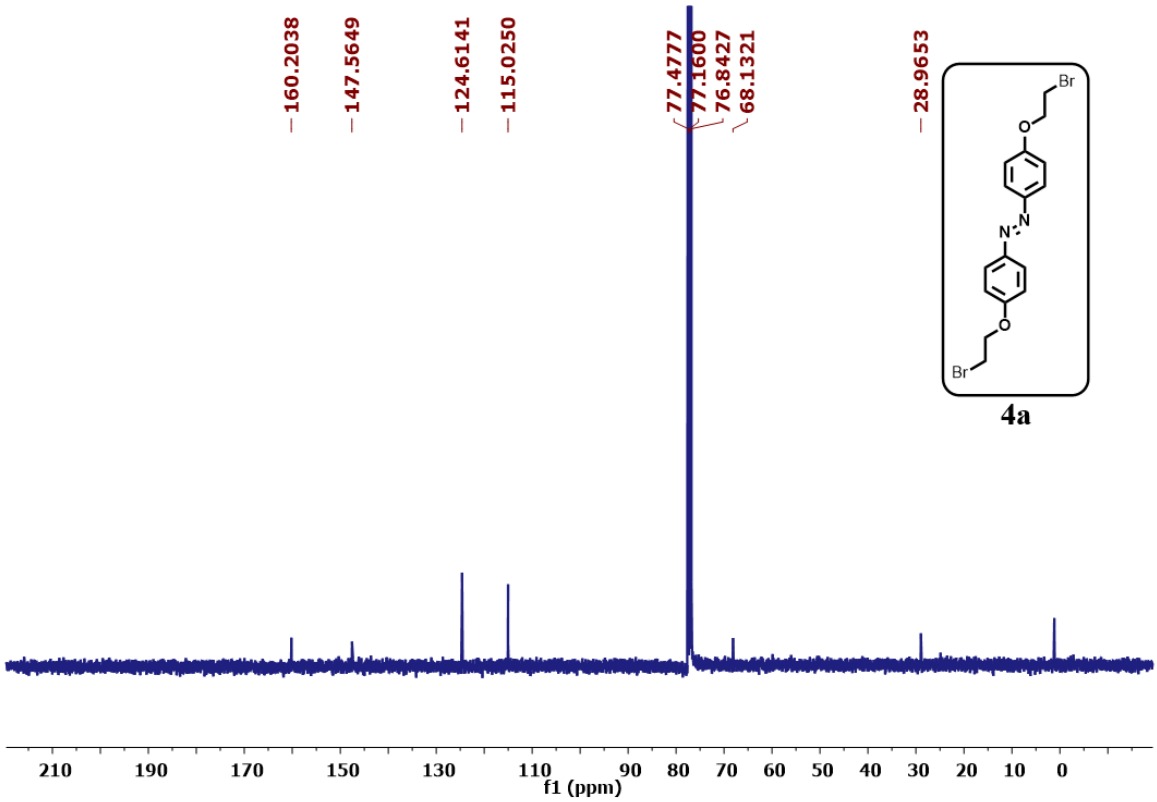

^{13}C NMR spectrum of ***(E)*-1,2-bis(4-(2-bromoethoxy)phenyl)diazene (4a)** in $CDCl_3$

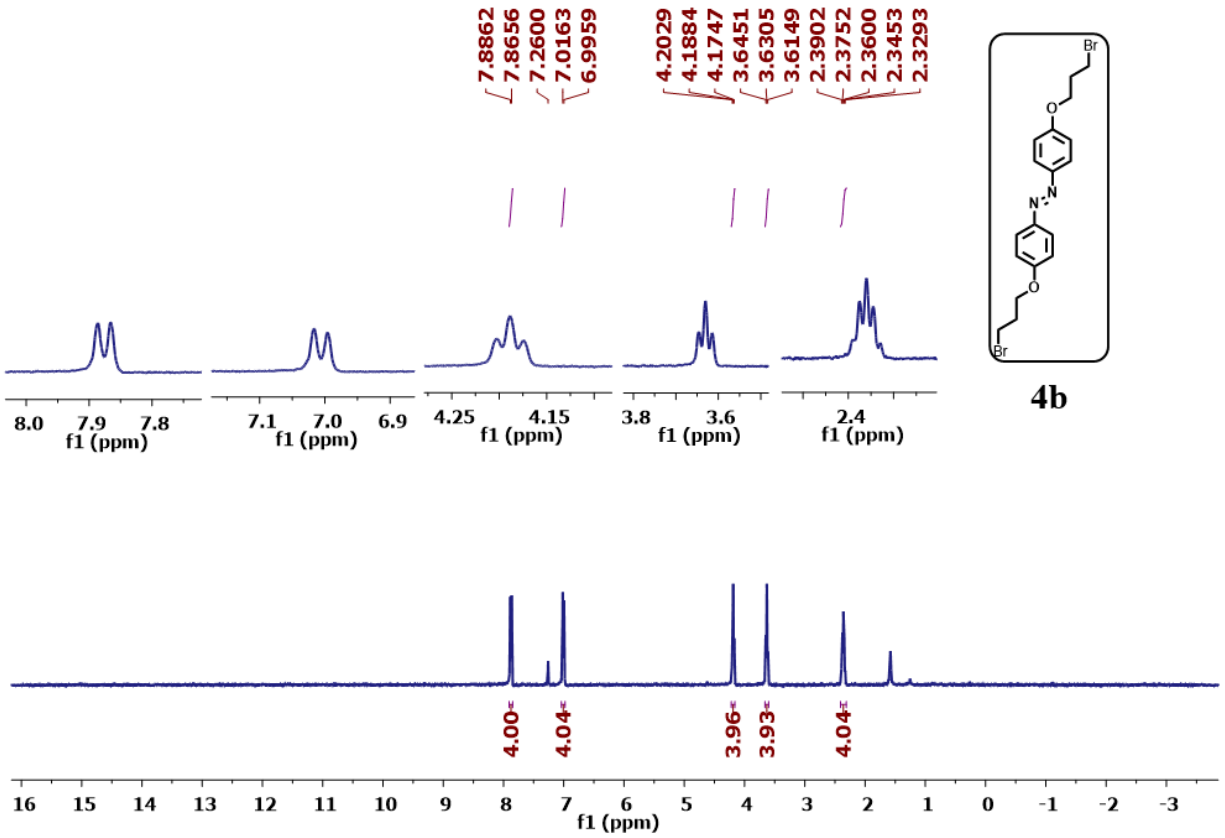

^{1}H NMR spectrum of ***(E)*-1,2-bis(4-(3-bromopropoxy)phenyl)diazene (4b)** in $CDCl_3$

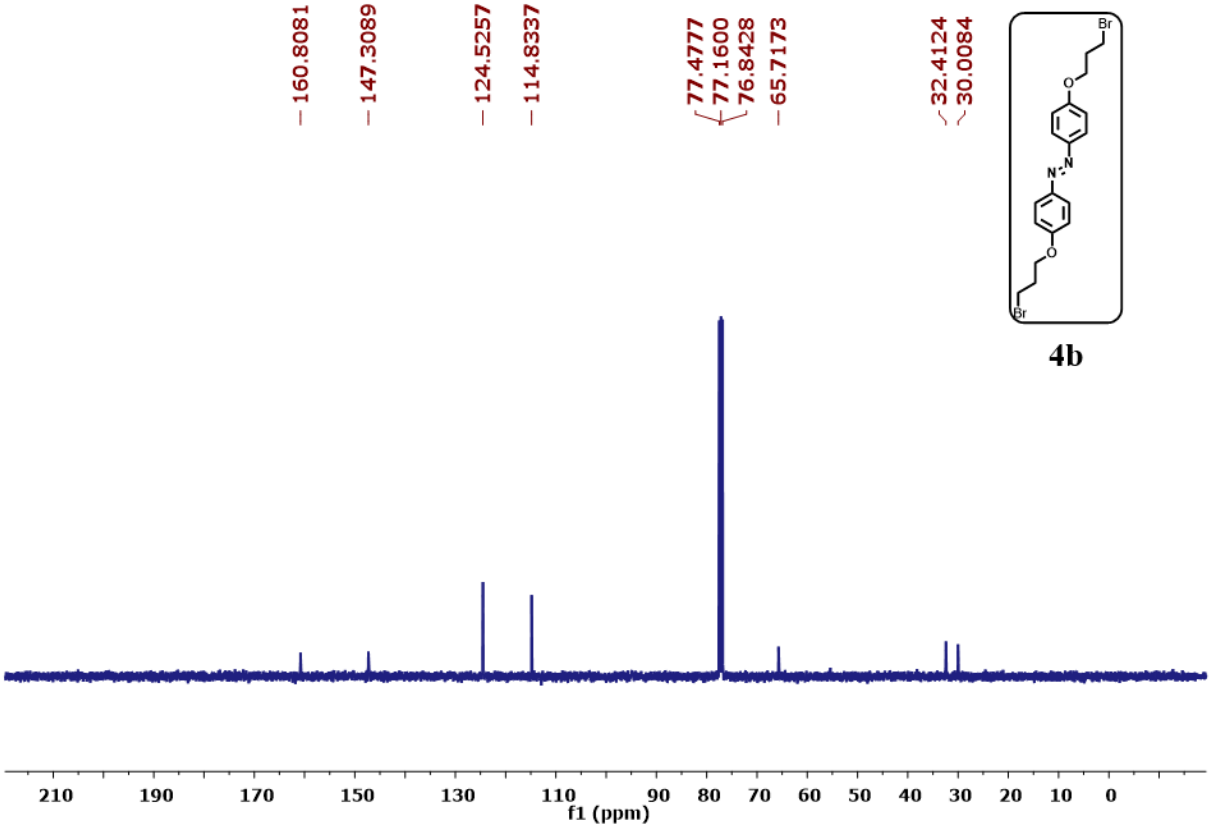

^{13}C NMR spectrum of ***(E)*-1,2-bis(4-(3-bromopropoxy)phenyl)diazene(4b)** in $CDCl_3$

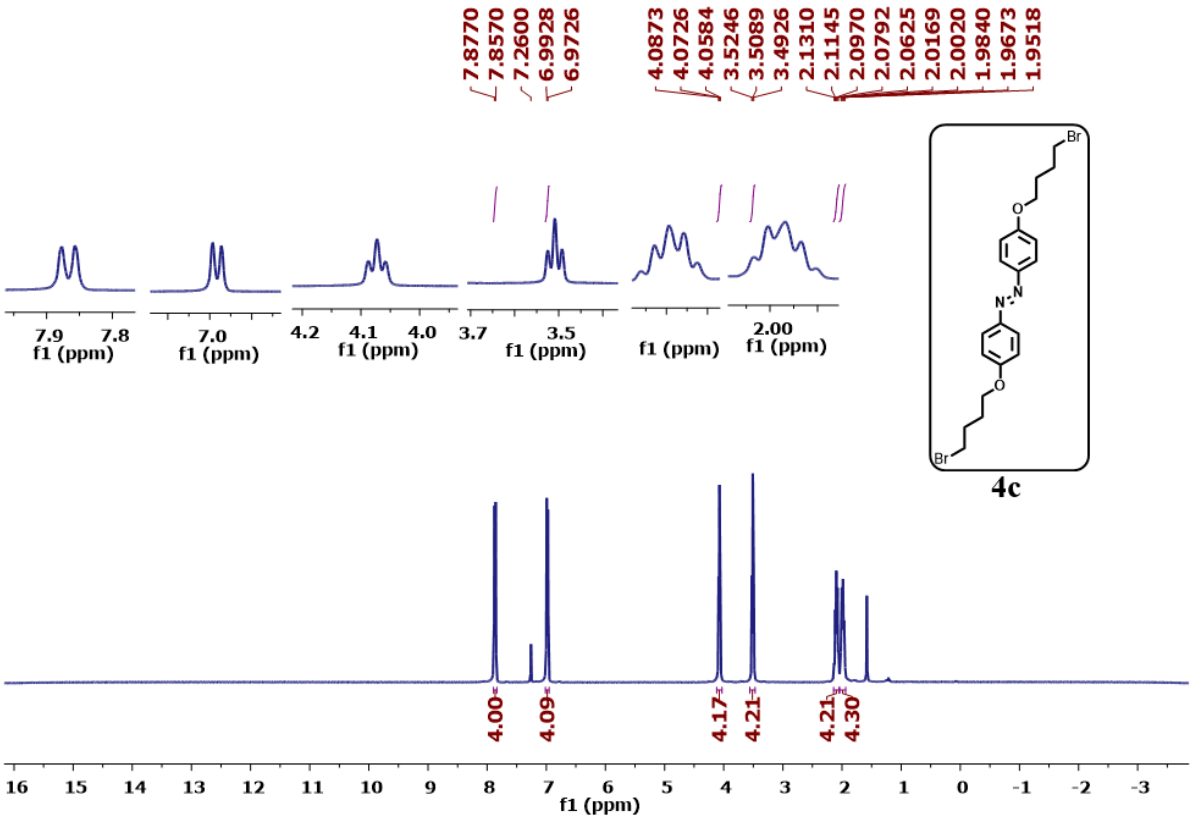

^{1}H NMR spectrum of **(*E*)-1,2-bis(4-(4-bromobutoxy)phenyl)diazene (4c)** in $CDCl_3$

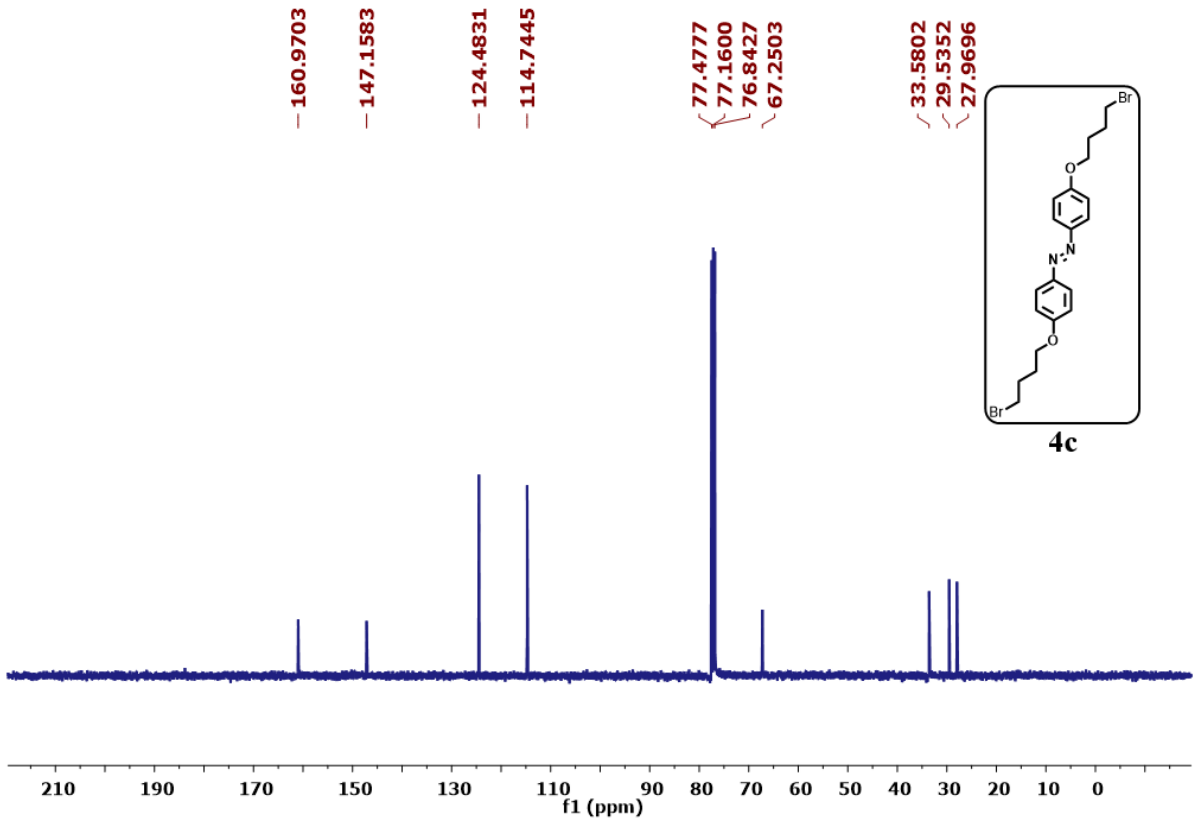

^{13}C NMR spectrum of **(*E*)-1,2-bis(4-(4-bromobutoxy)phenyl)diazene (4c)** in $CDCl_3$

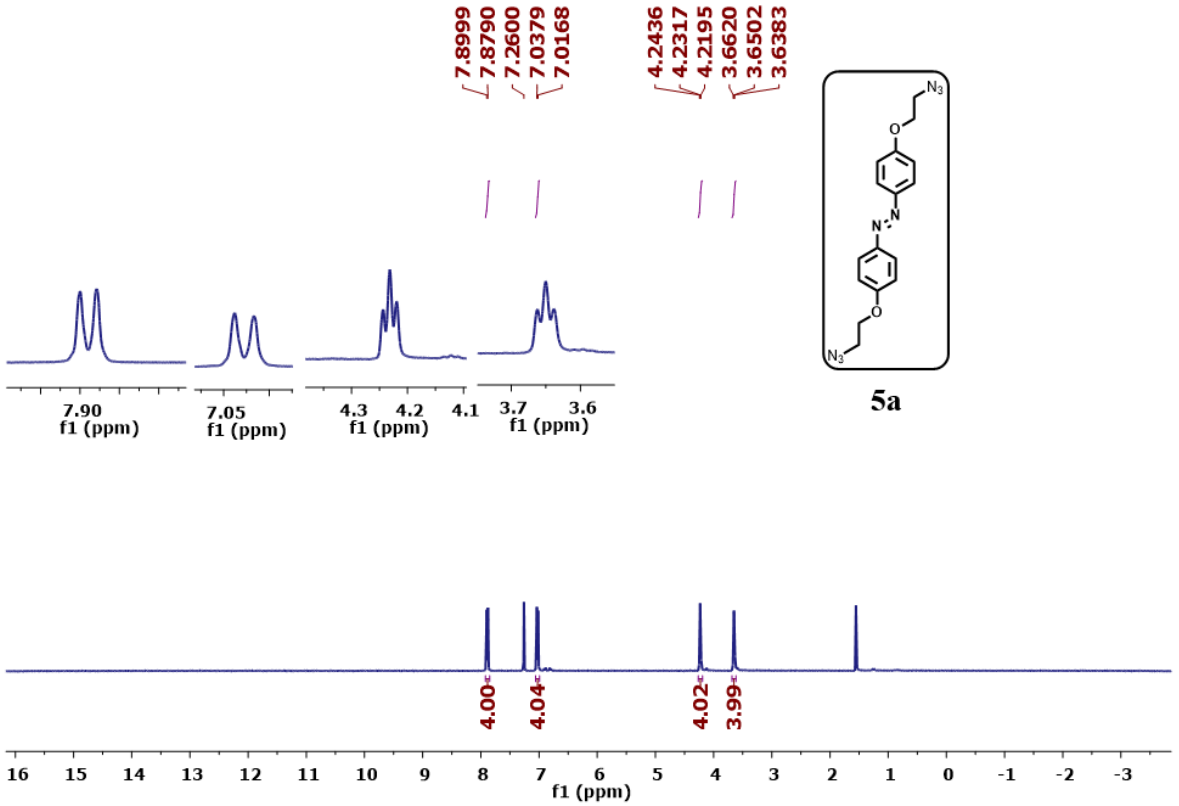

^{1}H NMR spectrum of ***(E)*-1,2-bis(4-(2-azidoethoxy)phenyl)diazene (5a)** in $CDCl_3$

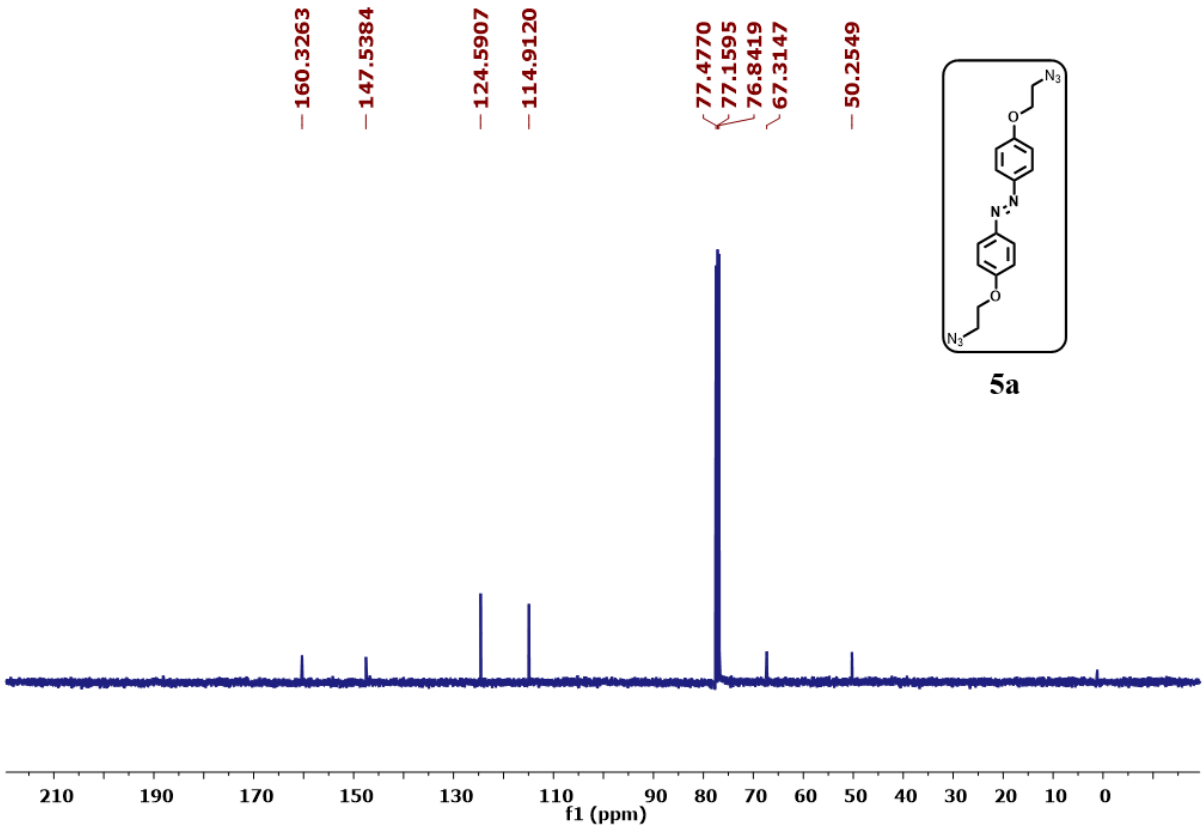

^{13}C NMR spectrum of ***(E)*-1,2-bis(4-(2-azidoethoxy)phenyl)diazene (5a)** in $CDCl_3$

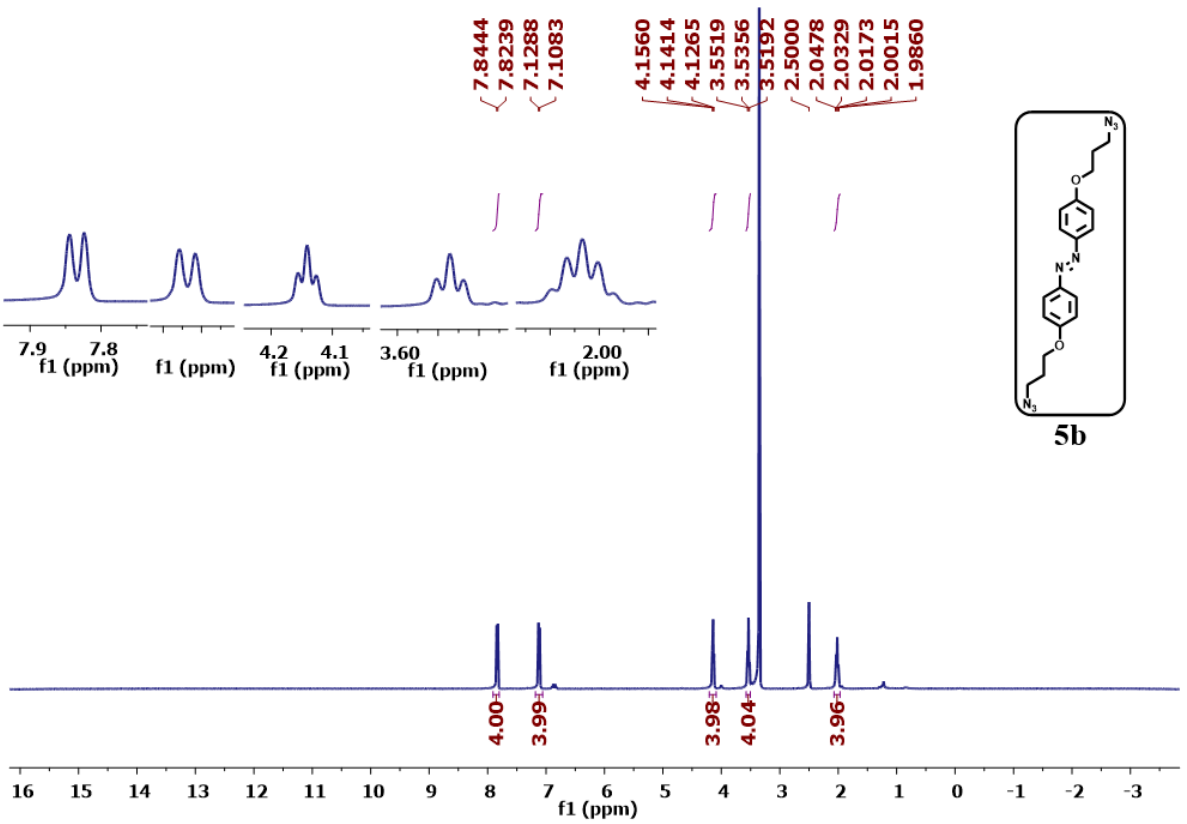

^{1}H NMR spectrum of ***(E)*-1,2-bis(4-(3-azidopropoxy)phenyl)diazene (5b)** in $CDCl_3$

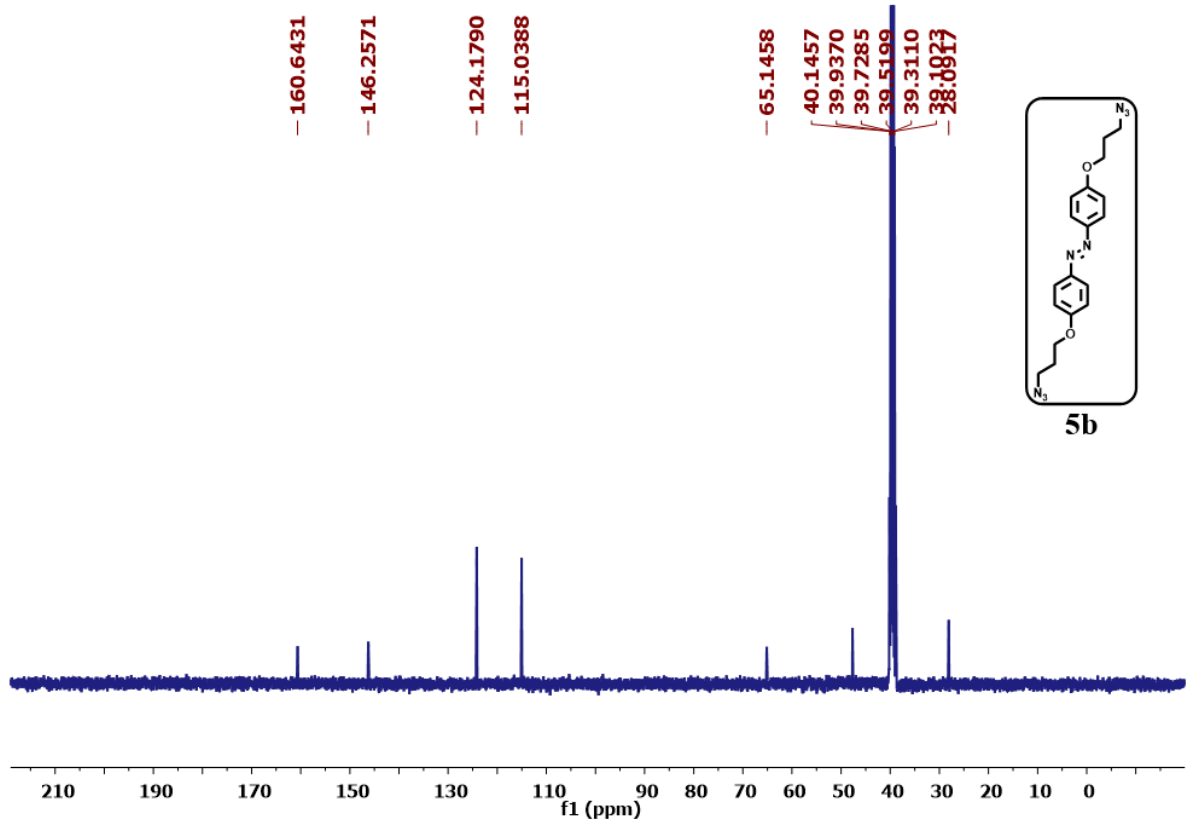

^{13}C NMR spectrum of ***(E)*-1,2-bis(4-(3-azidopropoxy)phenyl)diazene (5b)** in $CDCl_3$

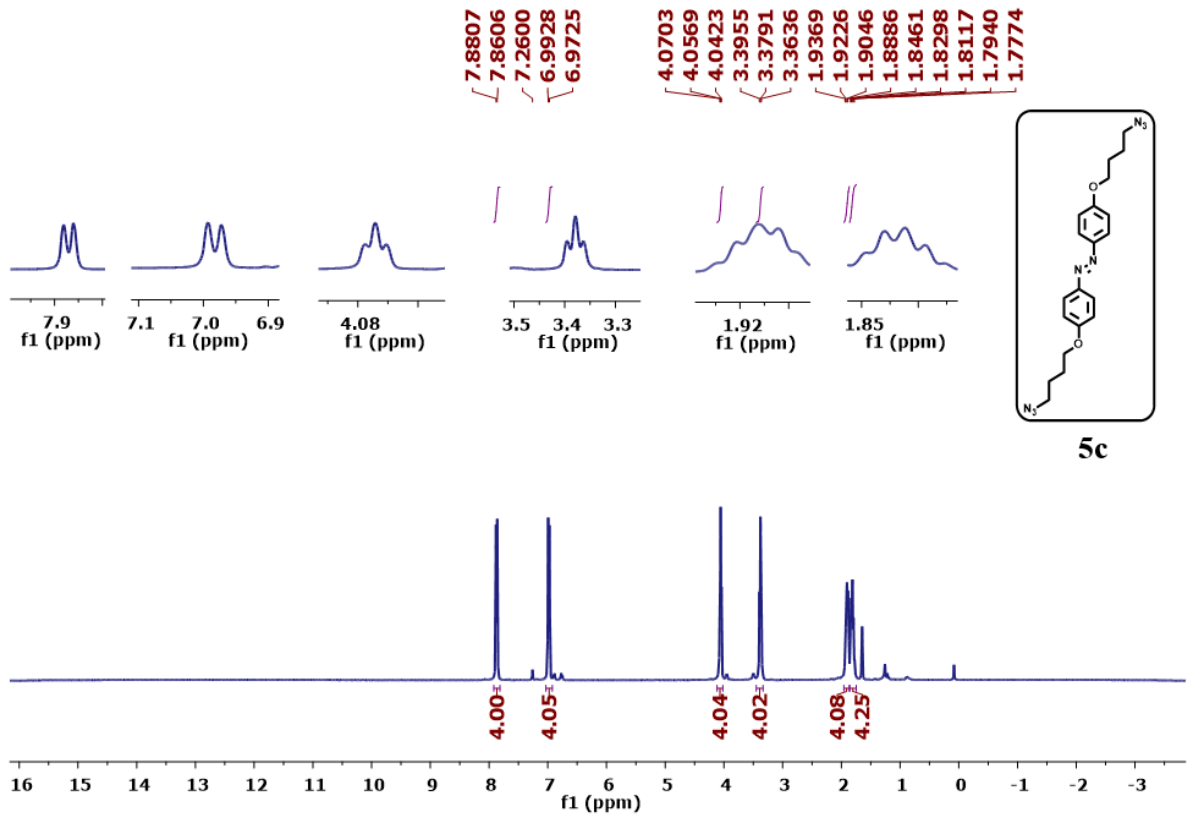

^{1}H NMR spectrum of **(*E*)-1,2-bis(4-(4-azidobutoxy)phenyl)diazene (5c)** in $CDCl_3$

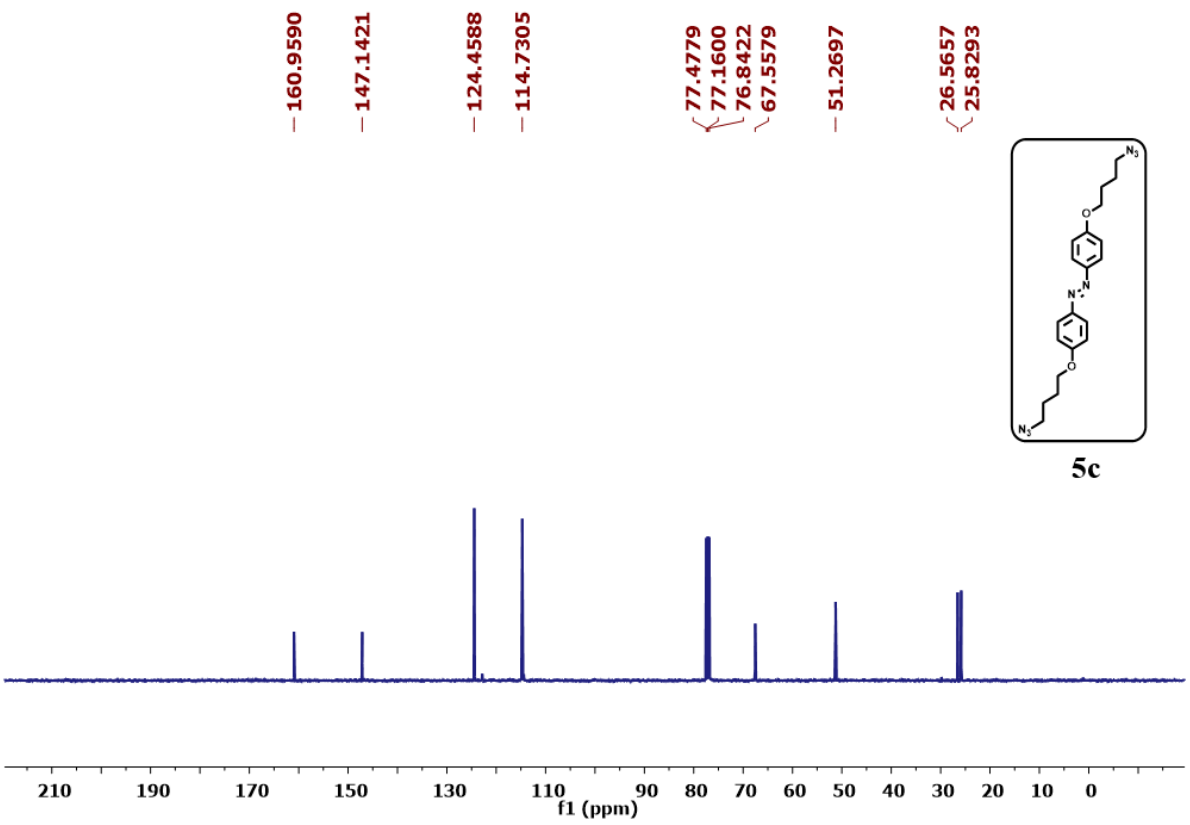

^{13}C NMR spectrum of **(*E*)-1,2-bis(4-(4-azidobutoxy)phenyl)diazene (5c)** in $CDCl_3$

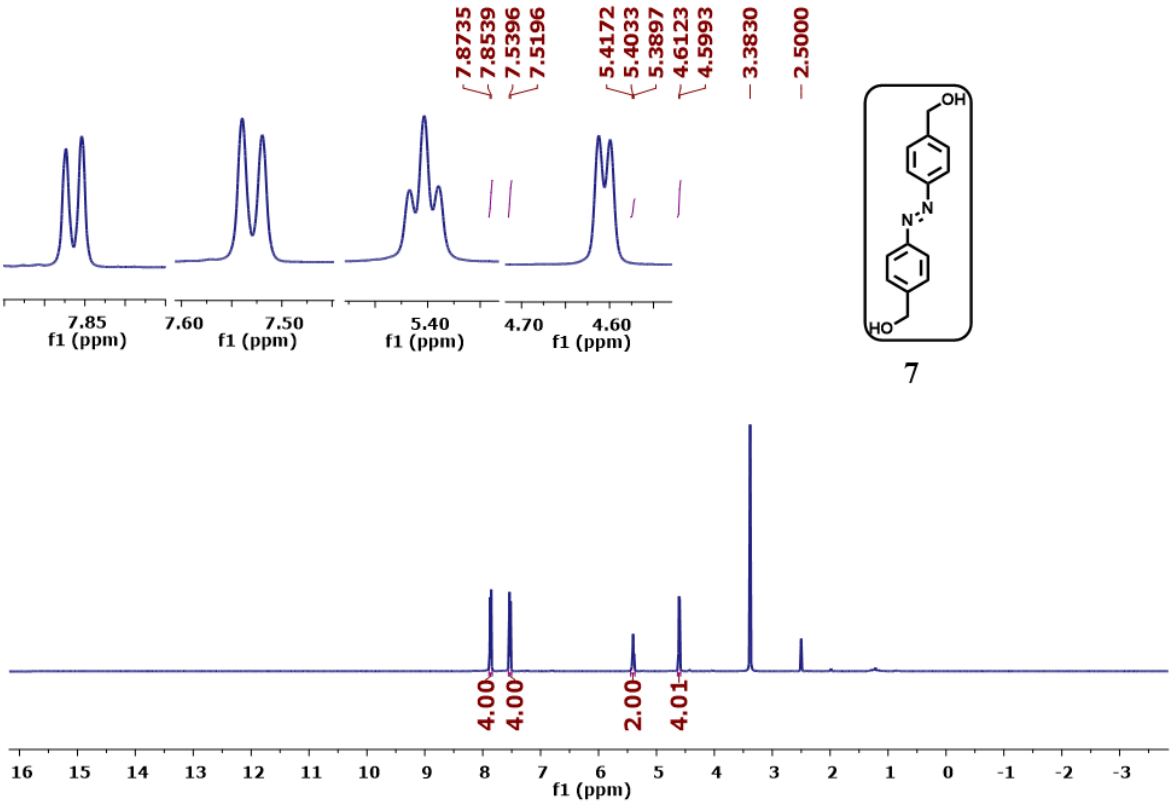

^{1}H NMR spectrum of ***(E)*-(diazene-1,2-diylbis(4,1-phenylene))dimethanol (7)** in DMSO-d_6

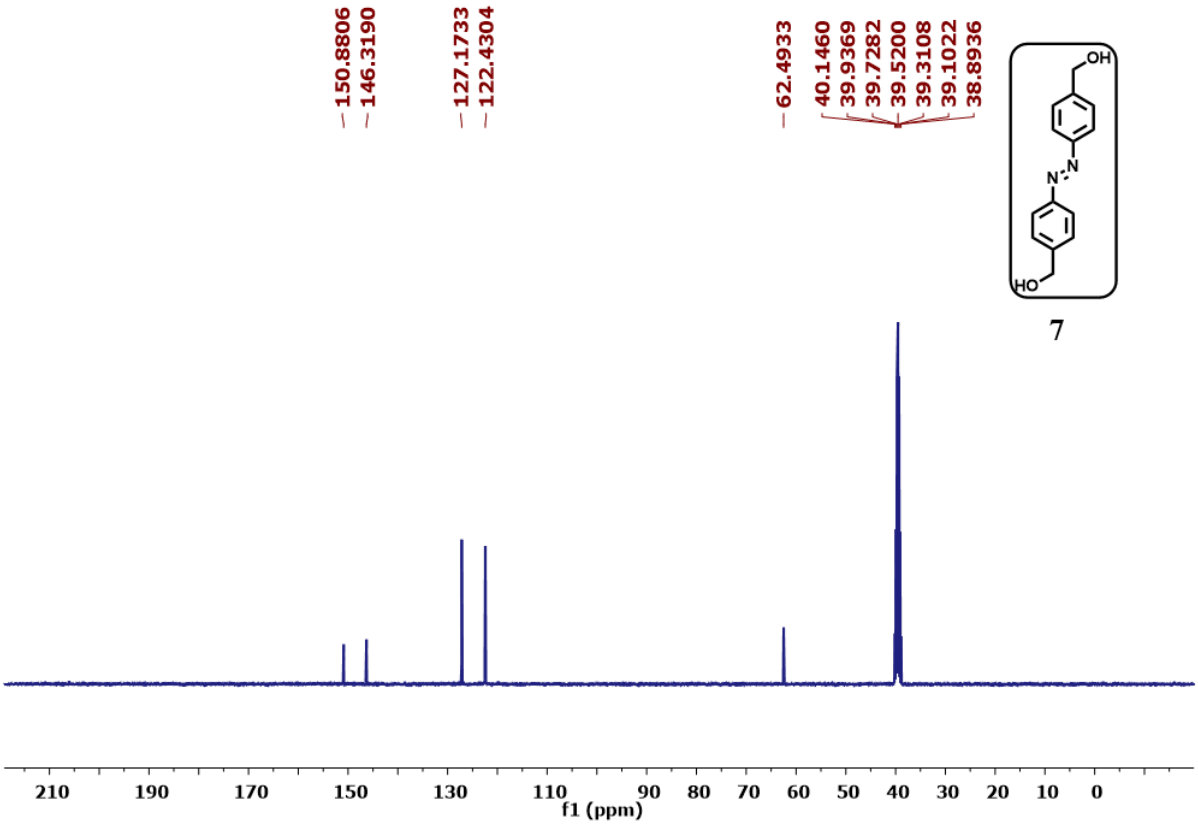

^{13}C NMR spectrum of ***(E)*-(diazene-1,2-diylbis(4,1-phenylene))dimethanol (7)** in DMSO-d_6

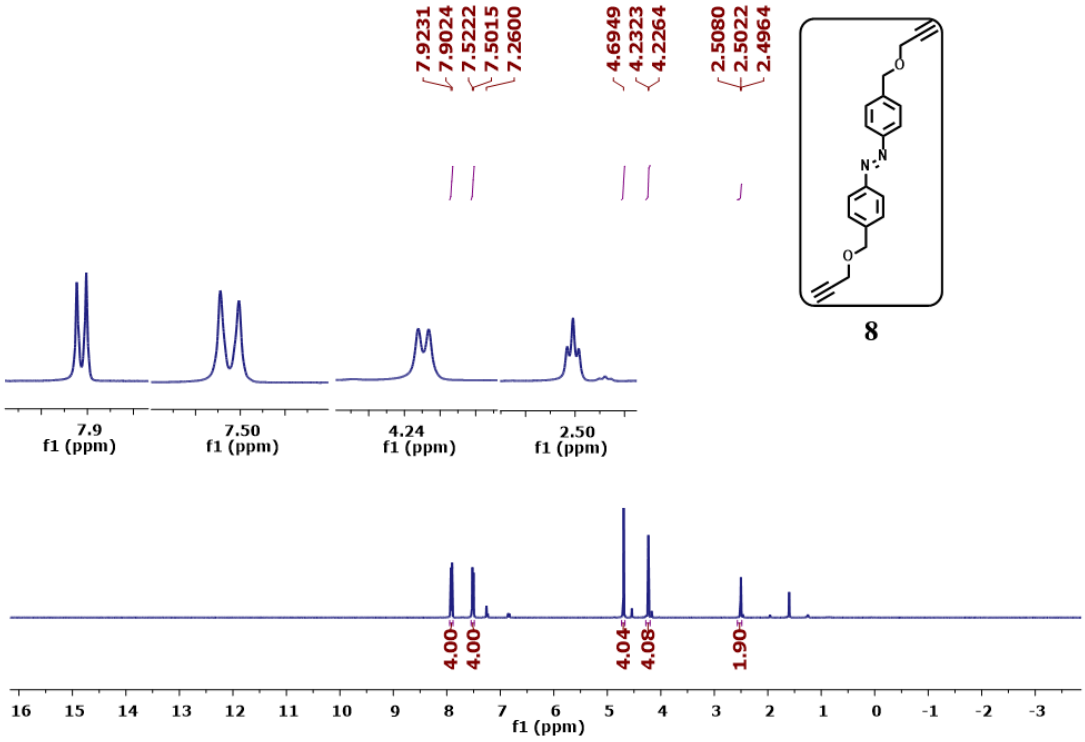

^{1}H NMR spectrum of ***(E)*-1,2-bis(4-((prop-2-yn-1-yloxy)methyl)phenyl)diazene (8)** in $CDCl_3$

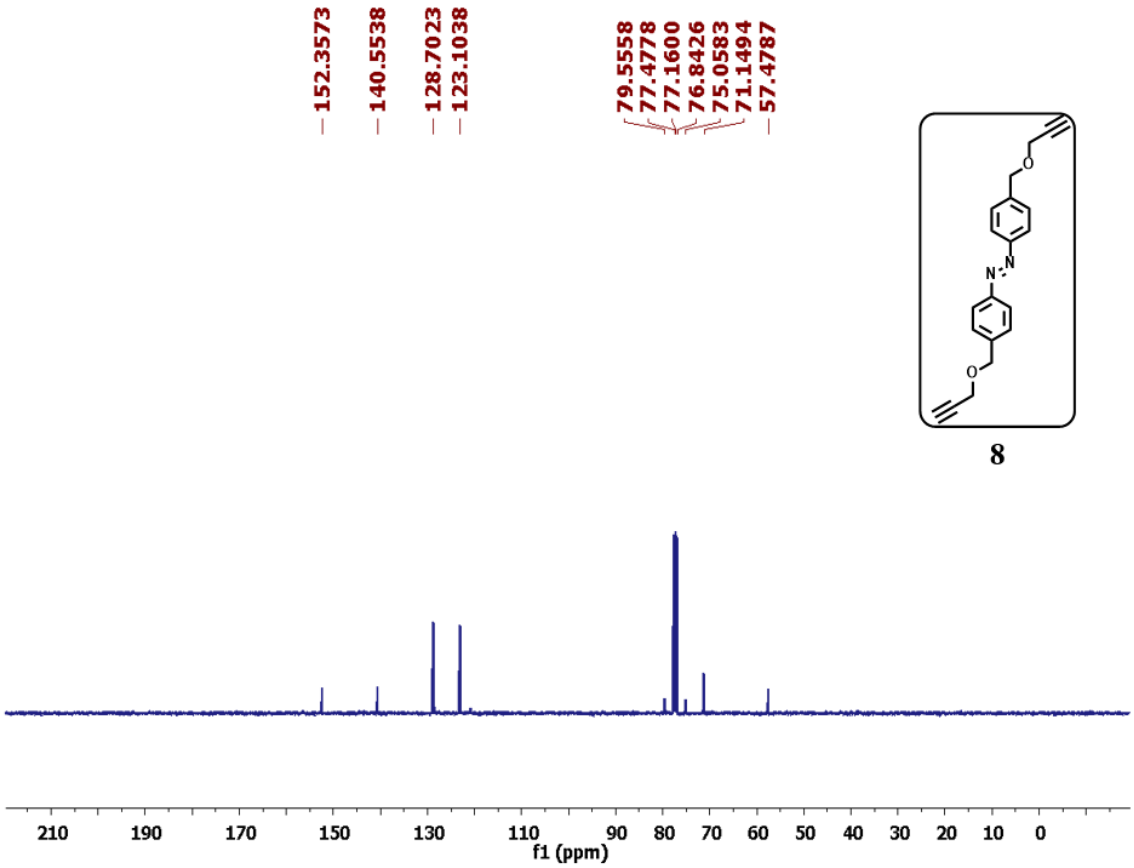

^{13}C NMR spectrum of ***(E)*-1,2-bis(4-((prop-2-yn-1-yloxy)methyl)phenyl)diazene(8)** in $CDCl_3$

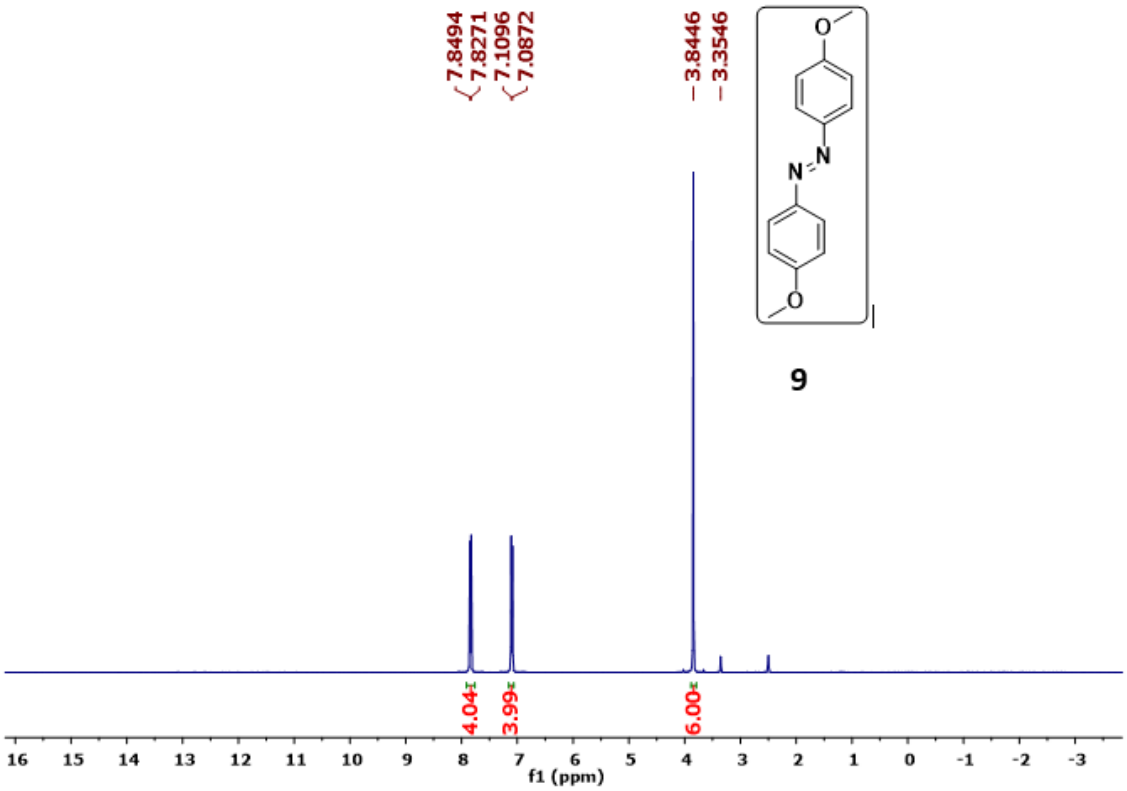

^{1}H NMR spectrum of ***(E)*-1,2-bis(4-methoxyphenyl)diazene (9)** in DMSO-d_6

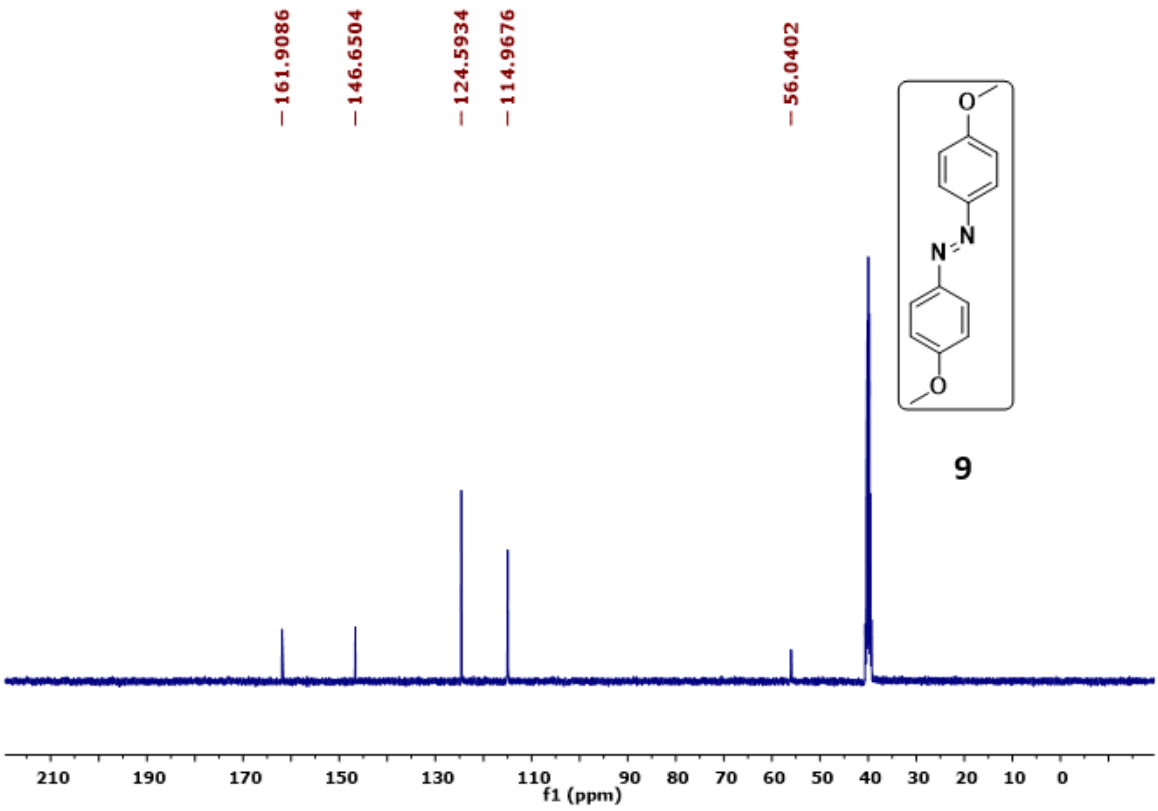

^{13}C NMR spectrum of ***(E)*-1,2-bis(4-methoxyphenyl)diazene (9)** in DMSO-d_6

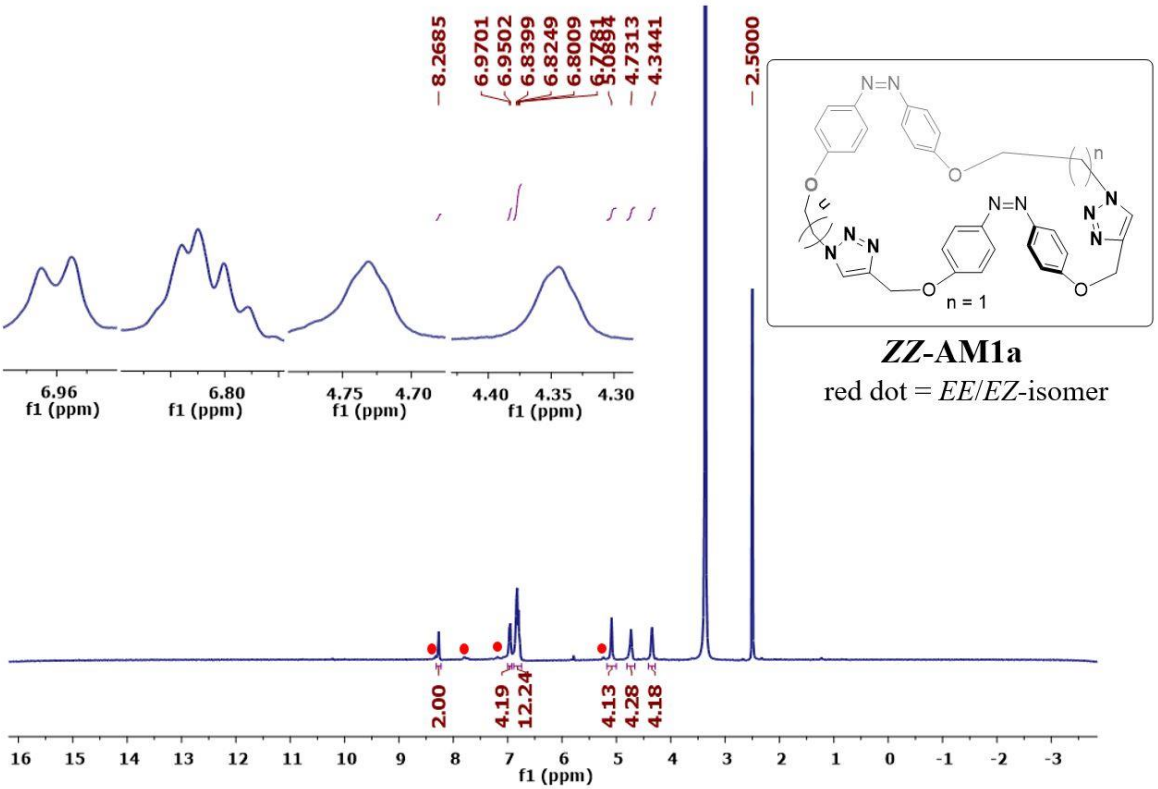

^{1}H NMR spectrum of ***ZZ*-AM1a** in DMSO-d_6 (red dot represents the *EE*/*EZ*-isomer)

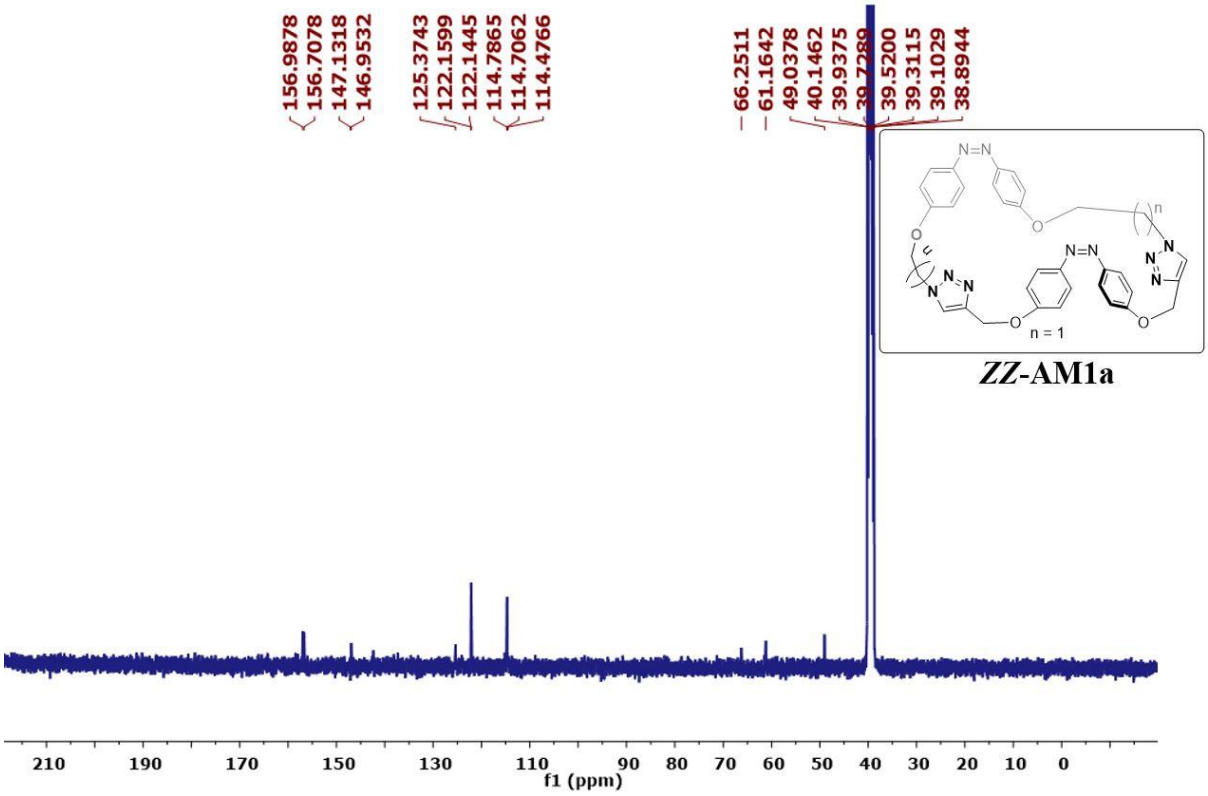

^{13}C NMR spectrum of ***ZZ*-AM1a** in DMSO-d_6

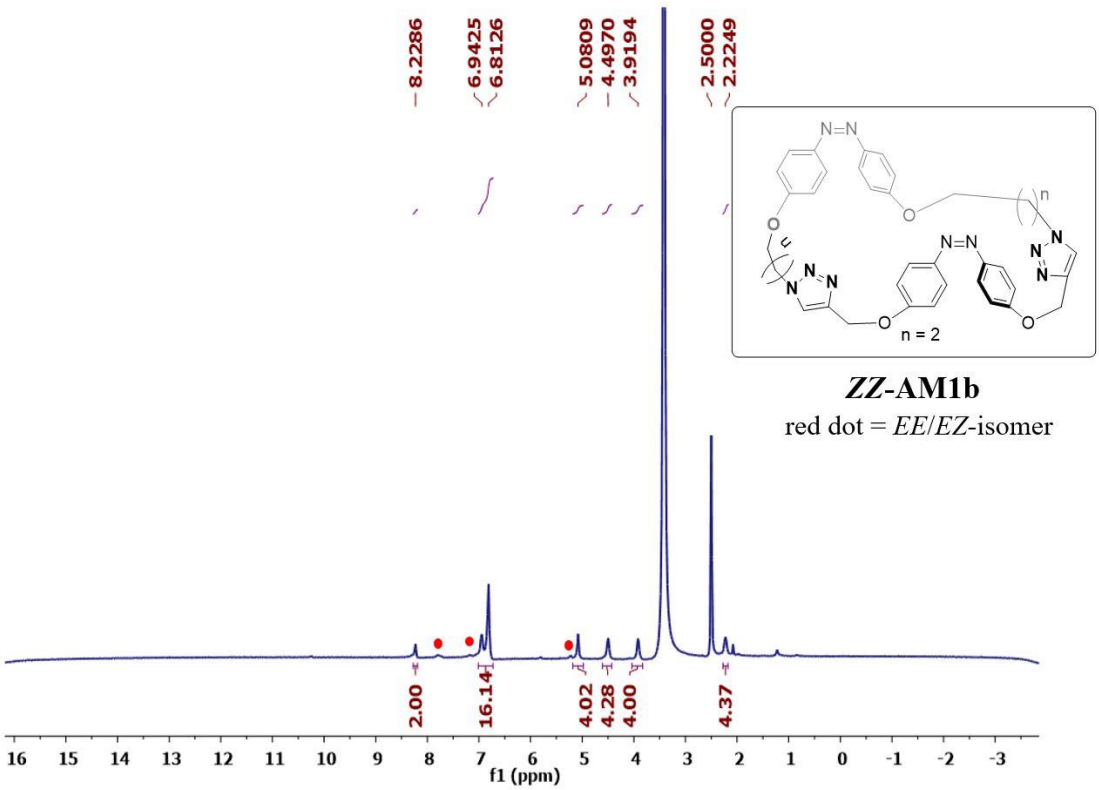

^{1}H NMR spectrum of ***ZZ*-AM1b** in DMSO-d_6 (red dot represents the *EE*/*EZ*-isomer)

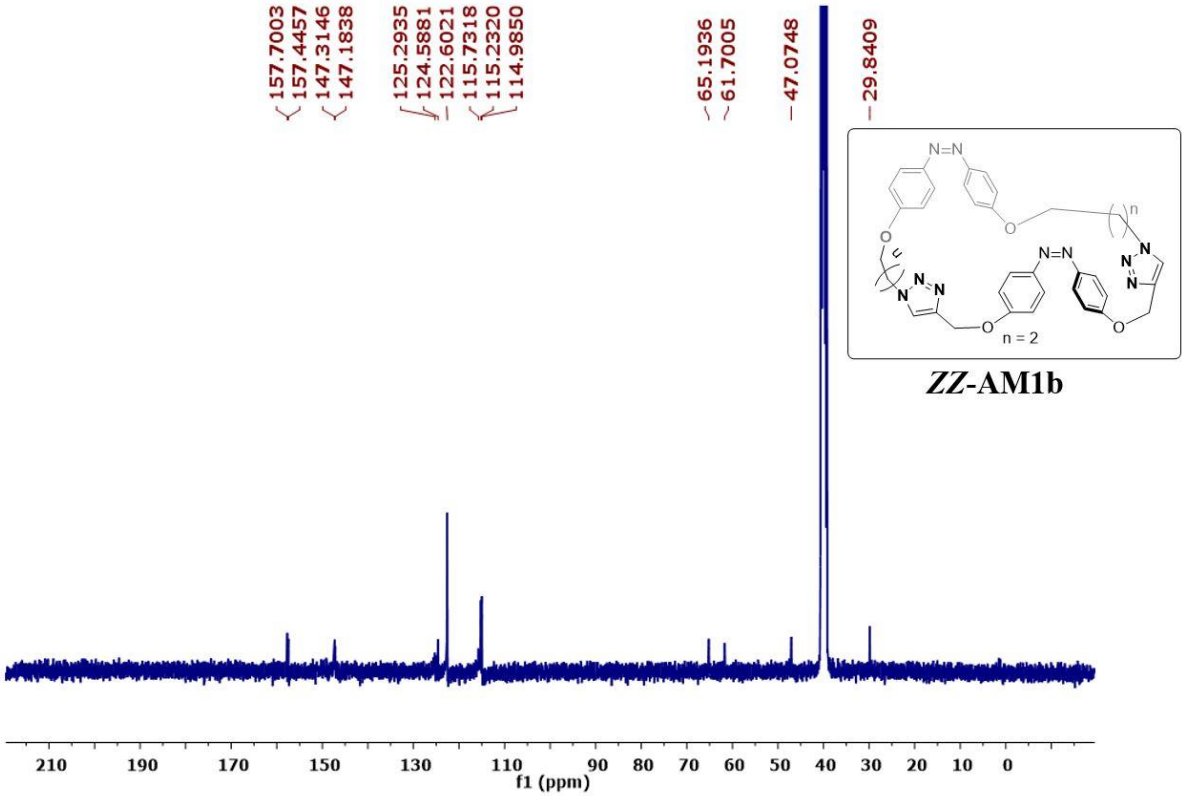

^{13}C NMR spectrum of ***ZZ*-AM1b** in DMSO-d_6

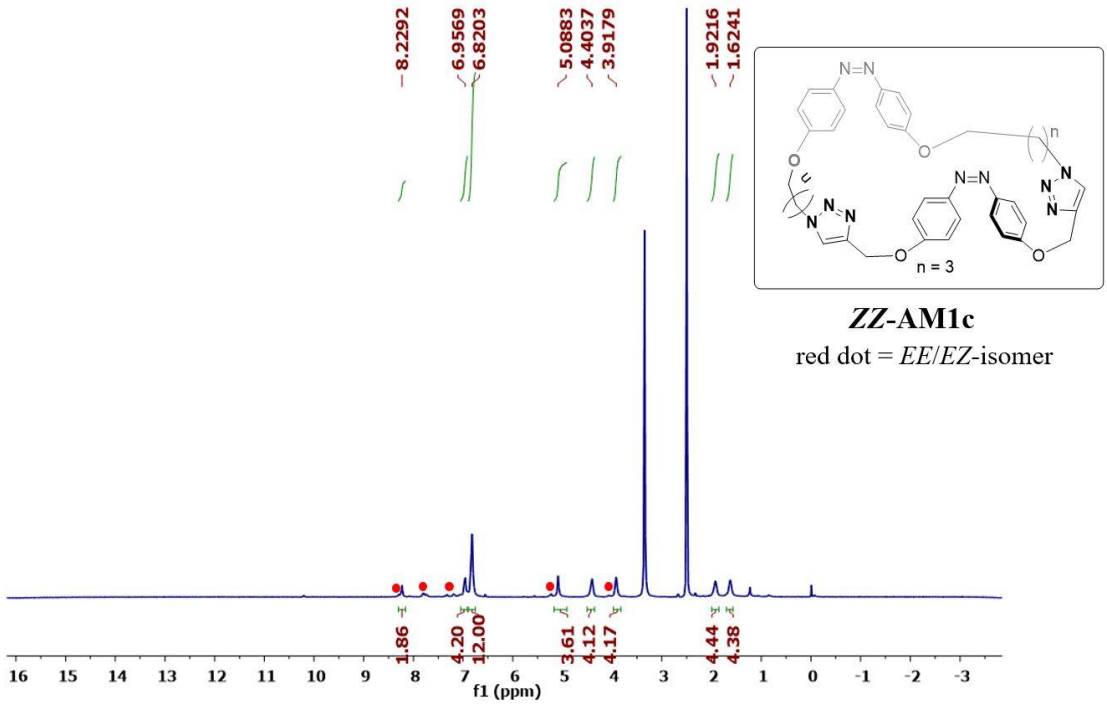

^{1}H NMR spectrum of ***ZZ*-AM1c** in DMSO-d_6 (red dot represents the *EE*/*EZ*-isomer)

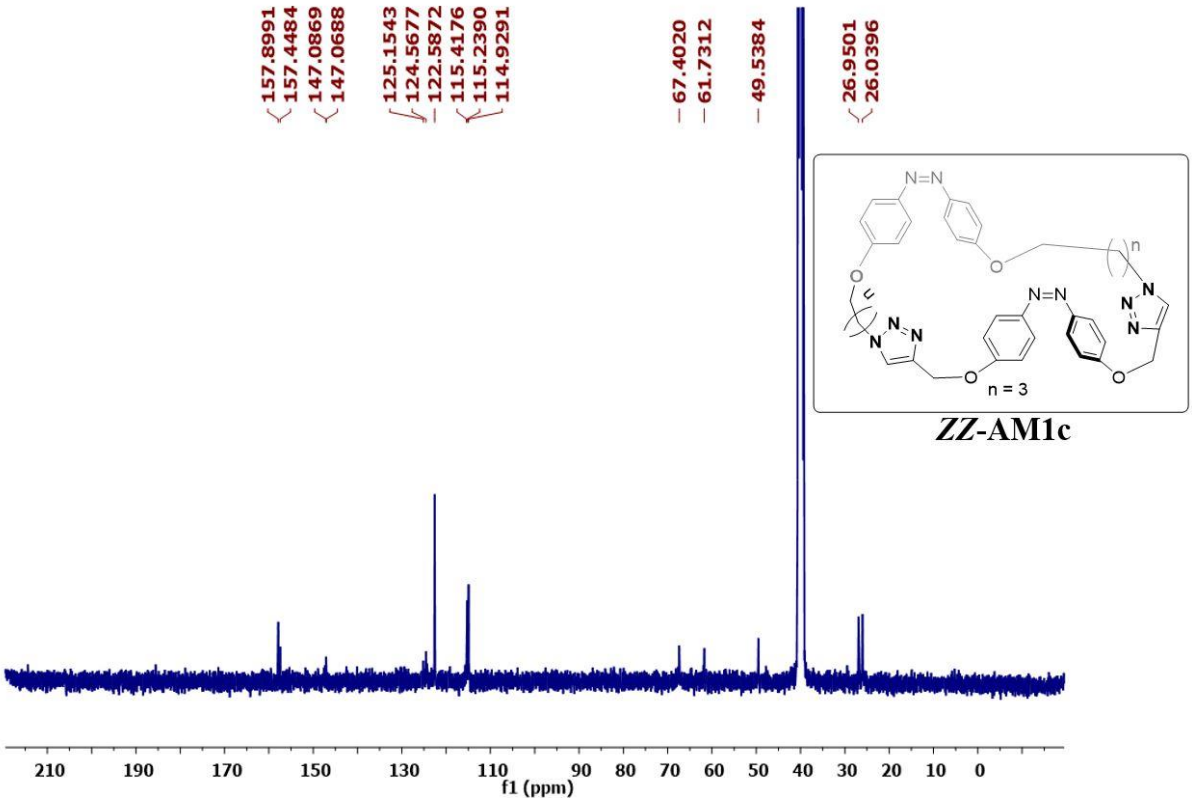

^{13}C NMR spectrum of ***ZZ*-AM1c** in DMSO-d_6

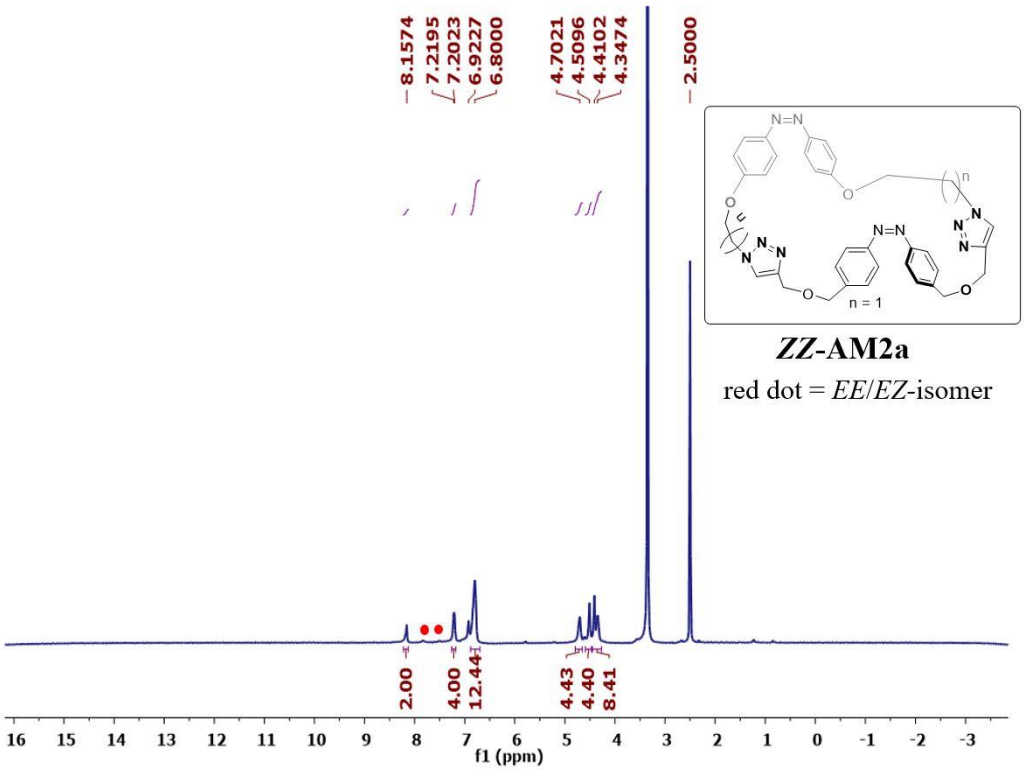

^{1}H NMR spectrum of ***ZZ*-AM2a** in DMSO-d_6 (red dot represents the *EE*/*EZ*-isomer)

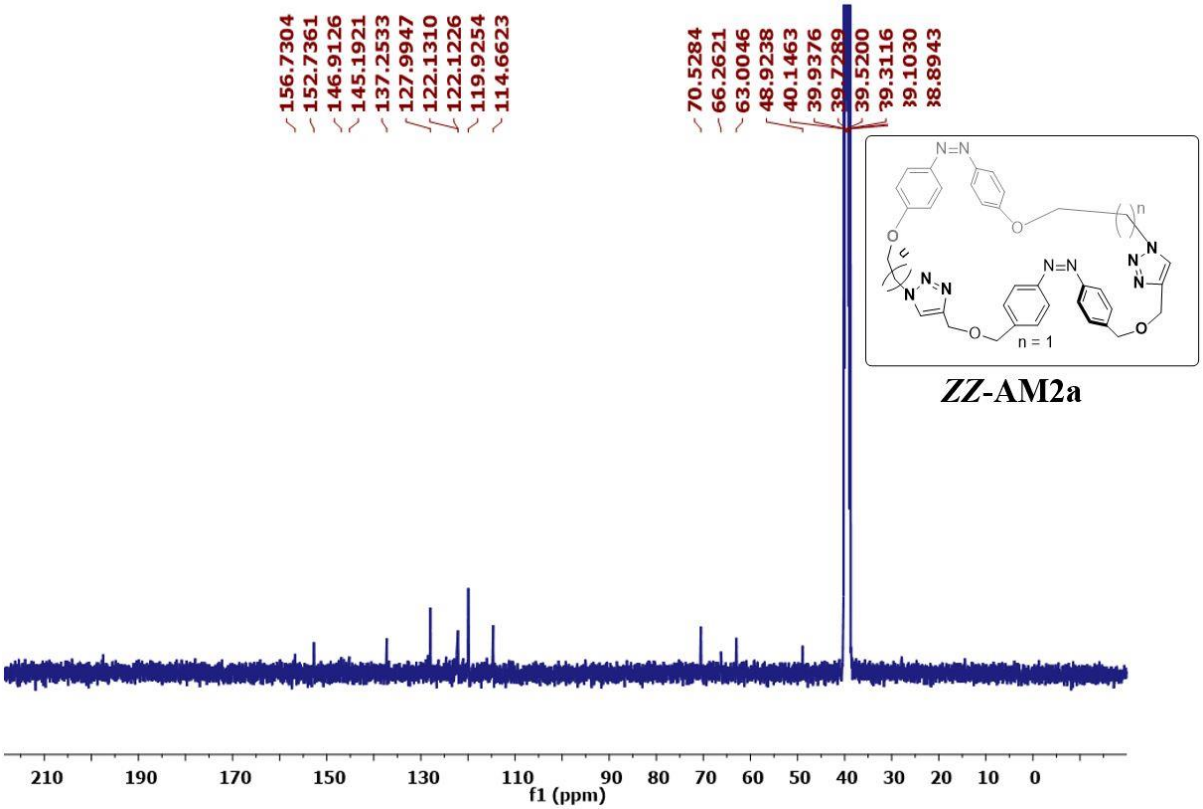

^{13}C NMR spectrum of ***ZZ*-AM2a** in DMSO-d_6

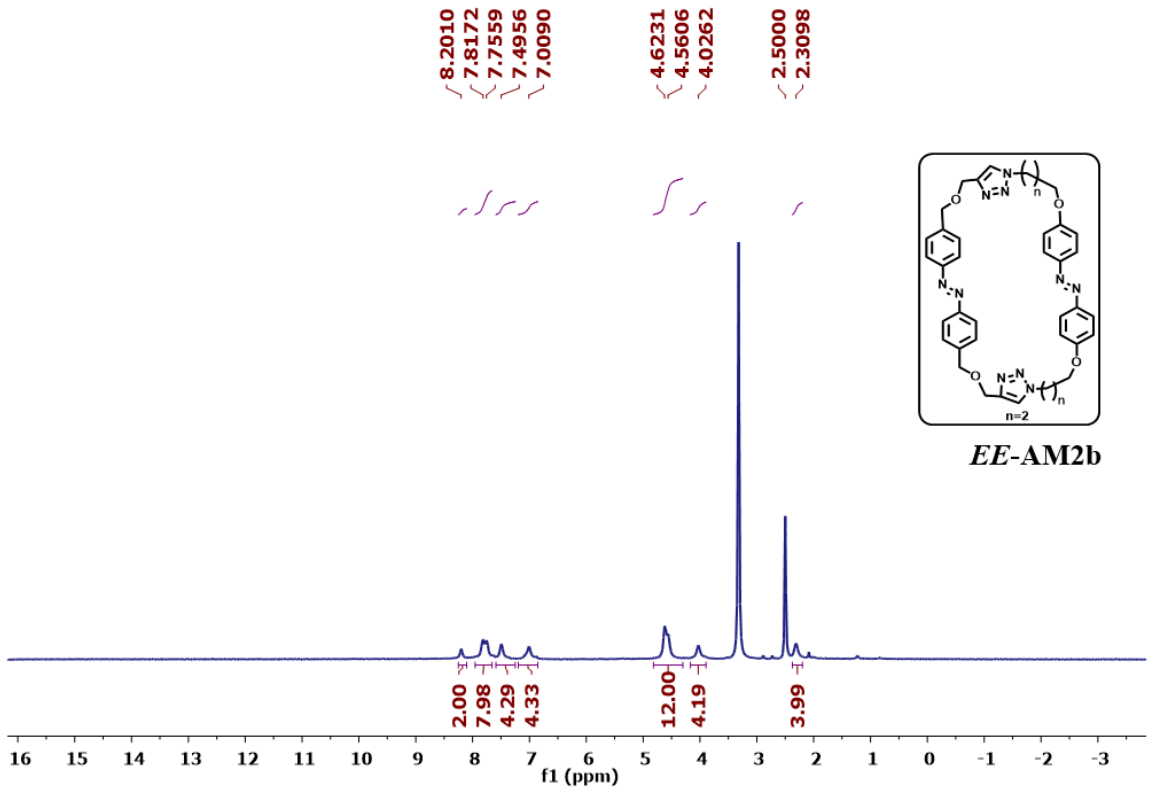

^{1}H NMR spectrum of ***EE*-AM2b** in DMSO-d_6

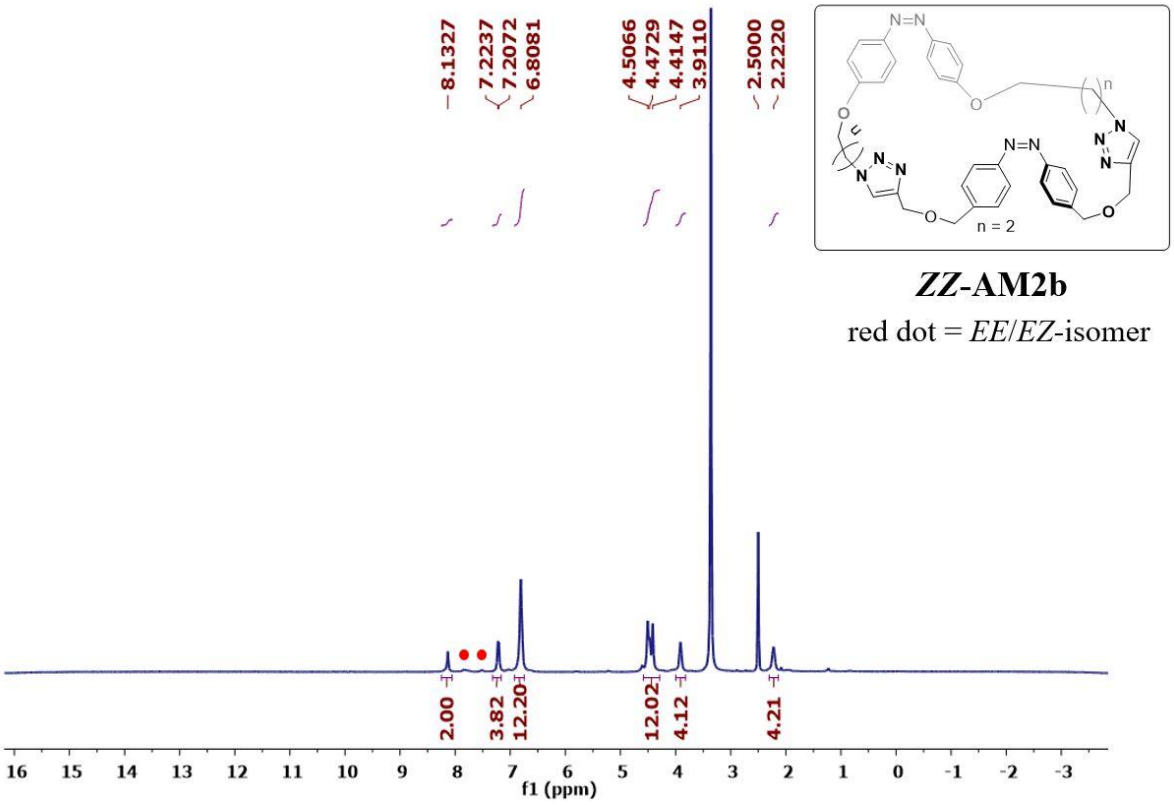

^{1}H NMR spectrum of ***ZZ*-AM2b** in DMSO-d_6 (red dot represents the *EE*/*EZ*-isomer)

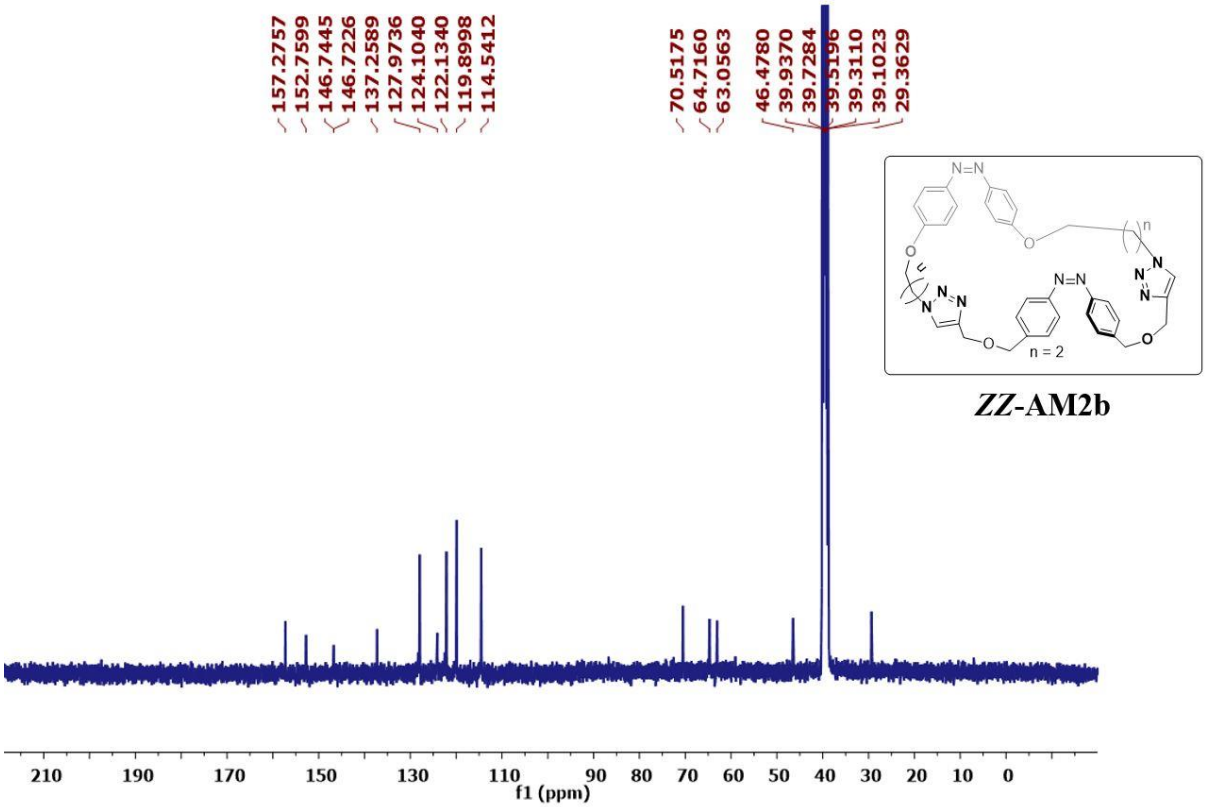

***ZZ*-AM2b**

^{13}C NMR spectrum of ***ZZ*-AM2b** in DMSO-d_6

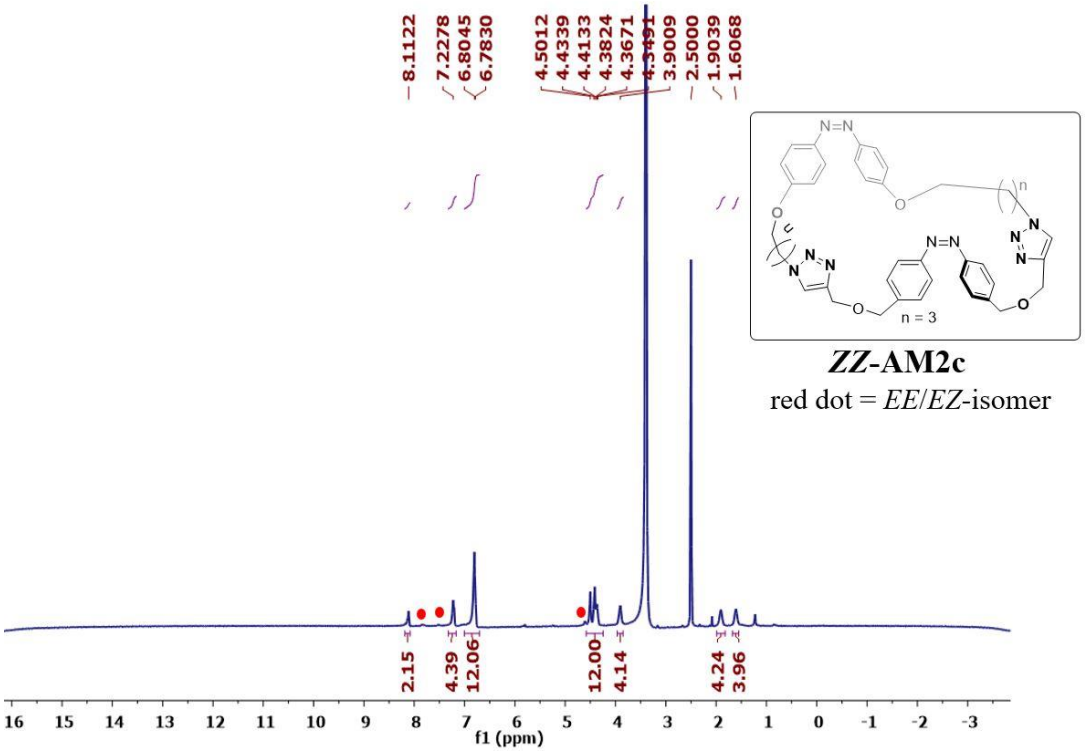

^{1}H NMR spectrum of ***ZZ*-AM2c** in DMSO-d_6 (red dot represents the *EE*/*EZ*-isomer)

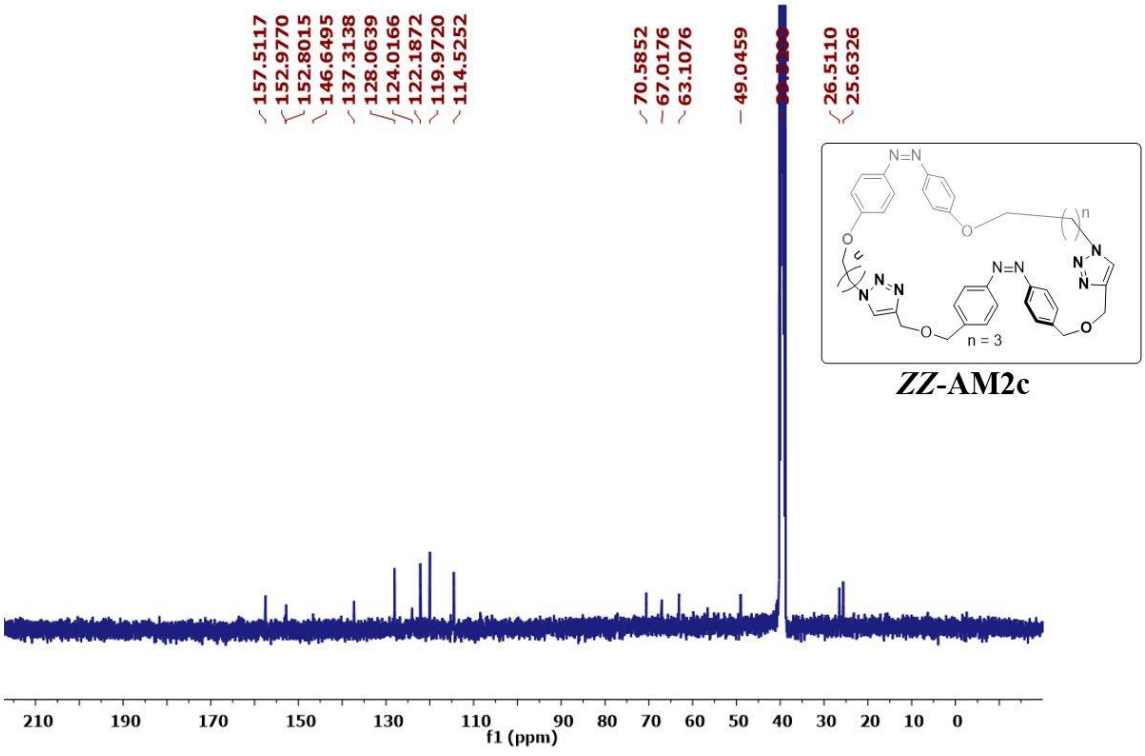

^{13}C NMR spectrum of ***ZZ*-AM2c** in DMSO-d_6

S10. Cartesian Coordinates

Cartesian coordinates of the optimized structures at M062X/6-311G(d,p) level of theory.

EE				***ZZ***			
C	1.38744498	2.47340391	2.45912298	C	-5.19958707	-2.00606102	1.91302601
C	1.54466394	2.85963593	1.12551898	C	-6.28925907	-2.63129902	1.31570200
C	2.81418193	2.89767695	0.55446794	C	-7.35370907	-1.87830302	0.82803200
C	3.93350995	2.57183995	1.31163091	C	-7.27777907	-0.49326902	0.85073001
C	3.78050299	2.17215394	2.63866691	C	-6.17142007	0.14887998	1.40858701
C	2.50233000	2.12261692	3.20014495	C	-5.14971407	-0.61974302	1.95847102
H	0.39160999	2.43021890	2.87922000	H	-4.38983507	-2.60187103	2.31593601
H	2.90344090	3.18142096	-0.48786705	H	-8.21213306	-2.38929202	0.40761600
H	4.92528594	2.59216996	0.86995089	H	-8.07565006	0.10436098	0.42520301
H	2.38162403	1.79089091	4.22669795	H	-4.29267007	-0.12940803	2.40708502
N	0.45188192	3.15872892	0.26449101	N	-6.38275907	-4.06842202	1.26173700
N	-0.61893807	3.36367991	0.85611404	N	-5.50806107	-4.73485702	0.69349800
C	-1.74740109	3.55144390	0.01012307	C	-4.45517206	-4.08126202	-0.04214599
C	-1.74937412	3.30250492	-1.36240394	C	-4.74448206	-3.22408501	-1.10369699
C	-4.10482710	4.02764888	-0.05856587	C	-2.10122406	-3.74472502	-0.40067898
C	-2.94076314	3.39133191	-2.06751390	C	-3.70720006	-2.62424501	-1.79452899
H	-0.82745213	3.00305193	-1.84302796	H	-5.77457006	-3.02135001	-1.36899199
H	-5.02946009	4.28803586	0.44471616	H	-1.07084506	-3.93090402	-0.12807298
H	-2.95900917	3.15282192	-3.12535991	H	-3.93173505	-1.94892101	-2.61416698
C	-2.92275208	3.93015088	0.65672310	C	-3.13798807	-4.38352202	0.27365601
C	-4.12738313	3.73700489	-1.42217587	C	-2.37962506	-2.85212601	-1.42946298
H	-2.88447605	4.11633687	1.72318310	H	-2.93675507	-5.08888602	1.07158301
C	-5.45970015	3.63340088	-2.11447684	C	-1.29522706	-2.09957201	-2.15283798
H	-6.08032415	4.51876488	-1.91784381	H	-1.37823805	-2.27065501	-3.23615498
H	-5.33623717	3.52951790	-3.19993184	H	-1.43490206	-1.02182101	-1.98008297
O	-6.07003812	2.48307787	-1.56668083	O	-0.02273006	-2.49013901	-1.70030097
C	-7.37890113	2.20980986	-2.00966380	C	0.98108394	-1.62982001	-2.18748797
H	-7.40023915	1.99541187	-3.08614680	H	0.84406494	-0.61664801	-1.78476996
H	-8.04417213	3.06303785	-1.81900078	H	0.93234795	-1.56416301	-3.28342497
C	-7.09617706	0.39949685	-0.22951983	C	2.61449994	-3.34377802	-1.13343197
H	-6.13047506	0.60616985	0.19729715	H	2.00808394	-4.14869102	-0.75739097
C	-7.80944010	1.01361285	-1.22614680	C	2.30720494	-2.17410501	-1.78097996
N	-8.97889809	0.34904784	-1.39274178	N	3.46280594	-1.51656901	-2.04359796
N	-9.02385106	-0.63779217	-0.55337179	N	4.45883394	-2.21337102	-1.59410596
N	-7.89518004	-0.61842116	0.15792718	N	3.96502294	-3.31718102	-1.04096596
C	-7.61834701	-1.63112817	1.16138017	C	4.87097494	-4.31650502	-0.47647996
H	-7.33784199	-1.12085318	2.08739117	H	4.25035294	-5.02863402	0.07169303
H	-8.55887600	-2.15560118	1.33055219	H	5.35357094	-4.84614102	-1.29917296
C	-6.51434501	-2.58455915	0.70824613	C	5.90775893	-3.66172602	0.42792804
H	-6.88755902	-3.22690215	-0.09240987	H	6.66033893	-4.40223302	0.70749804
O	-5.08681997	-4.41993815	1.44644208	H	6.40349894	-2.87089502	-0.13773095
C	-3.82423298	-4.03252313	1.12558205	C	5.28155893	-3.07003303	1.68418004
C	-3.29682399	-2.75335513	1.33768005	H	4.40696093	-2.46101103	1.42579604
C	-3.02561499	-5.02544912	0.55412302	H	4.96404693	-3.86055303	2.36741004
C	-1.98993600	-2.47323911	0.96330202	O	6.22437593	-2.27932203	2.40328905
H	-3.89374899	-1.96945414	1.78459607	C	6.32612993	-0.98562203	1.95044105
C	-1.72677100	-4.73671510	0.18371999	C	5.37880593	-0.04158803	2.34472905
H	-3.45692798	-6.00710512	0.40620702	C	7.39002993	-0.61374403	1.13718606
C	-1.19792601	-3.45925509	0.37697499	C	5.46314693	1.26160397	1.88380106
H	-1.57384101	-1.48451711	1.10740102	H	4.58612093	-0.34339303	3.01923605

H	-1.09529800	-5.48853809	-0.27385003	C	7.48951694	0.69975898	0.69694306
N	0.12742098	-3.26774808	-0.08966504	H	8.13957493	-1.35173603	0.87931006
N	0.59922497	-2.13232507	0.08812495	C	6.50393193	1.62469297	1.02643806
C	1.90563195	-1.95113705	-0.44319508	H	4.72720593	1.99616397	2.18647006
C	2.47600395	-0.68404205	-0.28690708	H	8.32142994	1.02464098	0.08392807
C	2.60819795	-2.94079304	-1.12901110	N	5.81535294	3.67770498	0.10723207
C	3.71759593	-0.40455403	-0.82908511	C	4.48903394	3.18787098	-0.14909594
H	1.92477395	0.07791494	0.25444094	C	3.44865094	4.03634798	0.20085006
C	3.85528193	-2.67218102	-1.67356513	C	4.20726894	2.00135698	-0.83502694
H	2.15600896	-3.91685304	-1.24244410	C	2.12411094	3.67878398	-0.03474594
C	4.40558592	-1.39489602	-1.53713614	H	3.68697294	4.98063398	0.67572306
H	4.17982092	0.57115797	-0.73073611	C	2.89785494	1.65887898	-1.10814495
H	4.37759693	-3.45047401	-2.21368915	H	5.00470594	1.34183998	-1.15708194
O	5.59339490	-1.01877300	-2.07090016	C	1.84510894	2.47494398	-0.68173495
C	4.98775202	1.79154194	3.47169088	H	1.33811994	4.35150998	0.28042105
H	5.32092102	2.65429194	4.05357688	H	2.68712494	0.74405699	-1.64576095
H	4.70809304	0.99974693	4.18194688	O	0.58987294	2.00806198	-0.94438996
O	6.09460200	1.40628996	2.69533385	C	-6.08809007	1.64993298	1.41398502
C	5.90841500	0.17144596	2.03447384	H	-6.85298107	2.07859698	2.07857002
H	6.18231202	-0.66265304	2.69316183	H	-5.11003907	1.97411398	1.78272002
H	4.85589999	0.04267096	1.75059587	O	-6.31060506	2.11634498	0.09206002
C	6.74678596	0.14826498	0.80059682	C	-6.20130606	3.52070698	-0.01906197
H	7.74471198	-1.85789800	0.60962877	H	-6.66719806	3.78770799	-0.96816297
C	7.51075896	-0.86163600	0.27431279	H	-6.75339606	4.01152098	0.79247203
N	6.80220793	1.20421899	-0.05546517	C	-4.78291406	4.00121098	0.00104903
N	7.55120291	0.89649401	-1.06235319	H	-4.07491705	4.33993999	-2.10915996
N	7.99223893	-0.34477899	-0.87911322	C	-3.94359306	4.32378199	-1.04011196
C	8.65685691	-1.03556997	-1.97180524	N	-4.08929206	4.17196498	1.15989404
H	9.05287393	-1.96825097	-1.56565426	N	-2.89255206	4.57458598	0.88799404
H	9.49330489	-0.42039296	-2.30417426	N	-2.78728806	4.67926098	-0.43986996
C	7.69063488	-1.30394397	-3.12798422	N	6.71898594	2.97045898	0.56930107
H	7.42488886	-0.35613397	-3.60036120	C	-0.51302406	2.82525198	-0.58686096
H	8.20413687	-1.92026996	-3.87029924	H	-1.37526006	2.15817998	-0.56591196
C	6.40331090	-1.99338399	-2.70211819	H	-0.39122506	3.22137998	0.42664304
H	5.88485688	-2.40092898	-3.57700318	C	-0.72288306	3.94728199	-1.60643595
H	6.60571792	-2.82069499	-2.00662421	H	-1.21311105	3.54505599	-2.49652296
C	-6.03143897	-3.45142316	1.86502311	H	0.24836995	4.33569999	-1.92453695
H	-5.62164896	-2.83975316	2.67753011	C	-1.52573006	5.10854399	-1.03116895
H	-6.85924695	-4.03181717	2.27535913	H	-1.74109405	5.85863599	-1.79318395
H	-5.68107403	-2.00873614	0.29839911	H	-0.98146006	5.59039198	-0.21779795
***EE*-pyrene**				***ZZ*-pyrene**			
C	-0.52361505	-4.72904503	0.97649498	C	5.29781295	-2.22190910	-1.74371701
C	-0.26955605	-4.12605403	-0.25798902	C	5.67157393	-3.50354410	-1.35368200
C	-1.32256005	-3.68240503	-1.05077102	C	6.71809593	-3.68800111	-0.45609000
C	-2.63389505	-3.85724102	-0.62803502	C	7.30267294	-2.58074912	0.14779799
C	-2.89579605	-4.45159503	0.60371798	C	6.89539297	-1.29110711	-0.18665502
C	-1.83141105	-4.87858503	1.40226798	C	5.91593197	-1.12444911	-1.16649203
H	0.31271395	-5.04530303	1.58572698	H	4.50666295	-2.10165010	-2.47554902
H	-1.09160304	-3.18308002	-1.98429002	H	7.02341791	-4.69530512	-0.19936899
H	-3.45999405	-3.49814402	-1.23156302	H	8.07532594	-2.72552112	0.89586499
H	-2.03511406	-5.32518803	2.37079698	H	5.61788299	-0.12043110	-1.44263304
N	1.03872995	-3.85786203	-0.74393601	N	5.04050091	-4.64684110	-1.93742499
N	1.94349395	-4.40651603	-0.09676201	N	3.83464591	-4.87791608	-1.78534599
C	3.25850995	-4.05705903	-0.50936901	C	2.95079592	-4.16150505	-0.89572400
C	3.54217795	-3.17315403	-1.55321501	C	3.28473793	-3.54286505	0.31797000

C	5.59435595	-4.17451903	0.05449300	C	0.59877892	-3.85430501	-0.38756300
C	4.85091195	-2.78212103	-1.76632900	C	2.27570793	-3.11727402	1.16638099
H	2.72626196	-2.76745203	-2.13749101	H	4.31196393	-3.42600306	0.63070400
H	6.39182295	-4.54466403	0.68945200	H	-0.44428808	-3.97296099	-0.65157900
H	5.08007596	-2.06142403	-2.54453100	H	2.54022494	-2.65850901	2.11468699
C	4.28379395	-4.58063203	0.27029199	C	1.60471392	-4.30492803	-1.23313400
C	5.88230095	-3.25771303	-0.95067700	C	0.92947693	-3.28753400	0.83867999
H	4.02353595	-5.26580703	1.06806799	H	1.36955491	-4.81926904	-2.15758199
C	7.24721895	-2.64426803	-1.06498400	C	-0.10967806	-2.94406597	1.87119099
H	7.99697795	-3.24808703	-0.53762400	H	0.06245692	-3.57790497	2.75491099
H	7.55574496	-2.54614403	-2.11457600	H	0.00149295	-1.89919197	2.19318198
O	7.14461395	-1.36145103	-0.47466500	O	-1.40944407	-3.16522895	1.37786499
C	8.35021395	-0.63102203	-0.48010499	C	-2.36729207	-3.00573593	2.40118299
H	8.73420296	-0.50330803	-1.50057699	H	-2.30102505	-2.00910292	2.85274297
H	9.11831095	-1.15223104	0.10762001	H	-2.18526408	-3.74594492	3.19370499 C
C	6.89138695	1.06593497	0.77845000	-4.19612208	-4.03779091	0.87031299	
H	6.00100995	0.52849097	1.05639200	H	-3.70721209	-4.77276893	0.25451800
C	8.03113195	0.70026696	0.10782601	C	-3.73499807	-3.17653591	1.83712099
N	8.84194296	1.78170196	0.01258401	N	-4.78247906	-2.43385589	2.27533698
N	8.26312495	2.79115396	0.58231801	N	-5.85327306	-2.79406088	1.63858998
N	7.08921295	2.37289696	1.05621401	N	-5.51875908	-3.76576189	0.79154399
C	6.13455395	3.32510497	1.59408900	C	-6.48305008	-4.18457289	-0.22430001
H	5.73863295	2.93354896	2.53401000	H	-5.98631010	-4.94284390	-0.83184800
H	6.70653595	4.22924996	1.80736201	H	-7.33745309	-4.64325987	0.27284500
C	5.02431196	3.59969297	0.58364200	C	-6.91182706	-2.97931089	-1.06684002
H	5.48001096	3.85923597	-0.37544000	H	-7.52172007	-3.32148089	-1.90562902
O	3.20867296	5.10517297	0.03024700	H	-7.53065705	-2.32063787	-0.45680503
C	1.96005396	4.57149297	0.07035900	C	-5.68414505	-2.23204491	-1.57686903
C	1.57986895	3.47571097	0.85317199	H	-4.98929505	-2.03863592	-0.75509303
C	1.02224396	5.21170597	-0.74304101	H	-5.16068806	-2.84474093	-2.31720102
C	0.24953195	3.07641897	0.87582399	O	-5.98628103	-1.00800392	-2.22607704
H	2.30543695	2.92716097	1.44081800	C	-5.94535701	0.13146509	-1.46507505
C	-0.29362804	4.79895597	-0.72419301	C	-5.58931899	1.30507908	-2.13078306
H	1.35466496	6.04321697	-1.35101200	C	-6.23419701	0.16580711	-0.10122605
C	-0.69740304	3.75381597	0.10853699	C	-5.49909697	2.50213008	-1.44053308
H	-0.06790905	2.23797397	1.48491599	H	-5.37380599	1.25067706	-3.19061306
H	-1.04569304	5.29060397	-1.32939901	C	-6.18033399	1.37861412	0.57719593
N	-2.08493404	3.48079097	0.09626499	H	-6.49693803	-0.72877088	0.44860396
N	-2.48613505	2.67350197	0.95071498	C	-5.78820197	2.54122310	-0.07494708
C	-3.89135305	2.45382698	0.90970098	H	-5.21202695	3.41030807	-1.95716809
C	-4.40461705	1.49076498	1.77813198	H	-6.44606099	1.42880413	1.62658793
C	-4.76163604	3.16650398	0.08650898	N	-5.02364093	4.64284510	0.66688890
C	-5.76297905	1.22332398	1.80385998	C	-3.70500494	4.44556107	0.13491990
H	-3.71310805	0.96078297	2.42361798	C	-2.92757596	3.32150206	0.39770292
C	-6.12162504	2.91063998	0.11133298	C	-3.12628792	5.54693305	-0.50018511
H	-4.35529704	3.92540898	-0.56799002	C	-1.59297096	3.28353403	0.01110892
C	-6.62679905	1.91996898	0.95729497	H	-3.34836397	2.47801107	0.93164793
H	-6.18363205	0.47732198	2.46650597	C	-1.81562792	5.49671703	-0.93377911
H	-6.77350504	3.48547498	-0.53135302	H	-3.72681690	6.43747606	-0.64258912
O	-7.94353805	1.57419098	1.03421497	C	-1.04035094	4.36205802	-0.67641209
C	-4.32061505	-4.64309702	1.07749797	H	-0.99401597	2.41872703	0.25809793
H	-4.67208205	-5.64036602	0.80147097	H	-1.35677490	6.33107801	-1.44896711
H	-4.35790406	-4.56808503	2.17441897	O	0.24103206	4.40017299	-1.12143809
O	-5.22393705	-3.74171902	0.48537297	C	7.48470499	-0.07968012	0.49494996
C	-5.04828805	-2.40975202	0.94101297	H	7.73341398	-0.31832711	1.53761797

H	-5.36059405	-2.33858302	1.99211597	H	8.40937899	0.24379986	-0.00602504
H	-3.99814105	-2.10568602	0.86915398	O	6.51904600	0.94199990	0.42979395
C	-5.86121905	-1.51342802	0.07863497	C	6.87190302	2.17682590	1.02443094
H	-8.02868505	-1.73743502	0.63482897	H	6.96787702	2.08618691	2.11244594
C	-7.22198205	-1.33493902	0.04694397	H	7.82842603	2.52796888	0.61517594
N	-5.31210905	-0.74018702	-0.89350303	C	5.75184804	3.10500292	0.69874193
N	-6.25459204	-0.09922302	-1.50822703	H	5.45871404	3.01480090	-1.52909307
N	-7.41462004	-0.45276302	-0.95201403	C	5.19816204	3.33966891	-0.53587607
C	-8.66550704	0.11774598	-1.43815803	N	5.00107605	3.74734194	1.62681892
H	-9.46811004	-0.33855702	-0.85567103	N	4.02669206	4.36322795	1.03178391
H	-8.78228604	-0.18272802	-2.48031403	N	4.13285006	4.12245893	-0.27529708
C	-8.68641904	1.63863798	-1.32235503	N	-5.90481695	3.77648111	0.65079291
H	-7.77478304	2.02046498	-1.78335203	C	1.05394904	3.24226798	-0.96219508
H	-9.53027304	2.01694698	-1.90644303	H	1.30626304	3.09414799	0.09694292
C	-8.85735404	2.14239498	0.11012497	H	0.52660403	2.35286598	-1.32575507
H	-8.80662404	3.23589698	0.14432197	C	2.29032105	3.49636195	-1.80160408
H	-9.83715405	1.84536298	0.48838497	H	2.87385803	2.57475794	-1.87690907
C	4.15086496	4.76094097	1.02923800	H	1.95865705	3.76530694	-2.80687308
H	3.64517195	4.55443497	1.97870100	C	3.15984407	4.62488094	-1.23758209
H	4.76634896	5.65324197	1.16450200	H	3.71315108	5.13211692	-2.02905610
H	4.41873096	2.70157197	0.42570400	H	2.55064908	5.36050896	-0.71305010
C	2.50994595	-1.96539803	2.12909999	C	2.97568501	1.28978298	2.24570395
C	1.12249795	-1.89161203	2.13943499	C	1.70524801	1.33215701	2.80629494
C	0.43823895	-1.14052003	1.17748199	C	0.59886200	0.83419602	2.10937995
C	1.18759795	-0.43890803	0.19663499	C	0.79060999	0.29634200	0.80892595
C	2.60760795	-0.49756503	0.20838699	C	2.09376399	0.24542197	0.24864696
C	3.25034295	-1.27767703	1.17322699	C	3.17548500	0.74116896	0.98209095
C	-1.00080805	-1.07852003	1.12820298	C	-0.73234400	0.85444005	2.66116795
C	0.51287896	0.31503197	-0.80940701	C	-0.33063202	-0.15686099	0.05153296
C	-0.90463804	0.34135297	-0.84327101	C	-1.63542801	-0.08697396	0.60514895
C	-1.64065405	-0.37873103	0.16224698	C	-1.79353601	0.40435306	1.95002695
C	-1.55264904	1.08090998	-1.83739502	C	-2.73193902	-0.44022895	-0.18401004
H	-2.63825904	1.09082298	-1.85774302	H	-3.72774902	-0.35131893	0.23641896
C	-0.81577404	1.80811498	-2.76290401	C	-2.54859303	-0.86267597	-1.49536804
C	0.57483696	1.79976397	-2.72732101	C	-1.27073503	-0.97918399	-2.02824504
C	1.25901696	1.04974897	-1.76766301	C	-0.14808102	-0.63261400	-1.27276504
C	2.69808596	0.98490497	-1.72126501	C	1.18967598	-0.71148503	-1.80136704
C	3.34042896	0.23433397	-0.79533100	C	2.25309598	-0.29665104	-1.07618304
H	4.42472296	0.15480297	-0.79673900	H	3.25734298	-0.35566607	-1.47871204
H	3.25958396	1.54196397	-2.46428300	H	1.32331797	-1.11178505	-2.80097403
H	-1.56101305	-1.63776603	1.87253398	H	-0.86683300	1.24957806	3.66216494
H	3.02151694	-2.57792103	2.86247999	H	3.81710101	1.70444897	2.78692194
H	0.55147794	-2.43663403	2.88367499	H	1.55855201	1.76297302	3.79056394
H	4.33234095	-1.37922003	1.13637100	H	4.17716900	0.69382694	0.56564395
H	-2.72521305	-0.34765802	0.10399098	H	-2.79513301	0.42352408	2.37056895
H	-1.32951504	2.39334998	-3.51637901	H	-3.40805903	-1.08151596	-2.11815804
H	1.14257896	2.37542297	-3.45041801	H	-1.13411503	-1.32077501	-3.04872303

Pyrene

C	0.00000000	0.00000000	3.50981800
C	0.00000000	1.20620900	2.82079100
C	0.00000000	1.22861500	1.42336000
C	0.00000000	0.00000000	0.71320800
C	0.00000000	-1.22861500	1.42336000
C	0.00000000	-1.20620900	2.82079100
C	0.00000000	2.45944800	0.67590000

C	-0.00000000	0.00000000	-0.71320800
C	-0.00000000	1.22861500	-1.42336000
C	-0.00000000	2.45944800	-0.67590000
C	-0.00000000	1.20620900	-2.82079100
H	0.00000000	2.14495900	-3.36378000
C	-0.00000000	0.00000000	-3.50981800
C	-0.00000000	-1.20620900	-2.82079100
C	-0.00000000	-1.22861500	-1.42336000
C	-0.00000000	-2.45944800	-0.67590000
C	0.00000000	-2.45944800	0.67590000
H	0.00000000	-3.39326300	1.22755000
H	-0.00000000	-3.39326300	-1.22755000
H	-0.00000000	3.39326300	1.22755000
H	0.00000000	0.00000000	4.59321300
H	0.00000000	2.14495900	3.36378000
H	-0.00000000	-2.14495900	3.36378000
H	0.00000000	3.39326300	-1.22755000
H	-0.00000000	0.00000000	-4.59321300
H	0.00000000	-2.14495900	-3.36378000

S11. References

1 A. Matsumoto, M. Kawaharazuka, Y. Takahashi, N. Yoshino, T. Kawai and Y. Kondo, *J. Oleo Sci*, 2010, **59,** *151-156*.

2 S. Kaneko, K. Asakura and T. Banno, *Chem. Commun*, 2017, **53,** *2237-2240.*

3 G. Wen, D. Zhang, Y. Huang, R. Zhao, L. Zhu, Z. Shuai and D. Zhu, *J. Org. Chem.*, 2007, **72,** 16, *6247-6250.*

4 F. P. H. Junior and N. L. Abbott, *Soft Matter*, 2008, **4,** *2225-2231*.

5 L. H. Urner, B. N. S. Thota, O. Nachtigall, S. Warnke, G. V. Helden, R. Haag and K. Pagel, *Chem. Commun.,* 2015, **51,** 8801-8804.

6 H. Mutlu and C. Barner–Kowollik, *Polym. Chem.*, 2016, **7,** 2272-2279.

7 a) C. E. Weston, R. D. Richardson, P. R. Haycock, A. J. P. White and M. J. Fuchter, *J. Am. Chem. Soc.,* 2014, **136,** 11878-11881; b) S. Devi, M. Saraswat, S. Grewal and S. Venkataramani, *J. Org. Chem.*, 2018, **83,** 4307-4322.

8 a) K. Ghebreyessus and S. M. Cooper, *Organometallics*, 2017, ***36,*** 3360–3370; b) S. Devi, A. K. Gaur, D. Gupta, M. Saraswat and S. Venkataramani, *ChemPhotoChem*, 2018, **2,** 806-810; c) I. I. Sahay and P. S. Ghalsasi, *ACS Omega,* 2019, **4,** 437-443; d) S. –L. Yim, H. –F. Chow and M. –C. Chan, *Chem. Commun.*, 2014, **50,** 3064-3066; e) S. Yagai, T. Karatsu and A. Kitamura, *Chem. Eur. J.*, 2005, **11,** 4054-4063; f) S. Lee, S. Oh, J. Lee, Y. Malpani, Y.-S. Jung, B. Kang, J. Y. Lee, K. Ozasa, T. Isoshima, S. Y. Lee, M. Hara, D. Hashizume and J. M. Kim, *Langmuir*, 2013, **29,** 5869-5877; g) Y. Huang and D. -H. Kim, *Nanoscale*, 2012, **4,** 6312-6317; f) R. Reuter and H. A. Wegner, *Chem. Commun.*, 2013, **49,** 146-148; g) F. Nüesch and M. Grätzel, *Chem. Phys.*, 1995, **193,** 1-17.

9 a) I. I. Sahay and P. S. Ghalsasi, *ACS Omega*, 2019, **4,** 437−443; b) S. –L. Yim, H. –F. Chow and M. –C. Chan, *Chem. Commun.*, 2014, **50,** 3064-3066; c) S. Yagai, T. Karatsu and A. Kitamura, *Chem. Eur. J.*, 2005, **11,** 4054-4063; d) S. Lee, S. Oh, J. Lee, Y. Malpani, Y.-S. Jung, B. Kang, J. Y. Lee, K. Ozasa, T. Isoshima, S. Y. Lee, M. Hara, D. Hashizume and J. M. Kim, *Langmuir,* 2013, **29,** 5869-5877; e) Y. Huang and D. -H. Kim, *Nanoscale*, 2012, **4,** 6312-6317; f) R. Reuter and H. A. Wegner, *Chem. Commun.*, 2013, **49,** 146-148.

10 F. Nüesch and M. Grätzel, *Chem. Phys.*, 1995, **193,** 1-17.

11 a) L. Mátyus, J. Szöllösi and A. Jene, Biology, 2006, **83,** 223-236; b) H. A. Benesi and J. H. Hilderbrand, *J. Am. Chem. Soc.*, 1949, **71,** 2703-2707.

12 Y. Zhao and D. G. Truhlar, Theor. *Chem. Acc.*, 2008, **120**, 215-241.

13 M. M. Francl, W. J. Pietro, W. J. Hehre, J. S. Binkley, M. S. Gordon, D. J. Defrees and J. A. Pople, *J. Chem. Phys.*, 1982, **77,** 3654-3665.

14 N. Ousaka, S. Yamamoto, H. Iida, T. Iwata, S. Ito, R. Souza, Y. Hijikata, S. Irle and E. Yashima, *J. Org. Chem.*, 2021, **86,** 10501-10516.

15 M. J. Frisch et al. Gaussian Inc., Wallingford CT, **2009**.